JUN 2 4 1955
UNIVERSITY OF
LIBRARY

GEOCHIMICA ET COSMOCHIMICA ACTA

EDITORIAL ADVISORY BOARD

L. H. AHRENS-CAMBRIDGE, MASS · **T. BARTH**-OSLO · **N. L. BOWEN**-WASHINGTON, D. C. **A. F. BUDDINGTON**-PRINCETON, N. J. · **L. CAPDECOMME**-TOULOUSE · **E. J. CONWAY**-DUBLIN · **P. ESKOLA**-HELSINKI · **P. GALLITELLI**-MODENA · **J. GOGUEL**-PARIS **D. GUIMARÃES**-BELO HORIZONTE · **A. HADDING**-LUND · **O. HAHN**-GÖTTINGEN **H. W. HARVEY**-PLYMOUTH · **F. HEIDE**-JENA · **A. HOLMES**-EDINBURGH · **G. E. HUTCHINSON**-NEW HAVEN, CONN. · **W. Q. KENNEDY**-LEEDS · **PH. H. KUENEN**-GRONINGEN **S. LANDERGREN**-STOCKHOLM · **F. MACHATSCHKI**-VIENNA · **B. H. MASON**-BLOOMINGTON, IND. · **A. MUIR**-HARPENDEN · **P. NIGGLI**-ZÜRICH · **J. ORCEL**-PARIS · **K. RANKAMA**-HELSINKI · **E. REINHARD**-BASLE · **TH. G. SAHAMA**-HELSINKI · **C. E. TILLEY**-CAMBRIDGE **H. C. UREY**-CHICAGO · **T. VOGT**-TRONDHEIM · **W. WAHL**-HELSINKI · **T. WATANABE**-TOKYO · **F. WHIPPLE**-CAMBRIDGE, MASS. · **R. WILDT**-NEW HAVEN, CONN.

EDITORS

C. W. CORRENS, GÖTTINGEN
E. INGERSON, WASHINGTON
S. R. NOCKOLDS, CAMBRIDGE
F. A. PANETH, DURHAM
L. R. WAGER, OXFORD
F. E. WICKMAN, STOCKHOLM

VOL. 2 NO. 1
1951

PERGAMON PRESS LTD · LONDON

Geochim. et Cosmochim. Acta

GEOCHIMICA ET COSMOCHIMICA ACTA

EDITORS

PROF. C. W. CORRENS, *Sedimentpetrographisches Institut der Universität, Lotzestr. 13, Göttingen, British Zone, Germany.*

DR. E. INGERSON, *United States Department of the Interior, U. S. Geological Survey, Washington 25, D. C., U.S.A.*

DR. S. R. NOCKOLDS, *Department of Mineralogy and Petrology, The University, Cambridge, England.*

PROF. F. A. PANETH, F. R. S., *Londonderry Laboratory for Radiochemistry, The University, South Road, Durham, England.*

PROF. L. R. WAGER, F.R.S., *Department of Geology and Mineralogy, The University, Oxford, England.*

PROF. F. E. WICKMAN, *Naturhistoriska Riksmuseets, Mineralogiska Avdelning, Stockholm 50, Sweden.*

1951 VOLUME 2 NUMBER 1

CONTENTS

Page

EDWARD GOLDBERG, AIJI UCHIYAMA and HARRISON BROWN: The distribution of nickel, cobalt, gallium, palladium and gold in iron meteorites 1

SOL R. SILVERMAN: The isotope geology of oxygen 26

H. v. BUTTLAR and F. G. HOUTERMANS: Photographische Messung des U- und Th-Gehaltes nach der Auflagemethode 43

H. BORCHERT: Zur Geochemie des Kohlenstoffs 62

HANS E. SUESS: Gas content and age of tektites 76

Book review:

R. L. MITCHELL: Spectrochemical Analysis by L. H. Ahrens 80

Publishing Offices: 2, 3 & 5 Studio Place, Kinnerton Street, London S.W. 1 (SLOane 8157–9). Subscription per volume (including postage) £ 4 4s. (U.S.A. $ 11·80). *Distributors:* All countries except U.S.A. and Germany—*Lange, Maxwell & Springer Ltd., 41–45 Neal Street, London W.C. 2.* U.S.A.—*The Academic Press Inc., 125 East 23rd Street, New York 10, N.Y.* Germany—*Lange & Springer, Reichpietschufer 20, Berlin W 35.*

PERGAMON PRESS LTD., 2, 3 & 5 STUDIO PLACE, KINNERTON STREET, LONDON S.W. 1

Geochimica et Cosmochimica Acta, 1951, Vol. 2, pp. 1 to 25. Pergamon Press Ltd., London

5856-294

The distribution of nickel, cobalt, gallium, palladium and gold in iron meteorites

EDWARD GOLDBERG *, AIJI UCHIYAMA, and HARRISON BROWN

Institute for Nuclear Studies, University of Chicago

(Received 22 June 1951)

ABSTRACT

The concentrations of nickel, cobalt, gallium, palladium and gold have been determined in 45 iron meteorites including representatives from all structural classes. Gallium was determined, in addition, in two specimens of troilite and in the metallic phase of two pallasites. The analytical procedures and the structural characteristics of the meteorites studied are described in detail.

It is found that most meteorites fall into three distinct classes, each class possessing a fairly narrow range of gallium concentrations: Class I, 40–100 ppm Ga; Class II, 20 ppm Ga; and Class III, 2 ppm Ga. Analysis of the structures, nickel contents and palladium and gold distributions leads to the same divisions.

All hexahedrites, nickel-poor ataxites and coarse and coarsest octahedrites possess gallium levels corresponding to Class I. Medium octahedrites are split between Classes I and II in the approximate ratio 1:2. All fine and finest octahedrites which posses nickel contents in the range 7·5% to 8·5% are in Class III.

The conclusions which might be drawn from these observations are discussed.

I. INTRODUCTION

Although the compositions of many iron meteorites are fairly well known with respect to their major constituents, iron and nickel, the distribution of the lesser constituents between iron meteorites of various types is known only poorly. As the pattern of the distribution of trace elements in meteorites probably was determined by the physical and chemical conditions under which the objects were formed, a careful quantitative study of the distribution of a number of elements might provide information concerning the origin of these extra-terrestrial fragments of matter.

Table 1. Gallium contents of meteorites as determined by GOLDSCHMIDT *and* PETERS [1]

Type	*Meteorite*	*Gallium Content (ppm)*
Iron	Canyon Diablo	5
Iron	Xiquipilco	10
Iron	Cape York	5
Pallasite	Brenham (metal phase)	5
Stone	Estherville (metal phase)	5

The elements gallium, palladium, and gold, all of which possess sufficiently low oxygen affinities to be concentrated primarily in iron meteorites rather than in stones, were chosen for this preliminary study. The concentrations of these three trace elements, together with the more abundant constituents nickel and cobalt, have been determined in a number of iron meteorites including representatives from

* Present address: Scripps Institution of Oceanography, La Jolla, California, U.S.A.

Table 2. Palladium and gold contents of meteorites as determined by Goldschmidt *and* Peters [3]

Meteorite	*Type*	*Palladium Content* ppm	*Gold Content* ppm
Coahuila	H	10	5–1
Sao Juliao de Moreira	H	10	10
Mount Joy	H	10	5–10
Arispe	Ogg	10	5–1
Arispe	Ogg	10	5
Corrizatillo		10	5–10
Magura	Og	5–10	5
Canyon Diablo	Og–Ogg	5–10	5
Cranbourne	Og	10	5
Cape York	Om	5	5
Xiquipilco	Om	10	10
N'Goureyma	Ob	5	1
Morradal	Ataxite (Ni rich)	10	5
Cape of Good Hope	Ataxite (Ni rich)	10	1
Krasnojarsk (iron phase)	Pallasite	10	5
Brenham (iron phase)	Pallasite	10	10–5
Estherville (iron phase)	Stone	10	1–5

all classes—hexahedrites (both granulated and normal), nickel-rich and nickel-poor ataxites, and coarsest, coarse, medium, fine and finest octahedrites. Three anomalous meteorites which do not fit into the usual structural classification scheme were studied as well.

Table 3. Palladium and gold contents of meteorites as determined by I. *and* W. Noddack [4]

Meteorite	*Type*	*Palladium Content* ppm	*Gold Content* ppm
Canyon Diablo	Og–Ogg	—	1
Bethany	Of	15	0
Xiquipilco	Om	20	—

Table 4. Average gallium, palladium and gold contents of iron meteorites as determined by previous workers

Element	Goldschmidt *and* Peters	I. *and* W. Noddack (1930)	I. *and* W. Noddack (1931)
Gallium	5	13	
Palladium	10	19	15–20
Gold	5	1·4	0–1

Gallium has been previously studied in iron meteorites by Goldschmidt and Peters [1], and by I. and W. Noddack [2]. The latter workers obtained an average gallium level of 13 parts-per-million. Goldschmidt and Peters found the gallium concentrations in specific meteorites to be as listed in Table 1.

Palladium and gold have also been studied in iron meteorites by Goldschmidt and Peters [3], and by I. and W. Noddack [2], [4], with results shown in Tables 2 and 3. The average values obtained by previous workers for the concentrations of gallium, palladium and gold in meteoritic iron are given in Table 4.

II. Analytical Methods

1. Nickel—Nickel was determined in all meteorites by the method utilized by Henderson [5]. The procedure involves the precipitation of nickel dimethyl glyoxime under carefully controlled conditions which prevent the coprecipitation of iron and cobalt. Nickel was determined in most meteorites examined in this study by two independent observers, and the availability of certain meteorites permitted us to cross-check a number of results with those previously obtained by Henderson utilizing the same technique.

Observer "A" in all cases dissolved the samples in HCl, discarding the residue (mainly schreibersite). Observer "B" dissolved the samples totally in aqua regia. In general, the results indicate that the two methods of dissolution yield results which are quite close to each other. There are certain notable exceptions, however.

The cases where cross-checking with Henderson was possible are shown in Table 5. It is seen that of the five cross-checked cases only one serious discrepancy exists, that of Linwood. The results reported in this work is the average of four separate determinations which yielded the individual values of 6·67, 6·65, 6·72 and 6·52 %.

Table 5

Meteorite	*Nickel Content %*		
	Observer A	*Observer B*	Henderson
Cedartown		5·58	5·48
Coahuila	5·61	5·65	5·59
Edmonton	12·64	12·68	12·57
Hill City	9·32		9·17
Linwood		6·64	5·98
Mount Joy	5·68	5·65	5·79
Sandia Mountains . .	5·94	5·94	5·92

The reproducibility of the nickel determinations can be judged on the basis of a series of independent runs made on pieces of the Canyon Diablo meteorite with the following results: 7·07, 7·12, 7·20, 7·09, 7·09, 7·12, 7·09, 7·13, 7·11, 7·11, and 7·09 %. The average of these runs is 7·11 % nickel and the standard deviation is 0·035. Thus the standard deviation corresponds to only 0·5 % of the nickel content of the meteorite. As a result, the authors believe the nickel values reported in this paper to be internally comparable to a precision of 0·5 % or better, all values being the average of at least two, and in most cases three or more, determinations.

In those few cases where major differences exist between the values reported by the two observers, the discrepancies must in general be attributed to the schreibersite contents of the meteorites or to inhomogeneity in composition. If a meteorite contains an appreciable concentration of schreibersite, the nickel content determined on the total meteorite will be higher than that determined on the metal phase alone. Only three cases were encountered in the present work where serious discrepancy exists between the results of the two observers (Arispe, Perryville and Spearman). In all of these cases, the results obtained by total sample dissolution were higher than those obtained by partial dissolution.

2. Cobalt—Cobalt was determined by a modification and further development of a method for determining cobalt in steel reported by Young and Hall [6]. As the method used by us has not been reported elsewhere, the procedure is given below in detail:

(1) Dissolve approximately 0·3 g of meteorite in minimum amount of aqua regia.
(2) Add 10 ml 6 M HCl, then dilute volume three-fold.
(3) Heat and pass in H_2S until precipitation is complete.
(4) Filter and wash precipitate with H_2S wash solution.
(5) Boil solution to eliminate H_2S.
(6) Add sodium phosphate reagent to solution (Reagent: 34·05 g of tri-sodium phosphate heptahydrate in one liter of water. 10 ml of reagent solution precipitates 0·05 g of iron). The

solution is usually cream-colored after addition of the reagent, although it may be a clear yellow solution if the acid concentration is high.

(7) Add concentrated NH_4OH to solution until a *p*H of 5·5 is reached (solution will be blue-grey).

(8) Add glacial acetic acid until a *p*H of 3·5 is reached (solution will be grey-white).

(9) Readjust *p*H to 3·5 with concentrated ammonium hydroxide.

(10) Bring solution to boil, allow to settle, then filter through a fritted Buchner.

(11) Wash with acetic acid wash solution at least five times (25 ml conc. acetic acid in 1000 ml water).

(12) Make filtrate acidic with HCl (3 ml 6 M HCl for every 100 ml of solution).

(13) Add fresh alpha nitroso beta naphthol reagent (Reagent: 10 g alpha nitroso beta naphthol in 100 ml of 1:1 acetic acid). Approximately 0·5 g of alpha nitroso beta naphthol (Eastman Kodak) are required for every 0·01 g of cobalt. The cobalt precipitate is brick-red. If copper is present the precipitate is brown.

(14) Digest at low heat, cool and filter.

(15) Wash precipitate several times with 5% hot HCl, then several times with hot water.

(16) Dry precipitate in platinum crucible and ignite in muffle oven at 800° C. The ignition should not take place at a temperature greater than 900° C or less than 750° C.

(17) Dissolve the residue in 1:1 sulfuric acid and transfer to a weighed porcelain crucible.

(18) Evaporate carefully, then ignite at 550° C in a muffle oven.

(19) Cool and weigh residue as cobalt sulphate.

Extensive checking of the above method on mock meteorite solutions and on meteorites lead us to the conclusion that the cobalt results reported in this paper are precise to within four per cent.

3. Gallium—The method utilized for the determination of gallium has been reported previously by Brown and Goldberg [7]. The meteorite samples were activated with neutrons, following which the radioactive gallium was chemically separated from the other activities present and counted. The chemical procedure was designed to make use of the fact that gallium is ether-extractable as the chloride, is amphoteric, and can be precipitated as the 8-hydroxyquinolate. Extensive testing indicates that the method as used in the present work permits the determination of gallium in the range of 1 to 100 ppm with a precision of 10% or better.

4. Palladium—As in the case of gallium, palladium was determined by neutron activation [7]. The chemical procedure for isolating the palladium activity was designed to make use of the fact that palladium forms a complex in excess ammonium hydroxide and can be precipitated conveniently as the dimethyl glyoxime. The method as used permits the determination of palladium at a 1 ppm level with a reproducibility of approximately 10%.

5. Gold—Gold was determined by neutron activation [8]. The chemical procedure for the separation of the gold from the other radioactivities consisted of the extraction of gold chloride from a 10% hydrochloric acid solution into ethyl acetate, followed by reduction of the gold chloride with hydroquinone. The method permits the determination of gold at a level of 1 ppm with a reproducibility of 10 to 15%.

Due to the self-shadowing effect in elements of high neutron cross-section [8], a constant correction factor has been applied to all gold values obtained, which factor is known with an accuracy of only 25%. Thus the actual concentration of gold present in a given specimen might differ by 25% from the amount reported. However, as this correction factor is constant for all samples studied, the results may be compared *with each other* with a considerably higher precision corresponding to the internal consistancy of 10 to 15%.

III. Descriptions of Meteorites Studied

The distribution of gallium, palladium and gold was studied in 45 iron meteorites, descriptions of which will be found below. We acknowledge the generosity of the following institutions and individuals for their cooperation in supplying us with material: The United States National Museum (Henderson) for gifts of Cedartown, Coahuila, Drum Mountains, Edmonton, Goose Lake, Hill City, Linwood, Maria Elena, Mejillones, Perryville and Sierra Gorda; The Institute of Meteoritics, University of New Mexico (La Paz) for gifts of Albuquerque, Henbury, Xiquipilco, and an Undescribed Iron from New Mexico; The Chicago Natural History Museum (Roy) for gifts of Canyon Diablo and Odessa; Dr. Cyril Smith of the University of Chicago for a gift of a specimen of Carlton. The balance of the meteorites, together with additional samples of Canyon Diablo, Henbury and Xiquipilco, were purchased from the American Meteorite Museum (Nininger), which was kind enough to make the specimens available to us for study.

The brief descriptions given below are those which have been either reported in the literature, or given to us in private communications.

1. Albuquerque—Found 13 miles WSW of Albuquerque, Bernalillo County, New Mexico, U.S.A. (35°0′ N, 106°48′ W). Recognized September, 1943. Described by Beck and Lapaz [9]. Weight 157·3 g. The bands of kamacite are regular and vary in thickness from 0·6 to 1·1 mm, placing the meteorite in the class 0 m. The taenite bands are narrow. The few schreibersite grains concentrate along the boundaries of the kamacite and taenite bands. Several large and many smaller plessite fields have been observed. Considerable lawrencite is present. A major discrepancy exists in the nickel analysis of this meteorite; Beck and Lapaz report 8·51 %, while this work gives 7·41 %.

2. Altonah—Found in Duchesne County, Utah, U.S.A. (40°34′ N, 110°20′ W), about 1932. Weight 21 kg. The meteorite is undescribed, but Nininger [10] has stated that it is a meteorite of the 0f class. In a private communication, Nininger says, "In Altonah I measured eight groups of kamacite bands totaling 52 bands and a total width of 18·6 mm or an average of 0·36 mm."

3. Arispe—Found in 15 miles NW of Arispe, Sonora, Mexico (30°15′ N, 110°0′ W), in 1898. Total known weight 398 kg. Described by Ward [11] and Wuensch [12]. A section surface shows numerous troilite nodules, up to 30 mm in diameter, with a surrounding envelope of schreibersite. The nodules sometimes contain small patches and angular fragments of nickel-iron and even occasionally masses of chromite 4 to 5 mm in diameter. Polished or etched surfaces sometimes show arborescent groups of crystals, as large as 10 by 18 mm in diameter, and apparently cohenite. Blades of schreibersite also occur, 3 mm in width by 45 mm in length. The *Widmannstätten* figures are sharp and clear, showing distinctly the octahedral structure of the iron. The kamacite plates are of unusual width, averaging 3 to 4 mm. In one instance, the length of the plate is 195 mm. The taenite films are comparatively small. The iron is further characterized by the almost entire absence of plessite. The nickel content determined in this investigation agrees well with that found by Whitfield (reported by Ward).

4. Bear Creek—Found near Bear Creek, about 25 or 30 miles from Denver, Colorado, U.S.A. (39°48′ N, 105°5′ W) in 1866. Weight estimated to be 200 kg. Work reviewed by Farrington [13]. Brezina [14] gives the width of the kamacite bands as 0·5 mm. This meteorite is listed by Farrington [13] and others as being of the 0f class. However, if we accept the bandwidth as determined by Brezina, this meteorite belongs to the 0m class. Cohen [16] gives a detailed description of the structure. The lamellae are long, straight, swollen, seldom grouped, and consist of strongly hatched granular kamacite, with very fine etching pits, and well-developed taenite. The plessite consists of grains whose size average 0·03 mm and varies from 0·02 to 0·10 mm. Schreibersite is very richly present. In part it forms large crystals up to 15 mm in length; in part there are smaller individuals which lie in the bands or are surrounded by swathing kamacite. Cohenite is possibly present. There are large troilite nodules surrounded by swathing kamacite.

Nininger (private communication) says: "It should be noted that all of the published writings on the structure of this meteorite were based upon the study of small pieces. While its structural pattern is very consistent if viewed in the large mass, there are local variations and contrasts which may readily lead to erroneous conclusions if not viewed in their environmental relations.

"Some have regarded this as a fine octahedrite; others as a medium octahedrite. Both conclusions can be defended. If one makes an intensive study of a small section he may come up with either of these classifications, or indeed, he might be forced to place it in the group of coarse octahedrites if he adheres strictly to the conventional band measurement long in use. For example: I measured 65 bands with a total width inclusive of intervening taenite of 31 mm. This is an average of a little less than 0·48 mm for kamacite and taenite combined. In Bear Creek the kamacite plate separation is abnormally great due not so much to the abundance of taenite as at first appears but rather to the fact that more often than not the taenite lamellae are replaced by narrow fields of plessite. Apparently this feature has been overlooked by some of the early writers.

"The above measurements were made in areas selected as representative of the predominant structure of the entire iron. However, at one point 5 bands lay side by side within a space of 1 mm, and two of the separating lamellae were found, on examination under a sufficient magnification, to be plessite rather than taenite. These 5 kamacite plates ranged from about 0·19 mm to less than 0·1 mm in thickness. Separated by a narrow field of plessite on one side of the group lay a normal kamacite plate measuring 0·6 mm, while on the other side beyond a narrow field lay a band of swathing kamacite 2 mm in width.

"In another part of the large slice a band of kamacite measured 3 mm wide and another 3·7 mm. Both of these were oriented in harmony with the adjacent plates which were of normal width. Each was also bordered by taenite. They were not swathing kamacite."

The most reliable previous analysis is that of J. L. Smith [17] who found 14·06% nickel, a value considerably higher than that found in this investigation.

5. Bristol—Found on the Holston River, 12 miles SE of Bristol, Sullivan County, Tennessee, U.S.A. (36°34′ N, 82°11′ W), about 1925, and recognized as a meteorite in 1937. Weight 20 kg. The meteorite is unstudied. Nininger (private communication) has measured the band-widths and has found them to average 0·24 mm. Thus, the meteorite belongs to the Of class.

6. Canyon Diablo—Approximately 30 tons of meteoritic iron have been recovered in the vicinity of Meteor Crater, near Winslow, Coconino County, Arizona, U.S.A. (35°10′ N, 111°7′ W), since 1891. Studies of the structure of this meteorite have been made by Meunier [18], Brezina [19], Nininger [20], and Perry [15]. The meteorite ranges in structure from coarse to coarsest, and contains numerous interlaminations of schreibersite and inclusions of graphite and troilite. The troilite inclusions are frequently 1 cm or more in diameter, and occasionally huge nodules of troilite and graphite from 10 to 15 cm in size are encountered. Carbon is present also in the form of microscopic diamonds. In general, the broad bands of kamacite are associated with very thin filaments of taenite. The kamacite bands vary in width up to a much as 4 or 5 mm. Young [21] has shown that the kamacite is body-centered cubic (a 2·870 Å), and the taenite is face-centered cubic (a 3·590 Å). A (110) plane of the kamacite is parallel to a (111) plane of the taenite.

Older analyses of Canyon Diablo vary widely. Moissan [22] obtained nickel values ranging from 1% to 7%. Later Whitfield [23] reported a value of 7·33%, which is in substantial agreement with the value determined by us. The question of the uniformity of the composition of Canyon Diablo will be discussed in detail later in this paper.

7.—Canyon Diablo No. 2—In 1936, while etching a group of freshly sectioned irons found in the region of Meteor Crater, Arizona, Nininger [20] noticed sections from two irons to be different from other Canyon Diablo sections. Schreibersite was not as abundant, and the kamacite band-widths were considerably smaller than in previously studied Canyon Diablo specimens. Taenite was more prominent than in normal specimens. In 1939, two other small individuals, which conformed to the same pattern, were discovered in another lot of specimens. Later additional specimens possessing the identical pattern were uncovered. Thus far, 1·6 kg of this material have been recognized. Nininger (private communication) has found that the kamacite bands average 1·4 mm in width.

Chemically, Canyon Diablo No. 2 appears to be decidedly different from the normal material, as will be discussed in detail later in this paper. HAWLEY [20] found the nickel content to be 8·42%, in reasonable agreement with our value of 8·22%.

8. Cape of Good Hope—Found in 1793, NE of Big Black River, between Sunday River and Bushman River, South Africa (34°0′ S, 27°30′ E). Weight 136 kg. The meteorite has been studied in detail by COHEN [16], who classifies it as a nickel-rich ataxite. The troilite of this meteorite occurs often with daubréelite ($FeS \cdot Cr_2S_3$) inclusions. The nickel content has been variously reported as 15·28, 12·27, 15·09, 15·23, 16·21, 14·32, and 15·67%, the latter value obtained by FAHRENHORST [16]. Our value of 16·48% is in reasonable agreement with this.

9. Carlton—Found in 1887 five miles south of Carlton, Hamilton County, Texas, U.S.A. (31°55′ N, 98°2′ W). Weight 81·5 kg. First described by HOWELL [24]. The nickel content as determined by EAKINS and reported by HOWELL is consistent with that determined in the present study. Work reviewed by FARRINGTON [13]. BREZINA [14] gives the width of the kamacite bands as 0·2 mm, thus placing the meteorite at the lower edge of the Of class. The meteorite has been further described by COHEN [25].

The bands consist of fine-grained kamacite and are long, straight, and often grouped. The taenite appears in relatively broad ribbons which are unusually sharp. The plessite is dark gray, compact and homogenous in the smaller fields. The richness in great schreibersite crystals is an important feature. These crystals are surrounded by swathing kamacite which often attains a considerable breadth. The swathing kamacite is not granular like the kamacite in the bands, but finely hatched. Troilite occurs sparingly. It appears almost entirely in short *Reichenbach* lamella which exceptionally reach a length of 5 to 10 mm. Curving of the *Widmanstätten* figures is frequent on the larger cavities of the exterior. The curving follows the cavity like an onion skin along the octahedral laminae and swellings between them.

10. Cedartown—Found about 1898 approximately 62 miles WNW of Atlanta, Polk County, Georgia, U.S.A. (34°0′ N, 85°16′ W). Total weight 11·6 kg. The meteorite has been described by PERRY and HENDERSON [26]. Several slices cut from the mass show a "normal" hexahedral structure, with two sets of *Neumann* lines crossing the entire surface of the slices. One set is conspicuous, the other scanty and less noticeable. Troilite inclusions are observed, some reaching dimensions of a centimeter, one large one being partly surrounded by graphite. Schreibersite is abundant, occurring as long oriented needles, rhabdites and irregular bodies. There are numerous small inclusions of troilite associated with schreibersite, the latter usually more or less completely surrounding the former. In such cases the troilite usually contains many minute white spots which apparently are kamacite. HENDERSONS determination of the nickel content of this meteorite agrees well with that reported in this paper.

11. Chihuahua City—Found in the southeastern part of Chihuahua City, Chihuahua, Mexico (28°40′ N, 106°7′ W), about 1907(?), and recognized as a new meteorite in 1929. Total known weight 54 kg. Described by NININGER [27], who classified the meteorite as a finest octahedrite. NININGER stated: "Within the small areas described a very fine octahedral crystallization is discernible. The size of the figures is apparently constant throughout the entire section of the meteorite, but their orientation and distinctness are local. The crystallization is very much like that of the Perryville iron, but the Chihuahua City meteorite differs radically from the former in its pronounced brecciation and in the distribution of its abundant dendritic schreibersite."

HENDERSON (private communication) writes: "There is no chance of Chihuahua City being a finest octahedrite. I would call the specimen we have an ataxite. It has a structure similar to what we used to call a 'brecciated hexahedrite.' This is a strange iron."

In the specimen studied by NININGER, there were found on the cutting surface, scattered somewhat irregularly 2–3 mm apart, tubercles or papillae rising perhaps 0·25 mm and averaging about a millimeter in diameter. In addition to the general sprinkling of these little protuberances, there were double rows of them traversing the iron in various directions, but seldom in straight lines. These tubercles were believed to be schreibersite.

Another peculiarity of the Chihuahua City specimen is the distribution of its troilite. Very compact and clean cut nodules of this substance are found, some circular and others triangular or rectangular. The usual arrangement is an inner nodule of troilite surrounded by a very narrow zone of schreibersite which, in turn, is bordered by a wide band of noncrystalline kamacite. The troilite seems to be of two varieties—one, brassy in color, takes a good polish

and resists the action of acids; the other is almost black, powdery, takes no polish, and is easily affected by acids. The nickel content as determined by Hawley [27] agrees well with the value determined by us.

12. Chilkoot—This meteorite was obtained in 1881 by the State Mining Bureau of California. It had been found a number of years previously near Chilkoot Inlet, Portage Bay, Alaska (59°20′ N, 136°0′ W). Total weight 43 kg. *Widmanstätten* figures can be dimly seen on the outer surface of the mass. Ward [28] stated that an etched face in his possession showed typical figures with an unusual abundance of taenite bands. He lists it as a medium octahedrite. On the label of Wards sample was found a chemical analysis with no analyst's name given. The reported nickel content of 7·11 % is lower than that determined in the present investigation.

13. Clark County—Found in 1937 in southern Clark County, Kentucky, U.S.A. (38°0′ N. 84°10′ W). Weight 11·3 kg. There is no published description of the structure of this meteorite, Nininger, who possesses the main mass, lists it as a medium octahedrite [10].

In a private communication, Nininger states further: "In Clark County 51 bands were measured with a total width of 54·6 mm or an average of 1·07. This includes the taenite which is very weak in this iron. A peculiarity of this meteorite which was not considered in my previous observations on it—slice No. 181·6 shows a large triangular area of kamacite measuring 4·5 × 4·5 × 5·5 cm with only a few small inclusions of taenite. It also shows several other smaller areas of the same kind. These in form and arrangement are similar to the plessite areas in other irons; but I am confident that they are regular kamacite. Plessite areas are very rare and are so small as to easily be overlooked. This meteorite probably deserves a re-classification, but to call it a coarse or coarsest octahedrite would be wholly misleading, in my opinion, for it is mainly composed of normal kamacite bands of the dimensions indicated above. I suspect that this large area of kamacite is merely a broad plate of normal thickness viewed broadside."

14. Coahuila—A number of masses have been found in the state of Coahuila, Mexico, in the neighborhood of 28°42′ N, 102°51′ W. The masses are sufficiently similar in composition and structure, and are in sufficiently close geographical proximity to warrant their being grouped together as members of a single fall. 2064 kg have been recovered. Various masses have been described by Brezina [29], Daubrée [30], Cohen [16], Huntington [31] and others. The iron shows a good cubical cleavage and gives etch lines which all are about the same intensity, but which vary considerably in length. Schreibersite occurs in small (mostly shorter than 1 mm) needle-shaped crystals which seem to be oriented. The troilite aggregates and single crystals are as a rule surrounded by a thin zone of schreibersite. Lamellae of daubréelite occur frequently with the troilite. Troilite also occurs in the form of *Reichenbach* lamellae, which attain a length of 10 cm and are always surrounded by a granular zone 1 to 1·5 mm wide. Most specimens of Coahuila are typical examples of "normal" hexahedrites. *Neumann* lines are abundant. X-ray analysis has shown [32] that Coahuila has a body-centered lattice, closely similar to that of α-iron, and possessing a parameter of $2{\cdot}88 \times 10^{-8}$ cm.

The older analyses of the Coahuila irons give nickel contents ranging from 3 to 7 %. The value reported in this paper is in good agreement with that reported by Henderson [33] who found 5·59 % nickel.

15. Costilla Peak—Found in 1881 on the north slope of Costilla Peak, Taos County, New Mexico, U.S.A. (36°55′ N, 105°30′ W). Total weight 35·5 kg. The meteorite has been studied by Hills [34] and by Brezina [19]. The former states, "The kamacite bands are from 1 to 2 mm in width and of considerable length. The taenite lines, which are irregular in trend and direction, are of capillary size and only visible through a lens or in strongly reflected light. Here and there are small nodules of troilite, from 1 to 10 mm in diameter, some of which enclose a dark-gray substance resembling graphite." Brezina states: "The lamellae are long, straight, grouped, 0·8 mm thick, the taenite weak, fields predominant, mostly containing repetitions of the lamellae. The kamacite and fields are granular; the former coarse, the latter fine. There are many troilite grains and plates distributed through the whole mass."

The nickel content of this meteorite as determined by Eakins [34] is slightly higher than that determined by us.

16. Deport—Found 1 mile east of Deport, Red River County, Texas, U.S.A. (33°31′ N, 95°18′ W) in 1926. Total weight 15 kg. Described by Palache and Gonyer [35]. The width of the kamacite bands classify this iron as a coarse octahedrite. The kamacite plates are closely

spaced with a minute amount of taenite separating the lamellae. The amount of plessite is small. Schreibersite is present, partly in irregular, nodular areas, more generally in rods. Several nodules of troilite were encountered, the largest 1 cm in diameter. This nodule is bordered by schreibersite and at one point by a small mass of graphite. The nickel content as determined by GONYER [35] is smaller than that determined by us.

17. Drum Mountains—Found in 1944 in an area of low hills lying between the Drum Mountains and the Little Drum Mountains, Township 15 South, Range 10 West, and approximately Section 29, Millard County, Utah, U.S.A. (39°31′ N, 112°54′ W). Total weight 529 kg. Described by HENDERSON and PERRY [36]. The meteorite is a medium octahedrite with bands averaging about 1 mm in width, but with occasional wider or narrower bands. The octahedral structure is highly developed, though somewhat irregular. Taenite is abundant, with many thickened or wedge-shaped lamellae having darkened cores due to incomplete transformation. A number of *Reichenbach* lamellae up to 2 or 3 cm in length are noticeable. A few nodular troilite inclusions were observed and also a number of small irregular inclusions. Schreibersite appears in irregular bodies. No rhabdites or fine phosphide particles were observed. Both troilite and Schreibersite are fairly abundant. Plessite fields are numerous.

Unfortunately, no material was available after gallium, palladium and gold analyses to permit our determining nickel and cobalt.

18. Edmonton—Found in 1942, four or five miles east of Edmonton, Metcalfe County, Kentucky, U.S.A. (36°50′ N, 85°30′ W). Total weight 10·5 kg. Described by HENDERSON and PERRY [37].

HENDERSON says (private communication): "There are definitely two sets of kamacite bands in this iron. The wider ones are independently oriented to the narrower ones. The wider ones swell and pinch and at their widest places they come to about 2 mm. At the narrowest places they are about 1·3 mm wide. The smaller bands are much more uniform in width and their sides are straight. I have found some that go up to about 0·3 mm but most of them are nearer to 0·2 mm." HENDERSON and PERRY originally classified this meteorite as Off, but HENDERSON now believes that it should be classified Of.

A few irregular inclusions of troilite surrounded by swathing kamacite may be seen, as well as a few small schreibersite bodies. The kamacite bands are bordered by tenous lamellae of taenite. Although in places the bands are closely grouped, plessite fields are relatively large and very abundant, and are mostly of the "dense" type, consisting mostly of imperfectly transformed gamma-alpha aggregate. A few plessite fields show spheroidized taenite in a ground mass of clear kamacite. The nickel content as determined by HENDERSON [37] agrees well with that reported in this paper.

19. Goose Lake—Found in 1938 near Goose Lake in northern Modoc County, California, U.S.A. (41°59′ N, 120°33′ W). Total weight 1167 kg. There is no detailed description of the structure of this meteorite. LEONARD [39] stated that it is a medium to coarse octahedrite. HENDERSON (private communication) says: "The Goose Lake meteorite is a coarse octahedrite. The kamacite bands present a remarkably symmetrical pattern on the etched slices of this iron, but there is some difference in their widths. A series of kamacite bands, selected at random, on one slice averaged 1·61 mm in thickness, while on another slice, an average of the same number of kamacite bands was found to be 1·51 mm thick. Some of the longer kamacite bands extend for 5 cm in length, but the average is perhaps nearer 3 cm. Taenite is abundant both in lamellae and irregular form, mostly darkened by reason of imperfect transformation and often including needles of kamacite. Plessite fields are numerous and extremely varied in character, ranging from light to dense with kamacite inclusions of great variety."

20. Henbury—Craters and fragments were found in 1931 seven miles WSW of Henbury, Central Australia (24°34′ S, 133°10′ E). Total recovered weight about 681 kg. Described by ALDERMAN [39] and by SPENCER [40]. An etched section of the iron shows wellmarked *Widmanstätten* figures of the medium octahedrite type. Besides kamacite, taenite and plessite, there are a few minute specks of troilite. The kamacite bands, instead of being straight, are wavy and in places much curved and distorted. Examination of the plates shown in reference [40] indicate that the band-widths range from 0·5 to 1·5 mm, with most bands possessing a width of about 0·8–1·0 mm. *Neumann* lines are well developed in the kamacite. Nickel has been determined by ALDERMAN [39], who obtained 7·54 %, and by HEY [40], who obtained 7·26 %. Our values are somewhat higher—7·73 % being found by one person as the average of six determinations, and 7·59 % being found by another as the average of two determinations.

21. Hill City—Found about 1946–47 near Hill/City, Graham County, Kansas, U.S.A. (39°20′ N, 99°50′ W). Total weight 11·7 kg. Henderson (private communication) has observed the band-widths to be 0·36 mm, thus placing the meteorite in the Of class. Henderson has found 9·17 % nickel, which agrees well with our value of 9·32 %. There is no published description of this meteorite.

22. Horse Creek—Found by the Niningers in 1937, twenty miles north of Springfield, Baca County, Colorado, U.S.A. (37°35′ N, 102°46′ W). Total known weight 570 g. This meteorite was originally classed as a finest octahedrite, but reexamination by Perry [15] showed it to be an anomalous meteorite consisting of pure kamacite with phosphide lamellae. According to Perry [15], "the structure resembles that of a fine octahedrite, although the phosphide lamellae are much finer, much more numerous and closely spaced, and of extreme regularity. Some are fairly thick; but for the most part they are very tenuous, appearing even under high magnification as extremely fine and straight black lines. Minute phosphide needles and extremely fine particles are thickly disseminated in the angular interstices of the octahedral pattern, being most abundant in the centers of such fields and sparse or absent near the bounding phosphide lamellae. Although the meteorite resembles an octahedrite, its planes are not octahedral, as the phosphide is tetragonal, and because of the relation of its space lattice with that of iron, it would precipitate on other than octahedral planes. Owing to the brittleness of the phosphide, the mass breaks easily with a nearly perfect cleavage along the planes of the phosphide lamellae." Our analysis of the nickel content of this meteorite gives a value of 5·87 %. The residue insoluble in aqua regia is unusually high, being 6·1 %.

23. Huizopa—Found in 1907 in a ruin near Huizopa, 60 miles west of Temosachic, Chihuahua, Mexico. Total known weight 130 kg. Described by Nininger [42]. The metal is very compact and possesses numerous small nodules of troilite. Almost one-third of the bands are of typical plain kamacite, which under a glass appears silvery-gray, compact and homogeneous, except for certain thin wavy lines which traverse it at various angles. The remaining bands are quite different. In these the kamacite is made up of fine grains of irregular form and variously oriented so as to give this portion a highly lustrous sheen when viewed under a lens. The average width of the bands is 0·20 mm. In addition to the regular arrangement of taenite, there occur in greater or less abundance wavy sheets of this alloy crossing the octahedral structure in various directions and in varying frequency. In some instances these are so abundant as to almost completely obscure the pattern. Henderson (private communication) observes that there is a very large amount of plessite. Nininger states that the plessite fields are comparatively scare and, like the kamacite, the plessite is of two types—the granular type, and a dark-gray alloy which is frequently beset with minute plates of taenite. Schreibersite is notably scarce.

The nickel content reported in this paper agrees well with the determination of Hawley [42] who found 7·90 %.

24. Indian Valley—Found in Indian Valley Township, Floyd County, Virginia, U.S.A. (36°55′ N, 80°30′ W) in 1887. Total known weight 14·2 kg. Described by Kurz and Weinschenk [43], and by Perry [15]. This iron is prevailingly a "normal" hexahedrite in structure. Nevertheless it is marked in some places by scattered grains with a strong sheen, appearing like snowflakes. The nickel content, as determined by Eakins [43], of 5·56 % agrees well with that determined in this work.

25. La Grange—Found in 1860 near La Grange, Oldham County, Kentucky, U.S.A. (38°25′ N, 85°30′ W). Total weight 51 kg. Described by Smith [44], and by Cohen [16], who observed that the lamellae are long, straight, considerably compacted, and about 0·15 mm broad, thus placing the meteorite in the Off class. Henderson (private communication) says: "The kamacite bands in the specimen of La Grange that I reexamined vary considerably in thickness. There are many that are about the widths reported by Cohen, but there are others that average between 0·3 and 0·4 mm in width. This iron is peculiar." A peculiar fibrous appearance, and a somewhat silken, oriented luster are characteristic of the kamacite. The few small fields are filled with dark plessite which appears rich in tiny glistening, uniformly distributed spangles. Minor constituents appear to be scarce and of small size.

The nickel content as determined by Burger [16] is but slightly lower than that determined by us.

26. Leeds—Recognized by H. H. NININGER in 1931 in a group of magnetite samples. The samples bore the label "magnetite from Leeds, Quebec." The location of Leeds is (46°18′ N, 71°20′ W). Total known weight 1·5 kg. NININGER (private communication) has found that the kamacite band-widths average 1·2 mm, thus placing the mateorite in the Om class. NININGER adds: "I find a condition somewhat similar to that described in Clark County, namely, certain bands are definitely coarse or coarsest, while in most parts the bands are of medium width."

27. Linwood—Found in 1940 or 1941, approximately $1\frac{3}{4}$ miles south and $1\frac{1}{4}$ miles west of Linwood, Butler County, Nebraska, U.S.A. (41°26′ N, 96°58′ W). Total weight 46 kg. Described by HENDERSON and PERRY [45]. The meteorite is a coarsest octahedrite possessing kamacite bands which vary in width from 2 to 4 mm. In some places polyhedral masses nearly half an inch across are found. The kamacite shows abundant *Neumann* lines. The individual kamacite areas are not granulated, yet the general structure of the octahedral pattern gives the impression of being granulated. No taenite lamellae or plessite is visible. The most distinctive feature of the meteorite is the silicate inclusions. These are numerous, colored black with carbon, and of irregular shapes, usually elongated or sprangling, with dimensions up to 2 inches or more. There are some small or irregularly-shaped masses of iron apparently isolated within the silicate areas. The bulk of the silicate is olivine.

The nickel value found in this work is considerably higher than that determined by HENDERSON [45].

28. Maria Elena—This meteorite was presented to the United States National Museum in 1935. Little is known concerning the earlier history of the mass, other than it was found on the Chilean Desert at about (22°20′ S, 69°40′ W). Total weight 15·5 kg. Described by MEEN [46]. The iron is a fine octahedrite with kamacite grains ranging from 0·1 to 0·4 mm in thickness. The majority are about 0·2 mm. The taenite lamellae are moderately abundant and very thin. Plessite areas are small and inconspicuous. Troilite is sparingly present as a few small nodules, the diameters of which are less than 3 mm, and as a few thin, short blades. Schreibersite was not recognized. MEENS [46] determination of nickel is much lower than that reported in this work.

29. Mejillones—One of the well-known "Chilean Hexahedrites" which, although scattered over a large area, may well have come from a single fall. Two bodies have been found near the Bay of Mejillones, Atacama, Chile (23°7′ S, 70°30′ W). The first, found in 1875, was very large. The second, found in 1905, weighed 14·5 kg. The first mass was described by DAUBRÉE [47], and the second by MERRILL [48]. PERRY [15] classifies Mejillones as a nickel-poor ataxite, but states: "It is often a matter of judgment whether a given iron should be termed a hexahedrite or a nickel-poor ataxite." The iron is an aggregate of macrograins, averaging about a millimeter in size, with diversely oriented sheen giving, with ordinary etching, an appearance of glistening flakes. The iron is filled with minute phosphide particles.

The nickel content determined by WHITFIELD [48] agrees with our value.

30. Morito—This meteorite has been known at least since 1600. It originally lay at El Morito, Chihuahua, Mexico (27°53′ N, 105°40′ W). The weight is approximately 11·000 kg. The iron has been described by SMITH [49], and by BREZINA [19]. Two small pieces show straight, strongly bunched lamellae 0·9 mm thick (Om). Taenite is scarce, fields are absent, and kamacite is much spotted. H. H. NININGER (private communication) says: "My observations on the etching pattern do not agree with those of BREZINA. I do not find the lamellae 'strongly bunched' at all. On the contrary, the lattice is quite open and regular, and instead of the plessite fields being absent I counted no less than 72 in an area of 40 sq. cm. The plessite does not stand out conspicuously, being about the same color as the kamacite but it is normally abundant. It presents a rather monotonous repetition of the same pattern. The edges of the field are commonly combed and the entire field is traversed by numerous ribbons of taenite, sometimes entire but often broken.

"55 bands of kamacite were measured, totalling 71 mm, or an average of 1·3 mm, but two groups were found to depart from the rule. One of 5 measured only 4·5 mm and another of 10 measured 9·5 mm. All measurements included the intervening taenite."

The nickel content as determined by SMITH [49] is much lower than that determined by us.

31. Mount Joy—Found in 1887 in Mount Joy Township, Adams County, Pennsylvania, U.S.A. (39°47′ N, 77°13′ W). Total weight 383·5 kg. It is possible that Mount Joy, Pittsburgh,

and New Baltimore are from the same fall. The meteorite has been described by Howell [50], Brezina [19], Berwerth [51], and Perry [15]. Brezina classified the meteorite as a breccia-like hexahedrite. Berwerth stated: "The preparation of the faces for exhibition showed without question that Mount Joy belongs to the octahedral irons, and by its very coarse structure should be placed among the last of the octahedral irons classed as having coarsest lamellae. The general structure of Mount Joy is that of a coarse-grained mass, the coarse grains of which are intergrown and so elongated with a certain regularity in one direction that the grains have a relatively short rod-like shape. From this shape and the position of the grains arises an appearance of *Widmanstätten* figures that is plain to the eye on a large section."

Perry states, on the other hand, that Mount Joy is a typical granular hexahedrite.

Berwerth described the meteorite further. The grains on the etched surface show two characters. Along the section, the course of the *Neumann* lines is shown plainly. In another part of the mass, the *Neumann* lines show only very weakly. Troilite is present only in relatively small quantity in scattered nodules of medium size. The troilite is regularly surrounded by a coating of schreibersite. Schreibersite also appears in larger skeletonlike crystals in the iron grains. Graphite seems to be everywhere lacking.

The nickel content determined by us agrees well with that determined by Henderson [52].

32. Nativitas—A mass of 1316 kg was found on a mountain slope near Nativitas, Zaragoza District, Tlaxcala, Mexico (19°14′ N, 98°15′ W). Nininger [53] gave the date of find as 1907, but later [10] changed the date to 1904. He considers the mass as possibly being a part of the meteorite Santa Apolonia, referred to by Ward [54].

Etching brought out a pattern of uniform and very long straight plates of kamacite averaging less than 1 mm in width. The taenite sheets which separate the kamacite plates are of a brassy lustre and average 0·34 mm in thickness. Lawrencite was identified. The nickel content determined by us is considerably higher than that determined by Hawley [53].

33. Odessa—More than a ton of meteoritic iron has been recovered from the neighborhood of some small craters found in 1922, nine miles southwest of Odessa, Ector County, Texas, U.S.A. (31°50′ N, 102°30′ W). The metal has been described by Merrill [55]. The structure is octahedral and of coarse crystallization. The etched surface is dull and lusterless, and abundantly sprinkled with small, angular areas of schreibersite. As the light is reflected from the etched surface at varying angles, the interior field gives the effect of having been cut parallel with the broad kamacite plates, while in the outer marginal portion they are cut more nearly at right angles. The suggestion is that of an intergrowth of two portions of unlike orientation. Taenite plates are thin and inconspicuous, as are plessite areas. Our nickel value for partial (HCl) dissolution agrees with the value of Shannon [55]. The value obtained by total dissolution is somewhat higher, possibly due to the presence of schreibersite.

34. Perryville—Found in 1906 near Perryville, Perry County, Missouri (37°40′ N, 89°50′ W). Total weight 17·5 kg. Described by Merrill [56], who classified the meteorite as a finest octahedrite—indeed so fine as to be almost microscopic. However, both Perry and Henderson (private communication) regard this meteorite as being an ataxite. Perryville, Chihuahua City and Horse Creek comprise a group of three meteorites possessing a most peculiar structure.

The nickel content as determined by Whitfield [56] agrees well with that determined by us using total dissolution.

35. Piñon—Found in 1928 or 1930, east of the Sacramento Mountains, in Township 198,, Range 18E, Section 22, Otero County, New Mexico, U.S.A. (32°40′ N, 105°6 W). Total weight 17·85 kg. Described by Nininger [57]. No lines or lamellae develop on etching; thus the meteorite is an ataxite. Microscopic examination of the etched surface revealed an abundant distribution of schreibersite in the form of needle-like crystals. Hawleys [57] determination of nickel agrees well with the value reported in this paper.

36. Puente del Zacate—A mass of 30·7 kg in the Museum of the Institute of Geology in Mexico, labelled Puente del Zacate, was described by Nininger [53] and found to be distinct from Coahuila. As Puente del Zacate is the location given for the Coahuila hexahedrites, there may have been an interchange of specimens or labels. Nininger [10] gives the location of the find as Morclova District, Coahuila, Mexico (28°42′ N, 102°51′ W), and the time as 1904. The iron appears to be distinct from Nativitas in several respects.

The crystallization of the meteorite varies from fine to medium. The regular kamacite bands measure for the most part about 1 mm in width, though some are narrower and a few

are wider. The widest measured were 1·6 mm. The general course of the bands is straight, with barely perceptible bendings, and the edges of the bands are undulating. Most of the roilite nodules encountered were compact and homogenous in structure, and show a very clean-cut line or separation between the troilite and the surrounding metal, with no intervention of schreibersite or carbonaceous matter.

Our value for the nickel content is considerably higher than that determined by HAWLEY [53].

37. Sacramento Mountains—Found in 1896 in the lower foothills of the Sacramento Mountains, Eddy County, New Mexico, U.S.A. (32°55′ N, 104°40′ W). Weight 237 kg. Described by FOOTE [58]. The meteorite is a medium octahedrite whose *Widmanstätten* figures are exceptionally regular and distinct. The nickel content determined by WHITFIELD [58] is somewhat lower than the value determined by us.

38. Sanderson—Found in 1936 near Sanderson, Terrell County, Texas (30°9′ N, 102°24′ W). Total weight 6·8 kg. This is an undescribed meteorite, but NININGER (private communication) has determined the kamacite band-widths and has found them to average 0·57 mm. This places the meteorite in the Om class.

39. Sandia Mountains—Found in 1925 in the Sandia Mountains, near Albuquerque, New Mexico, U.S.A. (35°0′ N, 106°40′ W). Total known weight 15 kg. Described by NININGER [59], who classified it a hexahedrite. PERRY [15] calls the meteorite a granular hexahedrite, stating: "This iron is transitional between hexahedrites and octahedrites, and, like a number of similar irons, has been classed by some as a coarsest octahedrite. In as much as the composition and microstructure are typical of hexahedrites, and no clear octahedral pattern is recognizable, the author would class it a hexahedrite."

Good agreement exists between HENDERSONS [52] determination of the nickel content and ours.

40. Sierra Gorda—One of the "Chilean Hexahedrites." This mass, which weighed 22 kg, was found in 1898 at 22 °53′ S, 69°18′ W. The only published data on this meteorite is that given by HENDERSON [33]. His nickel value agrees well with that reported in this paper.

41. Spearman—Found by H. H. NININGER near Spearman, Hansford County, Texas, U.S.A. (36°15′ N, 101°13′ W), in 1934. Total known weight 10·4 kg. This meteorite has not been described, but it has been listed by BARNES [59] as a medium octahedrite. E. P. HENDERSON (private communication) says: "We have a slice of this iron and the kamacite bands average 1·25 mm in width."

42. Tazewell—Found in 1853 about 10 miles west of Tazewell, Claiborne County, Tennessee, U.S.A. (36°26′ N, 83°34′ W). Total weight 27 kg. Investigations of this meteorite have been reviewed by FARRINGTON [13]. The meteorite has been described by SMITH [60], BREZINA [14], COHEN [25], and others. The meteorite is poor in kamacite, not in consequence of the small number of bands, but because of their narrow width (0·05–0·1 mm). The fields predominate in a considerable degree and show varied formation. One portion consists of dense and very dark plessite, and appears to be identical with the kamacite of the bands. Another portion of the fields appears bright and is composed of an intimate mingling of dense kamacite and numerous small, uniformly distributed leaves of taenite. In many places both sorts of plessite are represented by very nearly equal areas of considerable extent; in other places one sort predominates. Troilite and schreibersite inclusions have been found as well as very small particles of olivine and lawrencite.

The nickel content determined by us is higher than that determined by SMITH [60].

43. Willow Creek—Found about 1914 in Section 11, Township 40, R 83, near Willow Creek, Natrona County, Wyoming, U.S.A. (43°28′ N, 106°46′ W), and recognized as a meteorite in 1934. Total known weight 51·2 kg. Described by NININGER [61].

The iron is a medium octahedrite. The kamacite plates are, for the most part, 1·5 mm in width, but they are quite variable, and some were measured which were only 0·2 mm. In length they range all the way from less than a millimeter to as much as 30 mm. There are occasional broader, wavy bands of swathing kamacite. Many of the small nodules of troilite are surrounded by it in widths of one to two millimeters. Internally, the kamacite plates are characterized by very strong *Neumann* lines. These are very abundant, and under a lens appear almost as conspicuous as do the *Widmanstätten* lines. Plessite fields are very abundant and of varying

shapes and sizes. For the most part, the plessite is of dull gray color. In places it develops a flaky appearance, and in others the fields are traversed in part by narrow, strongly developed bands.

44. Xiquipilco—This meteorite, which was known before 1776, is commonly called Toluca, but, as Nininger [10] points out, its correct name should be Xiquipilco. Many masses have been recovered, totalling at least 18000 kg. Xiquipilco (now Jiquipilco) is located in Mexico State, Mexico, at about (19°24′ N, 99°44′ W). The many studies made on this iron have been summarized by Farrington [13]. Brezina [14] described a section of the iron, stating: "The Toluca iron shows lamellae 0·9 mm in breadth and frequently has very numerous large troilite inclusions with or without graphite with which the scaly troilite sometimes alternates. Schreibersite, especially in the vicinity of the troilite, is often well but irregularly developed." Cohen and Weinshenk [62] found that the taenite forms fine, isolated, very thin foliae between 0·03 and 0·25 mm in thickness. The latter authors undertook an extensive investigation of a 300 g specimen.

The nickel content determined by us is higher than that determined by Manteuffel and reported by Cohen [63].

45. Undescribed—A fragment of this meteorite, which has not as yet been named or described, was received from Professor L. La Paz of the University of New Mexico, who stated that it is a medium to fine octahedrite. It was given to us with the code number I.M. No. 2.

IV. Results and Correlations

The concentrations of nickel, cobalt, gallium, palladium and gold in the 45 meteorites studied are given in Table 6. Before we analyze the results, however, it is important that the significance of the data be ascertained by studying the variations in concentration of the elements with which we are concerned in individual meteorites.

Uniformity of Individual Iron Meteorites

It is frequently stated in the literature that individual iron meteorites may vary greatly in composition, and it is often pointed out in this connection that the nickel content of Canyon Diablo varies from as little as 1% to as much as 8%. If this should be true in general, then relatively small differences in composition between various meteorites would have little significance. Our studies, however, make it appear that the *metal phase* of an individual iron meteorite possesses a composition which is quite uniform.

The composition which one obtains for an iron meteorite will depend upon the method of sampling. If the sample size is small compared with the size of the kamacite and taenite lamellae, then the nickel content will vary considerably, due to the widely differing nickel contents of the two alloys. On the other hand, if the sample size is too large, it becomes difficult to avoid troilite, schreibersite and cohenite inclusions, the presence of which will give variable results. In view of this, we have attempted wherever possible to take samples for analysis which were sufficiently small to avoid major interference by inclusions, and yet which were sufficiently large and of such a shape as to give a fairly typical cross-section of the meteorite as a whole. In general, the sample sizes used were 200 to 300 mg in weight, and wherever possible the thickness was considerably less than the length or breadth. For example, a typical sample might have possessed the dimensions 1 mm × 5 mm × 6 mm. With such small samples one would, of course, expect to observe some variations in composition, but we found such variations to be much smaller than have been heretofore claimed.

Table 7 shows the individual results of a large number of nickel, gallium, palladium and gold determinations on each of four meteorites. It can be seen that the differences between the highest and lowest values are not large even in the cases of the two meteorites of coarse structure, Canyon Diablo and Odessa. It must be remembered also that a part of the variation shown in Table 7 is due to experimental error.

In the case of Canyon Diablo, the measurements were made on a variety of specimens which had come into our possession. In order to ascertain whether or not compositional differences exist between samples of Canyon Diablo whose locations of find are widely separated geographically, the nickel contents were determined on three small specimens of known and widely separated points of find. The specimens were located in the field with the kind help of Prof. L. La Paz and Mr. T. Johnson at the following locations near Meteor Crater: $\frac{1}{2}$ mile northeast of the rim, 1 mile northwest of the rim, and $2\frac{1}{2}$ miles northwest of the rim. The nickel contents of the specimens are shown in Table 8, and compared with the average of 11 nickel determinations on diverse samples of Canyon Diablo of unknown origin. It can be seen that the variations existing in these widely separated specimens are small.

Further tests of the variations in composition of individual meteorites were made on Henbury and Xiquipilco. The compositions of two individual specimens of each meteorite, obtained from different sources, were determined with results shown in Table 9. It can be seen that the differences in composition are in general not large.

The results presented above indicate strongly that individual iron meteorites, irrespective of size, possess compositions which are remarkably uniform throughout the metallic parts of their masses. Of the 45 meteorites studied by us, representing a cross-section containing about 8% of the total known number of iron meteorites, no case was found where major differences in composition exist within the metal phase of a given meteorite on a 200–300 mg scale. This result makes a further observation appear all the more interesting: With the exception of the hexahedrites and nickel-poor ataxites, which differ from one another only slightly in composition, only three pairs of meteorites were found to possess nearly identical compositions. Although the metal phase of a given iron meteorite appears to be chemically uniform throughout, each iron meteorite of the octahedral class in general appears to differ significantly from the others.

Gallium Groups

Figure 1 shows the gallium contents of the meteorites studied plotted on a logarithmic scale against the nickel concentrations. Inspection of the figure shows that the gallium levels are concentrated in three well-separated regions:

Region I	45–100 ppm
Region II	17–22 ppm
Region III	1·7–2·5 ppm

Only five of the meteorites studied were found to possess gallium contents lying outside of these rather narrow limits.

It is surprising that gallium concentrations should be "quantized" in this manner, particularly as no past evidence, based on a study of nickel contents or structure,

Ta-

Meteorite	*Class*	*Band Width*	*Nickel Content %*			
			*This Work**		*Previous*	
		mm	*A*	*B*	*C*	*Ref.*
1 Albuquerque	Om	0·6–1·1	7·41	7·37	8·51	[9]
2 Altonah	Of	0·36	8·45	8·64		
3 Arispe	Ogg	3–4	6·57	6·97	7·04	[11]
4 Bear Creek	Om	0·5	10·26	10·02	14·06	[17]
5 Bristol	Of	0·24	8·10	8·20		
6 Canyon Diablo	Og–Ogg	2·2	7·24	7·11	7·33	[23]
7 Canyon Diablo No. 2	Om	1·4	8·09	8·22	8·42	[20]
8 Cape of Good Hope	D	—	16·48		15·67	[16]
9 Carlton	Of	0·2	12·68		12·77	[24]
10 Cedartown	H	—		5·58	5·48	[26]
11 Chihuahua City	D	—	6·97	6·85	6·96	[27]
12 Chilkoot	Om	0·8	7·89		7·11	[28]
13 Clark County	Om	1·1	7·02			
14 Coahuila	H	—	5·61	5·65	5·59	[33]
15 Costilla Peak	Om	0·8–2	7·59	7·53	7·71	[34]
16 Deport	Og	1·5	8·40		7·97	[35]
17 Drum Mountains	Om	1			8·59	[36]
18 Edmonton	Of	0·25–2*	12·64	12·68	12·57	[37]
19 Goose Lake	Om–Og	1·6	8·44	8·48		
20 Henbury	Om	0·8–1·0	7·73	7·59	7·23	[40]
21 Hill City	Of	0·36	9·32		9·17	[41]
22 Horse Creek	D	—		5·87		
23 Huizopa	Of	0·2	7·76	7·87	7·90	[42]
24 Indian Valley	H	—	5·72	5·56	5·56	[43]
25 La Grange	Off	0·15	7·71		7·61	[16]
26 Leeds	Om	1·2	8·08			
27 Linwood	Ogg	2–4		6·64	5·98	[45]
28 Maria Elena	Of	0·1 -0·4	7·66	7·76	4·76	[46]
29 Mejillones	D	—	5·67		5·	[48]
30 Morito	Om	1·3	7·70	7·67	4·22	[49]
31 Mount Joy	H	—	5·68	5·65	5·79	[50]
32 Nativitas	Om	<1·0	7·83		7·39	[51]
33 Odessa	Og–Ogg	2·2	7·24	7·55	7·25	[55]
34 Perryville	D	—	8·12	9·63	9·66	[56]
35 Piñon	D	—	16·58		16·32	[57]
36 Puente del Zacate	Om	1·0	8·21		7·65	[53]
37 Sacramento Mountains	Om		8·17	8·03	7·86	[58]
38 Sanderson	Om	0·57	9·15	9·27		
39 Sandia Mountains	H	—	5·94	5·94	5·92	[52]
40 Sierra Gorda	H	—	5·61	5·56	5·58	[33]
41 Spearman	Om	1·25	8·00	8·78		
42 Tazewell	Off	0·05–0·1	16·69	17·5	14·82	[60]
43 Willow Creek	Om	1·5	8·75			
44 Xiquipilco	Om	0·9	8·31		7·54	[63]
45 Undescribed	Om–Of		8·03			

* See discussion of this meteorite in section III.

ble 6

Cobalt Content %			*Gallium*		*Palladium*		*Gold*	
This Work	*Previous*							
B	*C*	*Ref.*	*ppm*		*ppm*		*ppm*	
0·53	0·90	[9]	86·8	4	4·46	5	2·10	3
0·44			2·31	4	4·45	3	1·53	3
0·49			55·6	4	2·69	4	1·07	5
0·67	0·83	[17]	17·5	3	5·57	3	2·54	2
0·49			2·41	3	4·36	3	1·26	3
0·50	0·51		76·3	14	3·98	10	2·08	10
			85·6	5	5·30	3	1·58	3
	0·95	[16]	0·43	3	7·07	4	0·094	3
	0·63	[24]	13·0	5	6·52	4	2·06	3
0·53	0·22	[26]	63·2	3	1·65	4	0·715	3
0·49	0·40	[27]	46·3	3	2·52	3	1·00	3
	0·12	[28]	18·2	3	3·01	3	1·19	3
			7·36	3	2·37	4	0·452	2
0·53	0·78	[33]	64·5	3	1·44	3	0·743	3
0·54	0·44	[34]	19·7	3	2·02	3	0·586	3
0·53	0·41	[35]	61·8	8	4·45	3	2·04	3
	0·58	[36]	21·0	3	3·23	3	1·04	4
0·73	0·79	[37]	24·7	3	5·97	3	1·71	3
0·69			75·1	3	3·34	3	1·83	4
0·70	0·22	[40]	17·2	14	2·02	10	0·548	10
	0·46	[41]	2·35	3	6·23	3	2·32	3
			47·2	3	2·45	3	1·26	2
0·67	0·37	[42]	2·49	4	4·20	3	0·910	3
0·50	0·53	[43]	62·9	4	1·54	3	0·715	3
	0·62	[16]	2·11	5	3·95	3	1·23	3
			75·7	3	4·38	3	1·88	4
0·50	0·39	[45]	96·3	3	3·52	3	1·53	3
0·53	0·13	[46]	1·76	3	3·44	3	8·744	2
0·66		[48]	59·0	3	1·94	3	0·631	3
0·56	0·51	[49]	18·7	3	2·25	3	0·721	3
0·67	0·61	[50]	45·1	3	2·20	3	0·994	2
	0·51	[51]	20·8	2	2·29	4	0·606	3
0·49	0·74	[55]	69·3	10	4·15	10	1·97	10
0·68	0·55	[56]	37·9	3	3·07	3	0·903	3
0·87	0·67	[57]	2·39	4	9·88	3	0·815	5
0·63	0·54	[53]	17·2	2	2·57	3	0·945	3
0·55	0·52	[58]	20·4	3	2·34	3	0·685	3
			19·9	3	4·47	3	2·21	3
0·53	0·53	[52]	56·5	5	2·24	3	1·17	4
0·53	0·25	[33]	65·5	3	1·47	3	0·689	3
0·56			21·4	6	3·67	3	1·42	3
0·70	0·46	[60]	5·20	5	7·73	3	2·23	3
			19·5	5	3·70	3	1·33	3
0·53	0·66	[63]	55·2	14	4·72	10	1·81	12
			21·0	4	2·82	3	1·01	3

Table 7. Individual determinations of Ni, Ga, Pd and Au in four meteorites. Sample size: 200 mg. (The nickel content is in percent, all others on parts-per-million)

Canyon Diablo				*Odessa*				*Henbury*				*Xiquipilco*			
Ni	Ga	Pd	Au	Ni	Ga	Pd	Au	Ni	Ga	Pd	Au	Ni	Ga	Pd	Au
7·07	77·4	3·03	2·11	7·30	67·8	4·16	2·54	7·68	15·2	2·29	0·488	8·23	56·2	4·52	1·56
7·12	76·0	3·85	2·17	7·31	66·0	4·01	1·96	7·95	15·1	1·77	0·487	8·49	51·4	4·18	1·83
7·20	76·2	3·85	2·08	6·96	68·2	3·52	2·18	7·88	15·9	1·71	0·462	8·21	59·3	4·14	1·63
7·09	74·6	3·64	2·00	7·35	72·6	4·06	2·25	7·72	18·4	1·96	0·482		53·0	5·37	1·83
7·09	84·2	4·21	3·21		72·4	3·64	1·83	7·49	17·8	1·88	0·526		54·6	4·59	1·61
7·11	78·0	4·79	2·02		67·8	4·12	2·02	7·68	17·9	1·81	0·538		54·8	4·74	1·95
7·09	70·0	4·30	1·98		63·8	4·06	1·90		16·7	2·31	0·561		53·0	5·21	2·16
7·13	76·2	3·91	1·85		72·6	4·22	1·89		15·2	2·14	0·662		54·2	4·85	1·93
7·11	79·2	3·91	2·10		71·0	5·04	1·60		15·6	2·18	0·632		51·6	4·87	1·79
7·11	82·0	4·35	2·22		70·4	4·64	1·56		18·2	2·16	0·650		65·0	4·73	1·70
7·09	80·4								18·2				54·5		1·90
	76·8														1·81
	75·2														

Table 8. Nickel content of Canyon Diablo

Specimen	*Ni* %	*Number of Determinations*
1. Average of 11 diverse samples, location unknown .	7·11	11
2. Small fragment found 2½ miles NW of rim	7·20	2
3. Small fragment found ½ mile NE of rim	7·05	2
4. Small fragment found 1 mile NW of rim	7·06	2

Table 9. Comparison of compositions of specimens of Henbury and Xiquipilco obtained from different sources. (Nickel in percent, all others in parts-per-million. Number of determinations shown in parentheses)

	Ni	Ga	Pd	Au
		Henbury		
Source A	7·84 (3)	17·2 (14)	2·02 (10)	0·548 (10)
Source B	7·63 (3)	18·7 (3)	1·98 (3)	0·487 (1)
		Xiquipilco		
Source A	8·31 (3)	55·2 (14)	4·72 (10)	1·81 (12)
Source B		68·9 (2)	4·61 (3)	1·81 (2)

have indicated anything other than a continuum of meteorite types and compositions. In view of this, it is important that we investigate the meteorites within each gallium group for the purpose of determining whether any correlation with structure exists.

The meteorites belonging to gallium Class I possess nickel contents lower than 8·5%, and embrace all of the hexahedrites, nickel-poor ataxites and coarsest and coarse octahedrites. About 30% of the medium octahedrites belong to this class.

The low-nickel boundary for meteorites of Class I appears to lie in the neighborhood of 5·5%.

The meteorites of gallium Class II possess nickel contents greater than 7·5% and embrace 70% of the medium octahedrites, together with a few fine octahedrites of fairly high nickel content.

The meteorites of gallium Class III possess nickel contents greater than 7·5% and consist only of fine and finest octahedrites and nickel-rich ataxites.

The meteorites which possess nickel contents in the range of 7·5 to 8·5% are particularly interesting for they can belong to any of the three gallium classes.

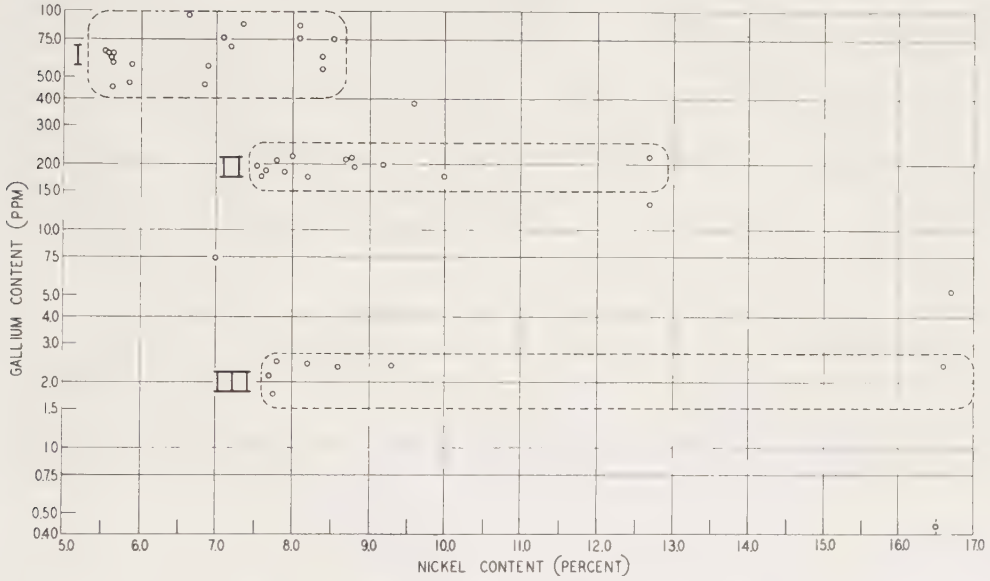

Fig. 1. Variation of gallium content of meteorites with nickel content.

A substantial fraction of the iron meteorites which are known possess nickel concentrations lying within this narrow range.

The general relationships between kamacite band-widths, nickel content and gallium content are shown in Figure 2, where nickel concentration is plotted against the band-width class in order of increasing coarseness. The gallium classes are found to lie within several fairly well-defined fields as shown in the figure. Meteorites lying in fields I, II, or III will with high probability possess gallium contents corresponding to gallium classes I. II or III respectively. On the other hand, a medium octahedrite possessing a nickel content of 7·5 to 8·5% might belong to either gallium Class I or to gallium Class II.

Palladium and Gold

The behavior of palladium and gold was found to be quite different from that of gallium. While the gallium concentration in general decreases with increasing nickel concentration and decreasing kamacite band-width, palladium and gold concentrations increase. In general hexahedrites possess the lowest palladium and gold concentrations and nickel-rich ataxites possess the highest.

Had it not been for the observations on the division of iron meteorites into the three gallium classes, a relationship between palladium and nickel and a similar

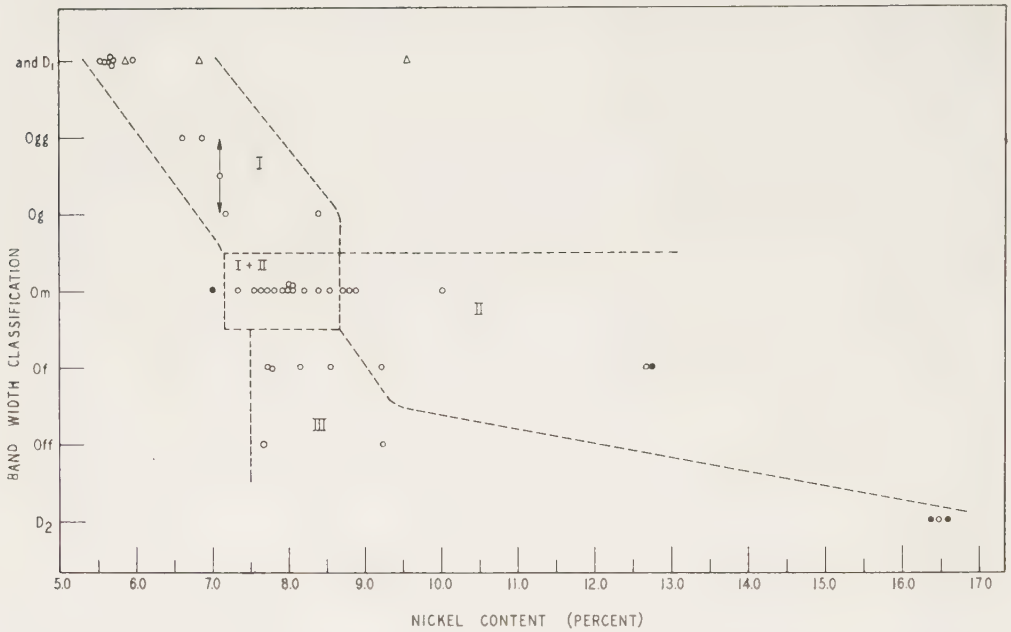

Fig. 2. Band width classification as a function of nickel content. The gallium groups lie in the fields designated I, II and III respectively. Meteorites which fit into gallium groupings are designated by open circles. Exceptions are designated by solid circles. The anomalous meteorites (Horse Creek, Chihuahua City and Perryville) are designated by triangles.

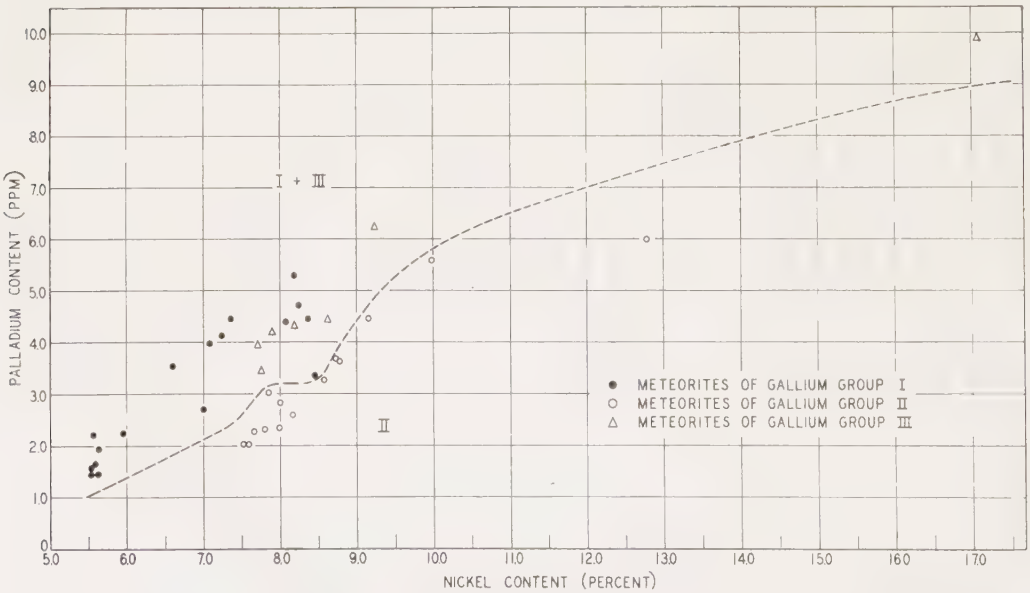

Fig. 3. Variation of palladium content of meteorites with nickel content. Note the separation between meteorites of gallium group II and the other gallium groups.

relationship between gold and nickel would have gone unnoticed: for a given nickel content, the meteorites belonging to gallium Class II possess lower palladium and gold contents than do the meteorites belonging to gallium Classes I and III. The palladium-nickel relationship is shown diagrammatically in Figure 3.

In general, palladium and gold increase with each other, but the relationship is not a smooth one. Here again dependence upon gallium Class is apparent. Meteorites of gallium Class I in general possess low palladium-gold ratios, meteorites of Class II possess intermediate ratios, and meteorites of Class III possess high ratios.

In general the ratios of palladium to gold lie in the range 1·8 to 4·6, but two nickel-rich ataxites possess unusually high ratios. Piñon possesses 9·88 ppm of palladium and 0·815 ppm of gold, giving a ratio of 12·1. Cape of Good Hope possesses 7·07 ppm of palladium and only 0·094 ppm of gold, giving a ratio of 75.

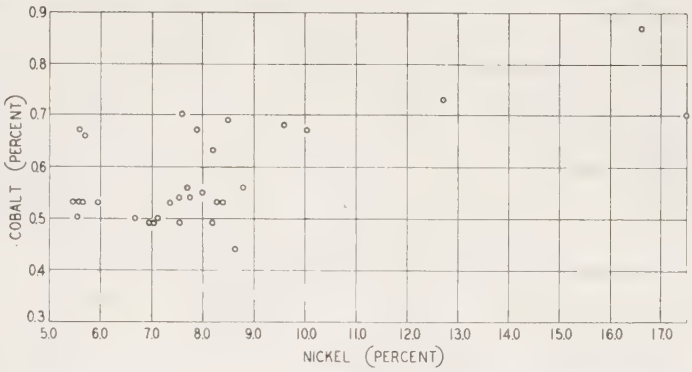

Fig. 4. Variation of cobalt content of meteorites with nickel content.

Cobalt

The most notable feature of the distribution of cobalt in iron meteorites is the small dependence of the cobalt level upon nickel content. The distribution of cobalt as a function of nickel content is shown in Figure 4. Inspection of the figure shows that cobalt values tend to concentrate around two levels, the first at about 0·53 %, and the second around 0·67 %. Only one meteorite was found to possess a cobalt concentration higher than 0·75 % (Pinon, a nickel-rich ataxite). Only one meteorite was found to possess a cobalt level lower than 0·47 % (Altonah, a fine octahedrite). There is no apparent correlation between cobalt distribution and the distribution of gallium, palladium and gold.

Hexahedrites and Nickel-Poor Ataxites

The chemical similarity of individual hexahedrites to each other and to nickel-poor ataxites is apparent from an inspection of Table 10. It has been stated previously by HENDERSON [33] that hexahedrites found in widely-separated regions

Table 10. Hexahedrites and nickel-poor ataxites

Name	Ni (%)	Co (%)	Ga *(ppm)*	Pd *(ppm)*	Au *(ppm)*
Sierra Gorda	5·56	0·53	65·5	1·47	0·689
Coahuila	5·65	0·53	64·5	1·44	0·743
Cedartown	5·58	0·53	63·2	1·65	0·715
Indian Valley	5·56	0·50	62·9	1·54	0·715
Mejillones	5·67	0·66	59·0	1·94	0·631
Sandia Mts.	5·94	0·53	56·5	2·24	1·17
Mount Joy	5·65	0·67	45·1	2·20	0·994

are frequently indistinguishable from each other on the basis of their nickel contents. This work supports that contention, and makes it appear further that individual hexahedrites and nickel-poor ataxites are frequently nearly identical with respect to their trace constituents.

It appears in addition that the anomalous ataxites (Chihuahua City, Horse Creek and Perryville) form a continuous series with ordinary hexahedrites and ataxites with respect to their trace element contents. Within this series, for example, palladium increases quite uniformly with decreasing gallium content, as is shown in Figure 5.

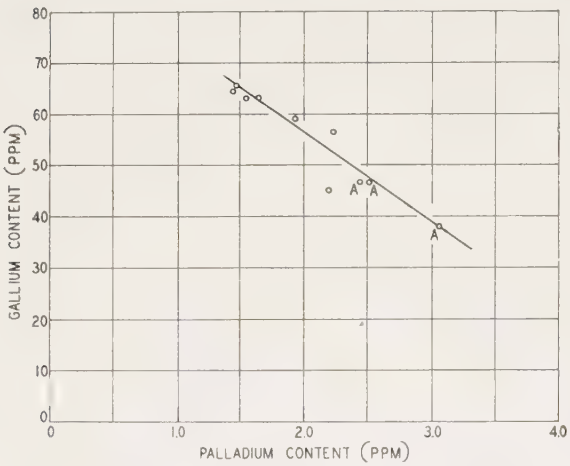

Fig. 5. Variation of gallium content of hexahedrites, ataxites and anomalous meteorites with palladium content. The symbol A designates the anomalous meteorites.

Troilite

Gallium was determined in samples of troilite obtained from Xiquipilco and Canyon Diablo. About 0·4 ppm were found in Canyon Diablo and 0·3 ppm were found in Xiquipilco. Clearly gallium favors the metallic phase over the sulfide phase with a concentration factor of the order of 150.

Pallasites

Gallium was determined in the metallic phase of two pallasites: Admire (Lyons County, Kansas, U.S.A.) and Springwater (Saskatchewan, Canada). The following concentrations were found:

Admire . . . . . 21·4 ppm Ga
Springwater . . . . . 17·9 ppm Ga

It is interesting and perhaps significant that these levels agree so well with the levels found in the iron meteorites belonging to gallium Class II.

Similarity of Canyon Diablo and Odessa

In our studies three pairs of meteorites outside the hexahedrite and ataxite classes were found to possess compositions and structures which are quite close to each other. The pairs are shown in Table 11. Of the three pairs, only one, Canyon

Table 11. Pairs of meteorites possessing similar compositions

Meteorite	*Class*	Ni (%)	Co (%)	Ga *(ppm)*	Pd *(ppm)*	Au *(ppm)*
Canyon Diablo .	Og	7·11	0·50	76·3	3·98	2·08
Odessa	Og	7·24	0·49	69·3	4·15	1·97
Henbury	Om	7·59	0·70	17·2	2·02	0·548
Costilla Peak . .	Om	7·53	0·54	19·7	2·02	0·586
Altonah	Of	8·45	0·44	2·31	4·45	1·53
Bristol	Of	8·10	0·49	2·41	4·36	1·26

Diablo-Odessa, is made up of meteorites which lie close to each other geographically. The Odessa craters lie about 600 miles east-southeast of Meteor Crater, Arizona (actually 3°20′ S and 8°37′ E).

Henderson, in a paper on the distribution of cohenite soon to be published, has pointed out the striking structural similarities of Canyon Diablo and Odessa and has independently reached the conclusion that these two meteorites, together with Wichita County, might be fragments from the same fall.

Any conclusion, however, as to whether or not Canyon Diablo and Odessa are in reality fragments of the same fall must await further studies.

Canyon Diablo No. 2

The interesting fragments from the vicinity of Meteor Crater which were discovered by Nininger and which he calls Canyon Diablo No. 2 have been studied carefully in an attempt to ascertain whether or not the fragments are really distinct from ordinary Canyon Diablo fragments. The two meteorites are compared in Table 12. Both meteorites belong to gallium Class I, but it seems clear that the

Table 12. Comparison of Canyon Diablo No. 1 and Canyon Diablo No. 2

	Class	Ni (%)	Co (%)	Ga *(ppm)*	Pd *(ppm)*	Au *(ppm)*
Canyon Diablo No. 1	Og	7·11	0·50	76·3	3·98	2·08
Canyon Diablo No. 2	Om	8·09		85·6	5·30	1·58

nickel content and palladium content in No. 2 are decidedly higher than in No. 1. One must conclude that either (a) Canyon Diablo No. 2 is a distinct fall (which is not impossible considering the thoroughness with which the area has been searched) or (b) fluctuations in composition of major consequence exist in Canyon Diablo. In view of the results of our studies, the latter possibility, although possible, appears improbable.

V. Summary and Conclusions

It is apparent that with few exceptions iron meteorites can be divided into three main classes which for convenience we can designate as Class I, Class II and Class III. The three classes are based on the major differences which exist between the gallium contents of the meteorites in each class, but marked differences exist also in their structures, and in the distribution of nickel, palladium and gold.

Inspection of Figure 2 shows that the determination of the kamacite bandwidths and the nickel content of a given meteorite are frequently sufficient to permit the assignment of the meteorite to one of the three classes. However, if the meteorite is a medium octahedrite possessing a nickel content in the range of 7·5% to 8·5%, the determination of one of the trace constituents is necessary in order to determine whether the meteorite properly belongs to Class I or to Class II.

Meteorites which possess nickel concentrations in the narrow range 7·5% to 8·5% are particularly interesting for they can belong to any one of the three classes. As these meteorites possess essentially the same nickel and cobalt contents, it is most interesting to inquire into the physical and chemical conditions which brought

about a division of these meteorites into three groups. Why did one meteorite containing 8% nickel take up only 2 ppm of Ga, while another possessing identical chemical composition with respect to major constituents took up 70 ppm?

A clue is offered by an inspection of the major differences between the meteorites of Class II and Class III. For a given nickel content a meteorite of Class III possesses a fine structure while one of Class II possesses a medium structure. It is well known that the development of structure in nickel-iron depends primarily upon (a) nickel content and (b) cooling rate. It would appear then that the "heat treatment" of the meteorites of Class III has been markedly different from that associated with Class II. When we consider that the meteorites of Class III possess trace element distributions differing markedly from those of Class II, we may conclude that the meteorites of Classes II and III were formed under physical and chemical conditions which differed considerably from each other.

Much experimental work must be done before the conditions which were associated with the formation of iron meteorites can be unravelled. Inspection of the data indicates that we are dealing with a very complicated situation. In particular, it is difficult to reconcile the data presented in this paper with the simple picture that meteorites had their origin in the breakup of a single small planet. On the other hand, it is difficult at this stage to say what alternate picture will account satisfactorily for the observations.

Acknowledgements—We would like to take this opportunity to express our thanks to Dr. E. P. Henderson and to Dr. H. H. Nininger for their help in carrying out this work. In particular we wish to express our gratitude for their help in describing the meteorites used in this work and for their determinations of kamacite band widths. We wish to thank also Mr. Stuart Perry, who was kind enough to read the manuscript and make constructive suggestions.

References

[1] Goldschmidt, V. M. and Peters, C.; Gesellschaft der Wissenschaften zu Göttingen, Math.-Phys. Kl. Fachgruppe III, 1931 (Nr. 10) p. 165. [2] Noddack, I. and W.; Naturwiss. 1930 **18** 757. [3] Goldschmidt, V. M. and Peters, C.; Gesellschaft der Wissenschaften zu Göttingen, Math.-Phys. Kl. Fachgruppe III, 1932 (Nr. 24) p. 377. [4] Noddack, I. and W.; Z. Phys. Chemie 1931 A **154** 207. [5] Henderson, E. P.; Amer. J. Sci. 1941 **239** 372. [6] Young, R. S. and Hall, A. J.; Ind. Eng. Chem. (Analyt. Ed.) 1946 **18** 262. [7] Brown, H. and Goldberg, E.; Science 1949 **109** 1. [8] Goldberg, E. and Brown, H.; Analyt. Chem. 1950 **22** 308. [9] Beck, C. W. and La Paz, L.; Pop. Astron. 1950 **18** 85. [10] Nininger, H. H. and A. D.; "The Nininger Collection of Meteorites," American Meteorite Museum, Winslow, Arizona, U.S.A. (1950). [11] Ward, H. A.; Proc. Rochester Acad. Sci. 1902 **4** 82. [12] Wuensch, A. F.; Colorado Sci. Soc. Proc. 1903 **7** 67. [13] Farrington, O. C.; Mem. Nat. Acad. Sci. 1915 **13**. [14] Brezina, A.; Jahrbuch K. K. Geologische Reichsanstalt 1885 **35** 151. [15] Perry, S. H.; The Metallography of Meteoric Iron, U.S. National Museum Bulletin 1944 No. 184. [16] Cohen, E.; Meteoritenkunde, Vol. 3 Stuttgart, 1905. [17] Smith, J. L.; Amer. J. Sci. (2)1867 **43** 66. [18] Meunier, S.; Revisions des Fers Meteorique (1893). [19] Brezina, A.; Ann. K. K. Naturhist. Hofmus. Wien 1895 **10** 231. [20] Nininger, H. H.; Pop. Astron. 1940 **48** 328. [21] Young, J.; Proc. Roy. Soc. Lond. 1926 A **112** 630; and Min. Mag. 1930 **22** 382. [22] Moissan, H.; Compt. Rend. 1893 **116** 288. [23] Merrill, G. P.; Amer. J. Sci. 1913 **35** 513. [24] Howell, E. E.; Proc. Rochester Acad. Sci. 1890 **1** 87. [25] Cohen, E.; Ann. K. K. Naturhist. Hofmus. Wien 1895 **10** 82. [26] Perry, S. H.; Smithsonian Misc. Collections 1946 **104** 3 No. 23. [27] Nininger, H. H.; Amer. J. Sci. 1931 **22** 360. [28] Ward, H. A.; Catalogue of the Ward-Coonley Collection of Meteorites (1900). [29] Brezina, A.; Sitzber. Wien Akad. 1881 **84** I 282. [30] Daubree, G. A.; Compt. Rend. 1881 **93** 555. [31] Huntington, A.; Proc. Amer. Acad. Arts and Sci. 1889 **24** 30; and 1889 **24** 313. [32] Smith,

S. W. J., Dee, A. A. and Young, J.; Proc. Roy. Soc. 1928 A **121** 477. [33] Henderson, E. P.; Amer. Mineralogist 1941 **26** 546. [34] Hills, R. C.: Proc. Colorado Sci. Soc. 1895 **5** 121. [35] Palache, C. and Gonyer, F. A.; Amer. Mineralogist 1932 **17** 357. [36] Henderson, E. P. and Perry, S. H.; Smithsonian Misc. Collections 1948 **110** No. 12. [37] Henderson, E. P. and Perry, S. H.; Smithsonian Misc. Collections 1947 **107** No. 13. [38] Leonard, F. C.; Pop. Astron. 1939 **47** 507. [39] Alderman, A. R.; Rec. South Austr. Mus. 1932 **4** 561. [40] Spencer, L. J.; Min. Mag. 1933 **23** 387. [41] Henderson, E. P.; private communication. [42] Nininger, H. H.; The Mines Magazine, Golden, Colorado 1932 **22** 11. [43] Kunz, G. F. and Weinschenk, E.; Amer. J. Sci. 1892 (3) **43** 424. [44] Smith, J. L.; Amer. J. Sci. 1861 (2) **31** 265). [45] Henderson, E. P. and Perry, S. H.; Proc. U.S. National Museum 1949 **99** 357. [46] Meen, V. B.; Amer. Mineralogist 1938 **23** 661. [47] Daubree, G. A.; Compt. Rend. **1875 81** 597. [48] Merrill, G. P.; Proc. Nat. Acad. Sci. U.S.A. 1924 **10** 309. [49] Smith, J. L.; Amer. J. Sci. 1871 (3) **2** 336. [50] Howell, E. E.; Amer. J. Sci. 1892 (3) **44** 415. [51] Berwerth, F.; Ann. K. K. Naturhist. Hofmus. Wien 1897 **12** 56. [52] Henderson, E. P.; Amer. J. Sci. 1941 **239** 407. [53] Nininger, H. H.; Proc. Colorado Mus. Nat. Hist. 1931 **10** No. 1. [54] Ward, H. A.; Catalogue of the Ward-Coonley Collection of Meteorites (1904). [55] Merrill, G. P.; Amer. J. Sci. 1922 (5) **3** 335. [56] Merrill, G. P.; Proc. U.S. National Museum 1912 **43** 595. [57] Nininger, H. H.; Pop. Astron. 1939 **47** 155. [58] Foote, W. M. Amer. J. Sci. 1897 (4) **3** 65. [59] Barnes, V.; Univ. of Texas Publication 2945 (June 1940). [60] Smith, J. L.; Amer. J. Sci. 1855 (3) **19** 153. [61] Nininger, H. H.; The Mines Magazine, Golden, Colorado, 1937 **27** 16. [62] Cohen, E. and Weinschenk, E.; Ann. K. K. Naturhist. Hofmus. Wien 1891 **6** 135. [63] Cohen, E.; Ann. K. K. Naturhist. Hofmus. Wien 1892 **7** 157.

Geochimica et Cosmochimica Acta, 1951, Vol. 2. pp. 26 to 42. Pergamon Press Ltd., London

The isotope geology of oxygen*

Sol R. Silverman**

Department of Geology and the Institute for Nuclear Studies, University of Chicago

(Received 22 June 1951)

ABSTRACT

Natural silicates vary in their O^{18}/O^{16} ratios by as much as 2·4%. This difference is largely due to an exchange reaction between silica and water during the processes of erosion and sedimentation, as a result of which sedimentary rocks are richer in O^{18} than are the igneous rocks. The temperature coefficient for the silica-water exchange has been estimated to be $-0{\cdot}128‰$ per degree Centigrade.

The O^{18} content of basic igneous rocks is low and confined to a narrow range (6·4 to 7·0‰). The alkalic and granitic igneous rocks are richer in O^{18}, and their isotopic ratios are more variable (7·7 to 12·2‰). In granitic rocks, quartz shows a greater preference for O^{18} than does orthoclase; the distribution coefficient is 1·20 in favor of the quartz.

The isotopic constitution of stony meteorites is identical to that of the basic igneous rocks, but tektites resemble the sedimentary rocks in their isotopic composition. The analysis of a granophyre-gabbro sequence revealed an isotopic gradient which suggests solid diffusion as the mode of origin for the intermediate rock. The mechanism of metamorphism has been studied from the standpoint of isotopic composition. The results are not conclusive, but suggest that metamorphism is associated with a depletion of O^{18}.

Introduction

The existence of measurable variations in the isotopic composition of the silicate oxygen of the lithosphere, and the significance of these differences have already been suggested [1], [2]. The purpose of this paper is to consider these variations and their implications in the light of current knowledge of isotopic phenomena.

The dependence of the energy, and consequently all thermodynamic properties, of vibrating and rotating molecules upon the masses of their constituent atoms [3], [4], [5] is responsible for the slight differences in the properties of isotopic substances. The validity of these fundamental principles have been assured by the success with which they have been used to predict the experimental results of isotope separations, isotopic exchange reactions, and isotopic reaction rates in the laboratory. The application of these principles, wherever possible, may serve to reveal the chemical and physical processes responsible for the distribution of oxygen isotopes in nature.

Oxygen is the most important element from a geochemical standpoint since it comprises about 46% of the lithosphere, 86% of the hydrosphere, and 23% by weight of the atmosphere. The relative abundances of oxygen isotopes in the hydrosphere [6], [7], [8] and in the atmosphere [9], [10], [11] have already been determined. The less accessible oxygen combined in the rocks of the lithosphere remains a relatively unexplored field.

Variations in the oxygen isotopic composition of limestones have been utilized in the determination of the temperatures at which these sediments have been deposited [8], [12], [13], [14]. The oxygen isotopic composition of some iron ores [15].

* The work described in this paper forms part of a dissertation submitted to the Faculty of the Division of the Physical Sciences of the University of Chicago in partial fulfillment of the requirements for the degree of Doctor of Philosophy.

** Present address: United States Geological Survey, Washington, D. C.

[16] and of the water contained in certain metamorphic rocks and minerals [17] have also been investigated.

TOKUDA and KASHIDA [18] measured the oxygen isotope abundances in silicates by treating the samples with potassium acid fluoride at 230° C, and the water formed by this reaction was purified in "an appropriate way" and its density compared with that of Osaka tap water. The sensitivity of this method in terms of the O^{18}/O^{16} ratio was reported to be about $\pm 1{\cdot}4‰$ ($\pm 0{\cdot}3$ ppm in density units), yet the authors state that they were unable to find any difference between igneous and metamorphic rocks. The slight differences reported by TOKUDA and KASHIDA are significant, but the absence of large differences may have been due to inherent purification difficulties in the density method for isotopic analyses and in some cases due to incomplete oxygen yields.

The oxygen separated from silicates by reaction with chlorine trifluoride and hydrogen fluoride [1], [2] have yielded O^{18}/O^{16} ratios reliable to $\pm 3{\cdot}0‰$. The isotopic abundances reported in this paper have been obtained from oxygen liberated by fluorine and hydrogen fluoride [2]. The average deviations in O^{18}/O^{16} ratios for duplicate measurements by this method were less than $0{\cdot}5‰$ for over 70% of the samples analyzed, and in only one case was the average deviation greater than $1{\cdot}0‰$.

TERRESTRIAL ABUNDANCES

The relative abundances of the three stable isotopes of oxygen, $O^{16}:O^{17}:O^{18}$, in air have been reported by NIER [19] as $2670 \pm 20:1:5{\cdot}5 \pm 0{\cdot}1$. The results of previous relative abundance measurements of the oxygen isotopes in nature have been compiled by THODE [20] and by BAINBRIDGE and NIER [21]. THODE's compilation, which denotes variations in O^{18} abundances ranging as high as 4%, is reproduced here as Table 1.

*Table 1. Distribution of O^{18} in nature**

Source	*Relative abundance of O^{18}*
Water:	
Fresh water, Lake Ontario	1·00
Ocean water	1·009
Atmospheric water vapor over Lake Ontario	0·991
Glacier water, Lake Louise	0·977
Dead Sea water	1·020
Air:	
Atmospheric oxygen	1·033
Atmospheric carbon dioxide	1·040
Photosynthetic oxygen	1·006
Rocks:	
Limestone	1·039
Cuprite	1·00
Swedish magnetite	1·00
Iron ores	1·00

* From THODE, H. G.; Research 1949 **2** 157.

The differences in O^{18} abundances given in Table 1 are encouraging because they are readily explained by theoretical principles. For example, it should be expected that the process of evaporation be accompanied by depletion of the heavy isotope in the vapor phase since the vibrational energy of a molecule is inversely proportional to the square root of its reduced mass. In other words, water molecules containing only the light isotope (O^{16}) should have a higher vapor pressure than water molecules containing the heavy isotope (O^{18}). Accordingly, fresh water is depleted in O^{18}

(Table 1) relative to ocean water. The same relation applies to water vapor derived from fresh water, as evidenced by a decrease of $9^0/_{00}$ in the O^{18} abundance of water vapor over Lake Ontario as compared to that of Lake Ontario water. The high concentration of O^{18} in Dead Sea water represents the anticipated enrichment of the heavy isotope in a residual liquid after loss of the O^{16}-rich water by evaporation. The water formed by the melting of glacial ice is $23^0/_{00}$ lower in O^{18} than fresh water. This is in agreement with the concept that isotopic fractionation could occur during the

Table 2. Oxygen isotopic composition in silicate rocks†

Sample and Number	O^{18}/O^{16} $^0/_{00}$	*Average Deviation* $^0/_{00}$	*Number of Determinations*
Chicago tap water	−3·2	—	1
Hawaii sea water No. RT–6	0·0	0·2	2
Columbia River basalt No. 79–PG–5	6·4	0·2	3
Disco basalt No. R–7696	6·6	0·7	3
Mt. Etna lava No. B–1–74	6·7	0·2	4
Dunite No. 25	6·8	0·5	2
Olivine basalt No. 1	7·0	0·1	3
Yellowstone obsidian No. 47	7·7	0·8	2
Gneissic granite No. 4	7·9	0·2	2
Nepheline syenite No. 14	8·3	0·0	2
Parícutin lava No. K–12	8·5	0·2	4
Cheshire orthoquartzite No. 410	10·2	0·0	3
St. Peter sandstone No. 46	10·9	0·2	2
Arkose No. 2698	11·4	0·5	2
Basal breccia No. 45	13·2	0·3	2
Quartz vein No. 89	14·0	0·2	4
Brazil quartz No. 26	14·0	0·2	2
Grafton orthoquartzite No. 778	14·7	0·3	2
Wishart orthoquartzite No. F–75	15·1	1·4	2
Potsdam sandstone No. 2039	15·5	0·0	2
Maquoketa shale No. 9	15·5	0·5	2
Atmospheric oxygen	19·2	0·9	2
Dover flint No. 2	29·3	0·5	2
Diatomite No. 13	30·3	0·0	2

† Sources and other information pertaining to these samples are listed in the appendix.

fusion of ice, in which case the O^{16}-rich water molecules, being the most energetic of the possible isotopic combinations, would be prevalent in the early fractions of the liquid phase.

The relative abundances of the oxygen isotopes in igneous, sedimentary, and metamorphic rocks, determined by mass spectrometric analysis of the oxygen liberated by the fluorine method [2], are listed in the order of increasing O^{18}/O^{16} ratio in Table 2. The values are given as deviations of the O^{18}/O^{16} ratio, in parts per thousand ($^0/_{00}$), from the same ratio in an arbitrary standard*. The results were adjusted to the Hawaii sea water value which was arbitrarily set equal to zero. On this scale

* The standard used in all analyses was the oxygen derived from pure quartz (Randville pegmatite, No. 10).

Chicago tap water has an abundance of $-3{\cdot}2\,^0/_{00}$, which supports our earlier contention that the cycle of evaporation and precipitation should deplete the heavy isotope in fresh water relative to sea water.

The analyses in Table 2 indicate that sediments are consistently higher in O^{18} than are the igneous rocks. This implies that the deposition of silica from solution is accompanied by enrichment of the heavy isotope in the precipitated phase. In accord with this conclusion, diatomaceous deposits (diatomite, No. 13), composed entirely of silica precipitated from solution, have the highest abundance of O^{18}. From the O^{18}/O^{16} ratios in sea water and diatomite, the equilibrium constant for the exchange reaction:

$$Si O_2^{16} + H_2O^{18} \rightarrow Si O^{16}O^{18} + H_2O^{16}$$

may be estimated to be 1·03 at the specific temperature of this precipitation. The equally high abundance of O^{18} in Dover flint (No. 2) implies that this material is

Table 3. Relation of isotope abundances in siliceous sediments to amount of authigenic silica

Sample	O^{18}/O^{16} $^0/_{00}$	*Per Cent Secondary Silica*	*Per Cent Increase in* O^{18}/O^{16} *Ratio Difference*
St. Peter sandstone No. 46	10·9	0	0
Basal breccia No. 45	13·2	10–15	12
Wishart orthoquartzite No. F–75	15·1	20	21
Dover flint No. 2	29·3	100	95
Diatomite No. 13	30·3	100	100

also a product of chemical precipitation. The correlation of the O^{18} abundances with authigenic silica content (Table 3) indicates that the enrichment of the heavy isotope in sediments is due to surface exchange between the clastic fragments and water.

Of the group of orthoquartzites considered in Table 3, only the St. Peter sandstone is uncemented. The complete absence of interstitial quartz is marked by its low O^{18} abundance relative to other sediments. The Dover flint and diatomite, representing the upper limits of chemically-precipitated silica, are about $20\,^0/_{00}$ higher (than St. Peter sandstone) in O^{18}/O^{16} ratios. The basal breccia, with siliceous overgrowths estimated at about 10–15%, is $2{\cdot}3\,^0/_{00}$ higher in O^{18} than the St. Peter sandstone. This increase is about 12% of the O^{18}/O^{16} ratio difference (Table 3, column 4) between St. Peter sandstone and diatomite. The Wishart orthoquartzite, which contains about 20% authigenic silica, is 21% of the above ratio difference higher in O^{18} than the St. Peter sandstone.

The arkose (No. 2698), a deposit attributed to a minimum of sedimentary action, fittingly shows an increase of only $0{\cdot}5\,^0/_{00}$ over the O^{18}/O^{16} content of St. Peter sandstone.

The relation of the Grafton and Cheshire orthoquartzites is also interesting. Both are from the same general locality; the Grafton occurs as a lens (100 ft in its greatest dimension) included in a deformed, but not recrystallized, shale. The Cheshire is a thick bed (1000 ft thick) unconformably overlying the pre-Cambrian Mt. Holly granite gneiss [22]. Petrographically, the Cheshire orthoquartzite is crystalloblastic

in texture. Original clastic grain boundaries are completely obliterated, and the undulatory extinction characteristic of metamorphic quartzites is evident throughout. Furthermore, the presence of traces of epidote and crystalline sericite serves to classify the rock as a metaquartzite [23] belonging to the epidote-amphibolite facies.

The Grafton also shows indications of metamorphic change, but not as intense as that encountered in the Cheshire. Clastic grain boundaries and overgrowths are still faintly visible, although crystalloblastic textures are prevalent.

The Cheshire orthoquartzite has an isotopic composition of $10{\cdot}2‰$, which is $0{\cdot}7‰$ lower than that of the St. Peter sandstone. The Grafton, which is the less completely metamorphosed of the two, is higher than the Cheshire by $4{\cdot}5‰$ in its O^{18}/O^{16} ratio. Since the O^{18} abundance of St. Peter sandstone has been taken to represent a lower limit for the undeformed sediments listed in Table 3, it is tempting to conclude that metamorphism results in a decrease in O^{18} content. This implies that metamorphic transformation is accompanied by a transfer of material.

*Table 4. Temperature coefficients for O^{18}/O^{16} fractionations in several exchange reactions**

Exchange Reaction	*Temperature Coefficient (‰ per degree Centigrade)*
$SO_4^{=}$—H_2O (liq.)	—0·188
$CO_3^{=}$—H_2O (liq.)	—0·176
$SiO_3^{=}$—H_2O (liq.)	—0·128
$PO_4^{\equiv}$—H_2O (liq.)	—0·068

* The values for the carbonate, sulfate, and phosphate exchange reactions have been calculated over the temperature range 0° to 25° C; that for the silicate covered the range 15° to 140° C.

The O^{18}/O^{16} ratios of the quartz vein (No. 89) and Brazil quartz (No. 26) are too high to class them among the igneous rocks. This is in accord with present theories which ascribe their origin to precipitation from vein-forming solutions [24]. The lower O^{18} concentrations in these samples than that of diatomite (No. 13) are believed to be due to higher deposition temperatures.

Ingerson [25] has estimated the formation temperature of Brazil quartz to be about 140° C. This figure is based on two "probable best values," 100° and 180° C. Assuming that the diatomite was precipitated at a temperature of 15° C, we have two points on the temperature-isotopic composition scale. Although this relation is not linear, it is not possible to consider it from any other viewpoint in the light of the crude and insufficient data used. Furthermore, because of the inherent differences between fresh and sea water, the O^{18} content of silica precipitated from fresh water should be lower than that deposited in sea water, and this may account for the slight difference between the diatomite (No. 13) and Dover flint (No. 2).

The fractionation factors at 15° C and 140° C (K_{15} and K_{140}) are 1·030 and 1·014, respectively, for the silica-water equilibrium, which indicates a difference of $-0{\cdot}128‰$ per degree centigrade. In 1947, Urey [5] noted the similarity in temperature coefficients for the carbonate-water exchange and the sulfate-water exchange and predicted at that time that similar coefficients should exist for the phosphate-water and silica-water exchanges. The temperature coefficients for the carbonate, sulfate, and phosphate exchange reactions have been calculated from experimental data [14] over the temperature range from 0° to 25° C. These values are given in Table 4 along with the temperature coefficient for the silica-water exchange reaction which has been computed as indicated above for the temperature range 15° to 140° C.

The significance of a diminishing isotopic fractionation with increasing temperature will become more evident in later sections of this paper. If we were to retain our erroneous assumption that the silica-water exchange constant is linearly dependent upon the temperature, the last traces of fractionation would be expected to vanish at about 160° C. In any event, at sufficiently high temperatures the thermal contribution to the vibrational energy of the silicate molecule would become great enough to eclipse the mass contribution due to the isotope effect. Under these conditions the exchange constant becomes equal to unity and no fractionation should occur.

The differences in oxygen isotopic abundances which exist between sedimentary and igneous rocks are the results of interactions and redistributions which have occurred since the formation of the earth's crust. Since fractionation of isotopes is not expected at high temperatures, it is reasonable to assume that the oxygen isotopes were uniformly distributed during the molten stage of the earth's crust. The composition of this completely mixed and uniform state shall be referred to as the primordial composition. To determine the primordial composition, it is necessary to obtain a sample of the lithosphere which has been unaltered by erosional processes and uncontaminated by remelted or assimilated sediments. Most geologists will agree that the Plateau and Oceanic basalts fulfill these requirements since they are believed to have arisen from the basaltic shell underlying the earth's crust. The samples selected as representative of this "Mother Magma" were an olivine basalt (No. 1) from Tahiti, the Columbia River basalt (No. 79–PG–5) from Oregon, and the Disco basalt (No. R–7696) from Ovifak, Greenland.

The olivine basalt is a good example of the Oceanic Province, the Columbia River basalt is typical of the Plateau basalts, and the noble metal content in the metallic phase of the Disco basalt bears a striking similarity to the composition of meteorites [26]. The analyses fall into the range of 6·4 to 7·0‰ (Table 2) and this range of oxygen isotopic composition may be regarded as the primordial composition. The dunite (No. 25), believed to have been formed at great depth, falls within this range with a value of 6·8‰.

The Mt. Etna lava (No. B–1–74), which has an isotopic abundance of 6·7‰, presented no problem, since these lavas are basaltic to andesitic in composition.

The alkaline and granitic rocks are somewhat richer in O^{18}, with values ranging from 7·7 to 8·3‰. Parícutin lava (No. K–12), although originally basaltic in composition, has been studied by Shand [27], who calls attention to granitic inclusions, and the high value (8·5‰) of this sample may be due to assimilation of alkalic rocks and sediments.

It is difficult to explain the higher O^{18} abundances in granitic rocks as compared with the basic rocks. If the granitic rocks have originated by differentiation from a magma, then on the basis of energy considerations, the earlier crystallizing fraction, *i.e.* the basic rocks, should be richer in the heavy isotope than the later fractions (granitic rocks). This is not the case, and the discrepancy is given further consideration below in the section dealing with fractional crystallization.

Since the increased O^{18} content of sediments is due to an exchange reaction associated with the precipitation of silica from solution, an equivalent amount of O^{18} must have been lost by the seas. Using the estimates of Kossina [28] and Kuenen [29] for the total masses of the oceans and sediments as $1{\cdot}4 \times 10^{24}$ g and $1{\cdot}9 \times 10^{24}$ g

respectively, it should be possible to calculate the primitive oxygen isotopic composition of the ocean. Accepting Krynine's [30] breakdown of continental sediments and Kuenen's [29] estimate for the ratio of continental to deep-sea deposits as 2:5, the overall weighted average for the isotopic composition of sedimentary rocks was calculated to be $23{\cdot}0\,^0/_{00}$.

Since water contains 89% by weight of oxygen, and sediments an average of 48%, the total oxygen content of the oceans is $1{\cdot}2\times10^{24}$ g, and for sediments, $0{\cdot}9\times10^{24}$ g. The isotopic composition of the oceans at present may be taken as $0{\cdot}0\,^0/_{00}$, the present overall value for sediments is $23{\cdot}0\,^0/_{00}$. Allowing that these deposits evolved from rocks with an original O^{18}/O^{16} ratio of $7{\cdot}0\,^0/_{00}$, and letting Y designate the primordial composition of the seas, then the balance may be expressed by:

$$1{\cdot}2\times10^{24}(Y-0{\cdot}0)=0{\cdot}9\times10^{24}(23{\cdot}0-7{\cdot}0)$$

and Y equals $12{\cdot}0\,^0/_{00}$.

Since deep-sea deposits (mainly clays, muds, and siliceous and calcareous oozes) are assumed to have precipitated chemically, or deposited as very fine clastic particles with very large surface area exposed to the action of sea water, a high value ($30{\cdot}0\,^0/_{00}$) was assigned to them in the calculation of the weighted average. If Kuenen's estimate of 5×10^8 cubic kms for the total volume of deep-sea deposits is too large by a factor of two, we then obtain for the primitive isotopic composition of the seas a value of $7{\cdot}5\,^0/_{00}$ which is close to the primordial abundance designated for igneous rocks.

In an earlier estimate, Clarke [31] has given 3×10^8 cubic kms as the highest possible volume of decomposed igneous rocks. Using this figure and retaining the computed average isotopic abundance for sediments as $23{\cdot}0\,^0/_{00}$, we are now concerned with $8{\cdot}4\times10^{23}$ g of rock of which 45% is oxygen. This results in a value of $5{\cdot}0\,^0/_{00}$ for the primordial isotopic abundance of the oceans.

Thus far we have barely taken into account the metamorphic and granitic rocks which are shown below to be generally richer in the heavy isotope than are the average basic igneous rocks. If these higher values are the results of sea water (or ground water) action preceding metamorphism and granitization, then the entire sialic layer underlying the continents to a depth of 30 kms must enter into our calculations. For a total land area of $1{\cdot}5\times10^8$ square kms, we are now concerned with a volume of $4{\cdot}5\times10^9$ cubic kms which weighs $1{\cdot}3\times10^{25}$ g. Deducting the $1{\cdot}9\times10^{24}$ g already taken as sedimentary deposits, $1{\cdot}1\times10^{25}$ g of sialic material remains to be considered. Ninety five per cent of this is granitic [32] and composed of about 48% by weight of oxygen. If we assign to the $5{\cdot}0\times10^{24}$ g of oxygen in these rocks an average value of $8{\cdot}0\,^0/_{00}$ for the O^{18}/O^{16} ratio, it will be necessary to add $4{\cdot}2\,^0/_{00}$ to our previous value for the primitive isotopic composition of the seas.

On the grounds that their contribution is negligible, the volume and isotopic composition of ground water, of the oxygen content of the biosphere, or of water vapor and fresh water on the continental masses were not considered in these calculations. Moreover, complete information is still lacking for a precise knowledge of the present distribution of the oxygen isotopes in the oceans. In view of these deficiencies and the questionable estimates used in the above calculations, it is not possible at this time to offer a reliable figure for the primitive composition of the oceans.

Cosmic Abundances

The only non-terrestrial materials that lend themselves to this method of investigation are meteorites. Four specimens in this category have been analyzed. Of these, the nortonite (No. 24) (achondritic stony meteorite) is the largest meteorite of any type of witnessed fall [33], [34]. Two tektites, moldavite (No. 38) and tektite (No. 40) are included in this group although their origin is still problematic. The results are given in Table 5.

Table 5. Oxygen isotopic abundances in stony meteorites and tektites

Sample	O^{18}/O^{16} ‰	*Average Deviation*	*Number of Determinations*
Nortonite No. 24	6·3	0·4	4
Stony meteorite No. 37	6·5	0·8	3
Moldavite No. 38	10·4	0·5	2
Tektite No. 40	10·4	0·1	2

The oxygen isotope ratios for the stony meteorites, 6·3‰ and 6·5‰, fall within the range assigned to the primordial composition of our planet, and may be taken as evidence that meteorites form a counterpart of the subsurface composition of the earth. Previous comparisons of the isotopic composition of iron [35] and oxygen [36] in terrestrial and meteoritic matter have led to the same conclusion. On the strength of observed isotopic shifts in the band spectra of M-type stars, McKellar [37] has concluded that the relative abundances of oxygen isotopes in stellar atmospheres show no significant departure from terrestrial abundances. This statement may now be extended to include the planetary bodies of the Solar System.

The higher isotope ratios for the tektite and moldavite bring them within the range of sedimentary rocks. This is interesting, since chemically the tektites resemble the aluminum-rich argillaceous sediments [38]. If tektites are derived from extra-terrestrial sources, do these data imply that erosional processes are operating on other planets? The analyses of the two samples given above neither add nor detract from the meager evidence for the nonterrestrial origin of tektites. Since all available information indicates that the structure and composition of all the planetary bodies of the Solar System are similar [39], isotopic abundances cannot be used to prove or disprove the extra-mundane origin of matter.

Fractional Crystallization

The process of fractional crystallization of one component from a melt may or may not be accompanied by fractionation of isotopes. This would depend upon the degree to which equilibrium is attained and the temperature at which crystallization occurs.

In the calculation of equilibrium constants by use of statistical mechanics, the fractionation factor is determined from the ratio of the partition functions Q_2/Q_1 for the molecules with different isotopic compositions. This ratio is given by the expression [5]:

$$\frac{Q_2}{Q_1} = \frac{\sigma_1}{\sigma_2} \pi_i \left\{ 1 - \frac{1}{24} \left[\left(\frac{h c \omega_{2i}}{k T} \right)^2 - \left(\frac{h c \omega_{1i}}{k T} \right)^2 \right] \right\}$$

where σ_1 and σ_2 are the symmetry numbers of the two different isotopic configurations [40], and the $hc\omega$ terms are the corresponding vibrational frequencies for each molecular configuration. π_i signifies the product over all the internal quantum states of the molecules.

At high temperatures the ratio of the partition functions, Q_2/Q_1, reduces to the ratio of the symmetry numbers, σ_1/σ_2, and the fractionation factor for the distribution of the oxygen isotopes between the two modifications (solid and liquid, or solid and solution) is determined by this ratio alone. For the oxygen exchange in the silicate ion, which has been shown to possess the same symmetry in both the liquid and the solid states [41], [42], [43], [44], the ratio of the partition functions Q_2/Q_1 (solid) approaches Q_2/Q_1 (liquid) as the temperature assumes high values. Under such conditions, the distributation coefficient for oxygen isotopes between solid and liquid states approaches unity, which implies that isotopic fractionation should not occur during crystallization at the temperature of silicate melts.

In order to verify this assumption, quartz and potash feldspar were separated from rocks of granitic composition, and the isotopic constitutions of these separated components were determined. If the rock was formed by crystallization from a melt at equilibrium conditions, the isotopic abundances of oxygen in the component minerals would disclose whether or not isotopic fractionation had occurred. The size of the mineral grains might be taken as a measure of the degree to which equilibrium was attained. Three sets of samples were analyzed, and these results are given in Table 6.

Table 6. Isotopic fractionation between quartz and potash feldspar

Sample	*Quartz*			*Potash Feldspar*			*Difference* *
	O^{18}/O^{16} ‰	*Average Deviation*	*Number of Determinations*	O^{18}/O^{16} ‰	*Average Deviation*	*Number of Determinations*	
Randville pegmatite No. 10 and 11 . . .	10·3	0·2	4	8·8	0·2	4	1·5
Balmoral granite No. 35	7·9	0·4	2	6·2	0·4	2	1·7
Graphic granite No. 31	13·1	—	1	11·3	—	1	1·8

* O^{18}/O^{16} (quartz) less O^{18}/O^{16} (potash feldspar).

In each case the quartz is richer in the heavy isotope than is the potash feldspar, and from the values in Table 6, the distribution coefficient for O^{18} enrichment between quartz and potash feldspar is 1·20 in favor of the quartz.

With regard to the equilibrium requirements, the Randville pegmatite is very coarse-grained, the graphic granite moderately so, and the Balmoral granite has a typical granular texture. Our criterion for equilibrium was apparently of no noticeable consequence to the isotopic fractionation in these rocks.

In a preceding section it was noted that granitic rocks were richer in O^{18} than the basic rocks which was incongruous with the prediction that the granitic minerals, being the latest crystallizing components of a magma, should have concentrated the

light isotope. The reaction principle [45] establishes a differentiation sequence in which potash feldspar crystallizes at a higher temperature than quartz, and here again the quartz is richer in the heavy isotope.

From the data presented in Table 2, it might appear that each mineral or group of minerals has a specific affinity for a definite oxygen isotopic composition. This thesis could be explained by way of the specific lattice energy associated with each mineral species, since the consequent specific bonding forces could be responsible for the selection of the different isotopes in fixed proportions during crystallization. Thus the isotopic composition of any mineral would depend solely on its chemical and structural composition and be independent of its mode of origin. This hypothesis can be discarded by noting the oxygen isotopic abundances in the three rocks in Table 6. Each is composed of approximately equal amounts of quartz and feldspar. The Balmoral granite has an average O^{18}/O^{16} composition of $7{\cdot}1^0/_{00}$ which is practically within the primordial composition range. The Randville pegmatite, with an O^{18}/O^{16} value of $9{\cdot}6^0/_{00}$, occupies a position intermediate to the alkalic rocks and sediments, and the graphic granite, averaging $12{\cdot}2^0/_{00}$, is well within the sedimentary class.

In certain respects, the choice of quartz and potash feldspar was unfortunate. These minerals are the major constituents of granitic rocks, and in view of the present uncertainty of a direct magmatic origin for granites, the results may be entirely irrelevant to the process of fractional crystallization from a melt. These minerals may have formed as a result of solid state reactions; or if the rock had originally crystallized from a melt, the present ratios may be the result of isotopic redistribution over a very long period of time at sub-solidus temperatures. Neither of these alternatives would be contradictory to our earlier assertion of a vanishing fractionation at high temperatures.

It should be noted that the basic igneous rocks have a narrow range of isotopic compositions ($6{\cdot}4$ to $7{\cdot}0^0/_{00}$), and from the standpoint of alteration and contamination, this justifies the acceptance of these rocks as representative material from the depths of the earth. The isotopic abundances of the acidic differentiates are more variable ($7{\cdot}1$ to $12{\cdot}2^0/_{00}$), and this suggests corresponding variations in modes of origin. The detrital constituent of an orthoquartzite, whether derived from igneous rocks, metamorphic rocks, or earlier sandstones, is thus a source of isotopic variation in itself, and the positive correlation of O^{18} abundance with amount of authigenic silica as shown in Table 3 must be discarded as fortuitous.

Diffusion in the Solid State

Among the foremost of the controversial subjects in geology today is the credence that many of the so-called igneous rocks (*i.e.* those presumed to have crystallized from a primary melt or magma) may have been formed by the introduction and incorporation of atoms or ions into pre-existing sedimentary, igneous, or metamorphic rocks [46]–[51]. The preferential diffusivity of certain ions through solids has been attributed to the differences in the chemical activities of the different ions [51], [52].

If we assume that a given source or center of migrating ions consists of an association of minerals with a definite oxygen isotopic composition, then at the temperature und pressure conditions at any point in this center molecules or ions with

differing isotopic constitutions will have different free energies, and consequently unequal migration tendencies.

The ions richer in the lighter isotope, in view of their higher chemical potential, will have a higher mobility than ions rich in the heavy isotope. For any given amount of movement, a gradual increase in the separation of isotopes should be experienced with increasing distance from the source. This principle of isotope separation by migration of ions through solids was discussed by Lindemann [53] in 1921, although subsequent attempts to separate isotopes by ionic migration through gels have been unsuccessful [54].

Laboratory methods are limited by space and time, but such limitations are non-existant in geologic processes. In order to determine whether isotopic separations of this kind have occurred in nature, it is necessary to select a series of properly-spaced samples of rocks from a region in which the silicate ion concentration increases gradually along a definite direction. If the silicate ion is the migrating particle, then the samples farthest from the source of migration should be enriched in the lighter isotope relative to the materials closer to the source.

A sequence which fulfilled these requirements was brought to the attention of the writer by M. W. Leighton, who was kind enough to supply the specimens and field details*.

The specimens were selected from a region in Bayfield County, Wisconsin, where, in a lateral extent of 20 ft, a granophyre passes gradationally into a gabbro. The granophyre is composed of approximately equal amounts of quartz and alkalic feldspar, while 82% of the gabbro is labradorite and the remainder a mixture of hypersthene and augite.

In all, six samples were selected to represent the transition from gabbro to granophyre. Running from north to south, the gabbroic end-member (No. W–187) passes into an intermediate rock (No. W–137–4), which is seven feet north of the site of specimen No. W–137–3. One foot away is No. W–137–2, and two feet farther south is No. W–137–1, which blendes into the main granophyric body (No. W–136–4). The samples are listed in Table 7 in the order of their position in the sequence.

The oxygen content of each member, taken as a measure of the silicate ion abundance, is given in column 5 of table 7 as the ratio of cc of oxygen per mg of sample. The trends in the isotope ratios and silicate ion concentrations meet the requirements given above for positive evidence for solid diffusion.

Table 7. Oxygen isotope abundances in the Bayfield County granophyre-gabbro sequence

Sample and Number	O^{18}/O^{16} ‰	*Average Deviation*	*Number of Determinations*	*cc O_2 / mg. Sample*
Gabbro No. W–187	6·1	0·4	4	0·28
Intermediate rock No. W–137–4	7·7	0·0	2	0·33
Intermediate rock No. W–137–3	8·4	0·3	4	0·35
Contact rock No. W–137–2	8·7	0·3	4	0·36
Granophyre No. W–137–1	9·0	0·2	3	0·39
Granophyre No. W–136–4	9·9	0·8	3	0·36

* A detailed description of the field relations by M. W. Leighton will appear elsewhere.

A petrographic analysis of any part of this rock sequence shows properties which indicate that the mineral assemblage is, directly or indirectly, the product of a crystallization process. Evidence of microscopic or macroscopic channelways which might explain the intrusion of foreign substances is absent. Neither is there any indication, in the form of embayments or other solution effects, that the rocks have assumed their present form as a result of assimilation processes.

In explaining the oxygen isotopic gradient in this extent of rock, it should be noted that in every laboratory method, to date, for isotope separation, reflux is necessary for the production of a measureable effect. If similar limitations apply to isotope separations produced in the course of geologic processes, a closed system must be conceived in which a cyclic geologic process can occur in order to account for the Bayfield County rock sequence. A silicate melt confined in a closed space in nature may experience isotopic separations as a result of the cyclic process known as the Soret effect, which is a crude equivalent of a thermal diffusion column in the laboratory [55]. The Soret effect could not have been responsible for the Bayfield County rock sequence on two counts. Ordinarily, in a Clusius-Dickel thermal diffusion column, the heavy isotope would be expected to concentrate at the "cold wall." In this case the gabbroic country rock would represent the "cold wall" in relation to the included silicate melt, and the rocks closest to the country rock are depleted in the heavy isotope relative to those crystallized at greater distances. Furthermore, the absence of sharp limiting boundaries in the Bayfield County sequence is evidence against the existence of the necessary "cold wall."

Gravitational forces may be discarded since the variation is horizontal. Another alternative is incomplete mixing.

Field evidence suggests that the granophyre has been intruded as a melt into the gabbroic country rock, or that some process of remelting has occurred. This is based on the presence of unoriented xenoliths of gabbro included in the granophyre. A common explanation given for this type of sequence is that the granophyre has been intruded into the gabbro, reacting with it to form the intermediate rock [56], [57]. A progressively decreasing assimilation of rocks low in O^{18} by a fluid high in O^{18} could account for the trend in isotope ratios found here. This requires that the granophyric melt reacts with, or partially remelts, the solid gabbro upon contact with it.

Bowen [58] has shown that the assimilation of a gabbroic solid by a granitic melt is extremely improbable, if not impossible. This is especially pertinent in this instance since the granophyre is believed to be the product of a "filter-press" type of action, being separated from an early gabbroic fraction at greater depth and forced upward to its present position. A residual melt arising in this manner would obviously not possess sufficient superheat to remelt a gabbro.

Petrographic studies of the intermediate rocks show features which cannot be explained by an assimilation mechanism. For example, idiomorphic hornblende crystals are completely enclosed by idiomorphic microcline crystals. Elongate prismatic hornblende crystals transect rows of other crystals without disturbing in any way the internal structures of the transected crystals. Plagioclase crystals are completely severed by other plagioclase crystals with no visible offset of the twinning lamellae in the transected plagioclases. Orthoclase with perthitic-type blebs of hornblende are common, and hematite-rich zones of reaction rim appearance occur

in plagioclase crystals with very distinct and straight inner borders. Idiomorphic crystal forms are prevalent, and nowhere is there any sign of solution effects or embayments. These are criteria for replacement mechanisms.

The O^{18}/O^{16} ratio of the granophyre is $9{\cdot}9^0/_{00}$, which is higher by about $1{\cdot}5^0/_{00}$ than the granitic rock with the highest O^{18} concentration in Table 2*. The O^{18}/O^{16} ratio falls to $6{\cdot}1^0/_{00}$ in the gabbro, which also shows many of the replacement features described above. This transition cannot be explained by assimilation, by crystal settling, or by incomplete mixing. On the grounds of the evidence presented above in the section on fractional crystallization, the oxygen isotopic gradient cannot be dismissed as the result of inherent specific isotopic compositions of the different mineral species. Above all, it is inconceivable that the oxygen isotopes of the intermediate rock could have assumed their present distribution as a result of direct crystallization from a silicate melt. Consequently, it must be concluded that oxygen in one form or another, is free to redistribute itself by some mechanism in solid rock.

There may be many mechanisms capable of producing the textural and chemical features described here, and whatever they may be, they must abide by the following restrictions:

1. The action of the mechanism should not transform the pre-existing rock completely into the liquid state, for then it would be difficult to avoid complete mixing.

2. The mechanism should not produce any microscopic or macroscopic inhomogeneities in the structure of the resulting rock.

In other words, this mechanism should involve the transfer of material by some process of permeation, solution, or diffusion in a solid.

The Effect of Metamorphism on Isotopic Composition

In a preceding section, a premature guess was ventured that metamorphism results in a decrease in O^{18} content. The Dutchess County metamorphic rock sequence is suited for further investigation of this possibility. This sequence consists of Paleozoic argillaceous sediments in southeastern New York state which show a progressively increasing intensity of metamorphism from northwest to southeast. The structure and petrology of the region have been described by Balk [59] and Barth [60].

The sequence of samples selected for analysis fall along a line perpendicular to the axis of the northeasterly trending geosyncline. The isotope abundances from this series may therefore be regarded as a measure of the effect of differing degrees of metamorphism on a sediment which is assumed to have had an originally uniform composition. The samples are listed in Table 8 in the order of increasing metamorphic change, with the exception of the black phyllite (No. 22), which was collected from a point about five miles northeast of the site of specimen No. 18. The locations of samples No. 22 and 18 are equidistant from the geosynclinal axis, and both should have experienced the same degree of metamorphic transformation.

The olive gray slate (No. 18) and the black phyllite (No. 22) have been assigned to the muscovite slate facies by Barth [60]. The black phyllitic slate (No. 20) falls

* This enrichment in O^{18} may be due to the preferential loss of the lighter isotope in the migration process.

on the biotite isograd*, but belongs to the muscovite slate facies; this sample comes from a locality five miles east-southeast of the source of specimen No. 18. The garnet schist (No. 19) is located about eight miles due east of the black phyllite (No. 22) site, and is well past the garnet isograd and belongs in the kyanite schist facies. The chlorite schist (No. 30), from a point two miles south of the garnet schist (No. 19) locality, also fits into the kyanite schist facies. The biotite garnet schist (No. 28), occuring five miles southwest of sample No. 30, falls just west of the sillimanite isograd, and also belongs to the kyanite schist facies.

The results listed in Table 8 indicate no immediately apparent correlations. The assumption that we are dealing with a sediment of initially uniform composition is not strictly true, since the Hudson River slate, of which the olive gray slate (No. 18)

Table 8. Isotopic abundances in rocks of the Dutchess County metamorphic sequence

Sample and Number	O^{18}/O^{16} ‰	*Average Deviation*	*Number of Determinations*
Olive gray slate No. 18	15·4	0·1	2
Black phyllite No. 22	12·1	1·0	2
Black phyllitic slate No. 20	15·7	0·4	2
Garnet schist No. 19	12·7	0·5	2
Chloritic schist No. 30	12·5	0·2	2
Biotite garnet schist No. 28	12·9	0·0	2

should have been a representative sample, is interbedded with lenses of conglomerate, arkose, and greywacke [61]. The authenticity of a sample taken from an average-sized hand specimen may therefore be questioned.

With the exception of the black phyllite (No. 22), the rocks of the muscovite slate facies (low grade of metamorphism) are higher in O^{18} than those of the more intensely metamorphosed kyanite schist facies, but this should not be taken as conclusive evidence for the depletion of the heavy isotope during metamorphism. It does suggest that isotopic analyses of rock sequences which extend over large areas are more subject to contamination from unrelated materials than are those selected from less widely scattered sources.

Conclusion

The fundamental principles of isotopic chemistry have been applied to a number of geologic problems. All conclusions and interpretations are based on the evidence reported in this paper. In no case has the investigation been sufficiently exhaustive to preclude the possibility of erroneous conclusions. More extensive studies will surely follow, because differences in isotopic abundances are extremely sensitive measures of the energy relations in chemical substances.

The writer is especially indebted to Professor H. C. Urey and Dr. P. Baertschi, without whose interest and assistance this work could not have been accomplished. The writer is also indebted to H. Ramberg, W. H. Newhouse, S. Epstein, M. Steinberg, and A. Mack for their helpful suggestions and assistance.

* See Plate 1, reference [59].

Sincerest thanks are due R. Balk, L. D. Bonham, H. Brown, H. B. Craig, G. W. de Vore, C. Emiliani, W. F. Fahrig, D. J. Fisher, I. Friedman, O. Joensuu, A. L. Kidwell, M. W. Leighton, F. J. Pettijohn, K. Rankama, D. M. Shaw, and C. C. Woo for supplying some of the specimens for these analyses.

Appendix

*Rock specimen descriptions**

Number	*Specimen and Data*
1	Olivine basalt, from Pt. Tahera, Tahiti.
2	Flint nodule, from Dover Cliffs, England.
4	Gneissic granite, from Little Ilk Creek, South Dakota. Migmatitic, with inclusions of biotite schist. Sample analyzed was free from biotite schist.
9	Maquoketa shale, from Belleview, Iowa (Upper Ordovician).
10	Randville pegmatite, (quartz), from Randville, Michigan. Oxygen from this sample used as standard.
11	Randville pegmatite, (orthoclase), from Randville, Michigan.
13	Diatomite, (diatomaceous earth), from Santa Barbara County, California.
14	Nepheline syenite, from Pulaski County, Arkansas.
18	Olive gray slate, from road cut 1·5 miles west of Lagrangeville, Poughkeepsie Quadrangle, New York, [59] p. 799: specimen No. 1.
19	Garnet schist, from site two miles south-southwest of Dover Plains, Clove Quadrangle, New York, [59] p. 804: specimen No. 9.
20	Black phyllitic slate, one-half mile north-northwest of Beekman, Clove Quadrangle, New York, [59], p. 799: specimen No. 4.
22	Black phyllite, from road cut north of Moores Mills, Clove Quadrangle, New York, [59] p. 799: specimen No. 2.
24	Nortonite (stony meteorite), fell at boundary of Norton County, Kansas, and Furnas County, Nebraska on February 18, 1948 [33].
25	Dunite, from Mooihoek, Union of South Africa.
26	Quartz, from Minas Gerais, Brazil [24].
28	Biotite garnet schist, from north side of Tennile River, just northeast of Webatuck, Clove Quadrangle, New York. Occurs as a lens in dolomitic marble immediately west of sillimanite isograd, [59] p. 802: specimen No. 8.
30	Chloritic schist, from road cut, two-thirds mile northwest of Dover Furnace, Clove Quadrangle, New York, [59] p. 802: specimen No. 7.
31	Graphic granite, Lincoln pegmatite, Custer, South Dakota. Quartz and perthitic microcline components separated by Dr. I. Friedman.
35	Balmoral granite, Scotland. Quartz and orthoclase components separated by Dr. I. Friedman.
37	Stony meteorite, from Varpais järvi, Finland. An analysis of this meteorite will be published by W. Wahl and H. B. Wiik.
38	Moldavite, a tektite from Radomilice, C.S.R.; this is Dr. Tucek's specimen No. 12.
40	Tektite (Americanite), Santa Mesa Site, Phillipines.
45	Basal Breccia, from Federal Exploration Mine, Menominee Range, Michigan. Upper Cambrian, Iron Formation.
46	St. Peter sandstone, from St. Paul, Minnesota.
47	Yellowstone obsidian, from Obsidian Cliff, Yellowstone Park, black variety, rhyolitic, [62] p. 98.
79-PG-5	Columbia River basalt, from Picture Gorge, Oregon.
89	Quartz vein, from 12th level, Dome Mine in Timiskaming conglomerate, Porcupine District, Ontario.

* Number in square brackets indicates literature references.

Rock specimen descriptions (Continued)

Number	*Specimen and Data*
410	Cheshire orthoquartzite, from road cut at north edge of Highway 9, on Bennington-Woodford town line, two miles east of Bennington, Vermont. Specimen is of Lower Cambrian age (Olenellus zone).
778	Grafton orthoquartzite, from 5/8 mile east-southeast of Southwest Hoosick, Grafton Quadrangle, New York.
2039	Potsdam sandstone, from Ablemans, Sauk County, Wisconsin.
2698	Arkose, Triassic age, from Fair Haven, New Haven, Connecticut.
B–1–74	Lava, from Mt. Etna, Sicily.
F–75	Wishart orthoquartzite, Huronian (?) age, from Gasson Lake, Labrador.
K–12	Lava, from active flow 100 m north of triangulation station "Paricutin," approximately 3 km northwest of volcano, Michoacán, Mexico. Collected May 20, 1948 by R. E. Wilcox.
R–7696	Disco basalt, from Ovifak, Greenland.
W–136–4 W–137–1 W 137 2 W–137–3 W–137–4 W–187	Granophyre-gabbro sequence, T 45 N; R 5 W, SW¼, Sec 25-Bayfield County, Wisconsin. These specimens will be described fully at a later date by M. W. Leighton.

References

[1] Baertschi, P.; Nature, Lond. 1950 **166** 112. [2] Baertschi, P. and Silverman, S. R.; Geochim. et Cosmochim. Acta (in press). [3] Herzberg, G.; Molecular spectra and molecular structure, I. Spectra of diatomic molecules, 2nd Edition, pp. 162–168, New York: D. Van Nostrand Co., 1950. [4] Herzberg, G.; Molecular spectra and molecular structure, II. Infrared and Raman spectra of polyatomic molecules, pp. 227–238, New York: D. Van Nostrand Co., 1945. [5] Urey, H. C.; J. Chem. Soc. for 1947 562–581. [6] Wirth, H. E., Thompson, T. G. and Utterback, G. L.; J. Amer. Chem. Soc. 1935 **57** 400–404. [7] Gilfillan, Jr., E. S.; J. Amer. Chem. Soc. 1934 **56** 406–408. [8] Epstein, S., Buchsbaum, R., Lowenstam, H. and Urey, H. C.; Bull. Geol. Soc. Amer. 1951 **62** 417–426. [9] Greene, C. H. and Voskuyl, R. J.; J. Amer. Chem. Soc. 1936 **58** 693–694. [10] Greene, C. H. and Voskuyl, R. J.; J. Amer. Chem. Soc. 1939 **61** 1342–1349. [11] Dole, M.; J. Amer. Chem. Soc. 1935 **57** 2731. [12] Urey, H. C.; Science 1948 **108** 489–496. [13] McCrea, J. M.; J. Chem. Phys. 1950 **18** 849–857. [14] Urey, H. C., Lowenstam, H., Epstein, S. and McKinney, C. R.; Bull. Geol. Soc. Amer. 1951 **62** 399–416. [15] Dole, M. and Slobod, R. L.; J. Amer. Chem. Soc. 1940 **62** 471–479. [16] Dontsova, E. I.; Akad. Nauk. SSSR Doklady 1950 **71** 905–906. [17] Vernadsky, W. I., Vinogradov, A. P. and Teis, R. V.; Compt. Rend. (Doklady) Acad. Sci. URSS 1941 **31** 573–576. [18] Tokuda, T. and Kashida, T.; Collected Papers from the Faculty of Science, Osaka University Series C 1949 **2** (No. 6) 1–2. [19] Nier, A. O.; Phys. Rev. 1950 **77** 789. [20] Thode, H. G.; Research 1949 **2** 157. [21] Bainbridge, K. T. and Nier, A. O.; Relative Isotopic Abundances of the Elements, Prelim. Rept. No. 9, Nuclear Science Series, Washington, D. C.: National Research Council, 1950, p. 12. [22] Bonham, L. D.; The Structural Geology of the Hoosick Falls Area, New York-Vermont, in relation to the Theory of Taconic Overthrust., 1950, Ph. D. Thesis, University of Chicago. [23] Pettijohn, F. J.; Sedimentary Rocks, p. 237, New York: Harper and Bros., 1949. [24] Johnston, Jr., W. D. and Butler, R. D.: Bull. Geol. Soc. Amer. 1947 **57** 639–641. [25] Ingerson, E.; Amer. Mineralogist 1947 **32** 387. [26] Goldschmidt, V. M.; J. Chem. Soc. for 1937 655–673. [27] Shand, S. J.; Eruptive Rocks, 3rd Edition, p. 260, London: Thomas Murby and Co., 1947. [28] Kossina, E.; Veröffentl. Inst. Meereskunde, Univ. Berlin, N. F., A, Heft 9, 1921. Cited by Rankama, K. and Sahama, T. G.; Geochemistry, p. 264, Chicago: Univ. Chicago Press, 1950. [29] Kuenen, P. H.; Amer. J. Sci. 1946 **244** 563. [30] Pettijohn, F. J.; *op. cit.*, p. 4. [31] Clarke, F. W. and Washington, H. S.; The Composition of the Earth's Crust, p. 30, U.S. Geol. Surv., Prof. Paper 127, 1924. [33] Daly, R. A.; Igneous Rocks and the Depths of the Earth, pp. 32–41, 173–189, New York: McGraw-Hill Book Co., 1933. [33] Beck, C. W. and La Paz, L.; Amer. Mineralogist 1951 **36** 45–59. [34] La Paz, L.; Science 1948 **107** 543. [35] Valley, G. E. and Anderson,

H. H.; J. Amer. Chem. Soc. 1947 **69** 1871–1875. [36] Manian, S. H., Urey, H. C. and Bleakney, W.; J. Amer. Chem. Soc. 1934 **56** 2601–2609. [37] McKellar, A; Public. Astronomical Soc. of the Pacific 1949 **61** 235–245. [38] Rankama, K. and Sahama, T. G., *op. cit.*, p. 31. [39] Brown, H. and Patterson, C.; J. Geol. 1948 **56** 85–111. [40] Mayer, J. E. and Mayer, M. G.; Statistical Mechanics, pp. 195–199, New York: John Wiley and Sons, 1940. [41] Rice, O. K.; Electronic Structure and Chemical Binding, 1st Ed., pp. 392–393, New York: McGraw-Hill Book Co., 1940. [42] Warren, B. E.; Z. Krist. 1933 **86** 349–358. [43] Zachariasen, W. H.; J. Amer. Chem. Soc. 1932 **54** 3841–3851. [44] Sosman, R. B.; The Properties of Silica, pp. 245–246, New York: Chemical Catalog Co., 1927. [45] Bowen, N. L.; The Evolution of the Igneous Rocks, pp. 54–62, Princeton: Princeton Univ. Press, 1928. [46] Origin of Granite, Geol. Soc. Amer., Memoir 28, 1948, pp. 1–139. [47] Reynolds, D.; Geol. Mag., 1947 **84** 209–223. [48] Read, H. H.; Geol. Assoc. London Proc. 1943 **54** 64–85. [49] Read, H. H.; Geol. Assoc. London Proc. 1944 **55** 45–93. [50] Perrin, R. and Roubault, M.; J. Geol. 1949 **57** 357–379. [51] Bugge, J. A. W.; Norsk, Videns.-Akad. i Oslo, I Math. Naturv. Kl. (No. 13) pp. 1–59. [52] Ramberg, H.; Norsk. Geol. Tidsskr. 1944 **24** 98–111. [53] Lindemann; Royal Soc. London Proc. 1921 **99** 102–104. [54] Aston, F. W.; Mass Spectra and Isotopes, 2nd Ed., pp. 259–260, New York: Longmans, Greene, and Co. 1941. [55] Wahl, W.; Amer. J. Sci. 1946 **244** 417–441. [56] Tyrrell, G. W.; The Principles of Petrology, 2nd. Ed., p. 164, New York: E. P. Dutton and Co., 1929. [57] Fenner, C. N.; Amer. J. Sci. 1929 **18** 251. [58] Bowen, N. L.; *op. cit.*, pp. 175–223. [59] Balk, R.; Bull. Geol. Soc. Amer. 1936 **47** 685–774. [60] Barth, T. F. W.; Bull. Geol. Soc. Amer. 1936 **47** 775–850. [61] *Ibid*; pp. 777–778. [62] Allen, E. T. and Day, A. L.; Hot Springs of the Yellowstone National Park, p. 98, Washington, D. C.: Carnegie Institution of Washington, 1935.

Geochimica et Cosmochimica Acta, 1951, Vol. 2, pp. 43 to 61. Pergamon Press Ltd., London

Photographische Messung des U- und Th-Gehaltes nach der Auflagemethode

H. v. Buttlar und F. G. Houtermans

II. Physikalisches Institut der Universität Göttingen

(Received 15 May 1951)

1. Einleitung

Die modernen Kernemulsionen (nuclear research emulsions) lassen sich bequem zur Messung geringer Beimengungen an radioaktiven Elementen in irgendwelchen Substanzen benutzen [1]. Ihr Hauptvorteil liegt in der vollständigen Registrierung der emittierten α-Teilchen [2] über längere Zeiträume, wobei die Empfindlichkeit durch hinreichend große Belichtungszeiten prinzipiell beliebig gesteigert werden kann. Dies wird nur begrenzt durch den bekannten spontanen Rückgang des latenten Bildes, der als Fading bezeichnet wird. Diese Erscheinung macht sich jedoch erst bei Belichtungsdauern über mehrere Monate störend bemerkbar. Die Aufgabe dieser Arbeit ist, zu untersuchen, wieweit die Auflagemethode, die den Vorteil der einfachen Durchführbarkeit hat, zu einer quantitativen Methode der Aktivitätsmessung verwandt werden kann.

Nach Picciotto [3] gibt es drei Möglichkeiten für die Durchführung solcher Experimente: Man kann eine Lösung der zu untersuchenden Substanz in die Platte einziehen lassen, ein Pulver auf die Plattenoberfläche streuen und mit einer zweiten Emulsion (Stript Emulsion) abdecken oder einen festen Körper in direkten Kontakt mit der Plattenoberfläche bringen. Die hier durchgeführten Experimente benutzen die letzte Methode (Auflagemethode).

Empirisch kann man die Strahler, insbesondere mineralogische Objekte, grob in zwei Klassen teilen, je nachdem die Aktivität homogen über die Auflagefläche verteilt ist oder nicht. Als nichthomogenen Strahler würde man etwa ein Gestein mit aktiven Einschlüssen bezeichnen. Bei diesen ist eine Aktivitätsmessung schwierig, wenn sich das Material auf Gebieten von der Größenordnung der Reichweite der α-Strahlen in seiner chemischen Zusammensetzung ändert.

Diese Arbeit beschäftigt sich mit dem anderen Fall, daß die Aktivität in Gebieten groß gegen die Reichweite homogen verteilt ist (z. B. Zirkon, Monazit, Titanit. Apatit). Es wird festgestellt, mit welcher Genauigkeit sich Aktivitätsmessungen durchführen und etwa aus der Reichweiteverteilung der Spuren Schlüsse über die Natur der im Material vorhandenen α-Strahler ziehen lassen.

Unter der Voraussetzung, daß die Aktivität räumlich homogen über den Strahler verteilt ist, werden zunächst theoretische Aussagen über die zu erwartende Spurendichte und die Längenverteilung der α-Bahnprojektionen auf die Schichtebene der photographischen Platte gegeben und diese dann experimentell geprüft und angewandt. Dabei stellt sich heraus, daß sich durch Aufnahme einer Statistik der Längen der Bahnprojektionen auf den Uran- und Thoriumgehalt sowie das Verhältnis [Th]/[U] schließen läßt.

2. Berechnung der zu erwartenden Spurendichte und Längenverteilung der Bahnprojektionen

(a) Allgemeine Formel für die Grenzflächenaktivität.

Unter „Grenzflächenaktivität" I sei die Zahl der pro Sekunde aus einem Quadratzentimeter der Grenzfläche des strahlenden Halbraumes austretenden Teilchen verstanden.

Betrachtet wird ein Halbraum, in dem pro Kubikzentimeter und Sekunde $\dot{N}$ elementare Emissionsprozesse stattfinden. $f(x)dx$ sei die Wahrscheinlichkeit dafür, daß ein emittiertes Teilchen in einer Entfernung zwischen x und $x+dx$ vom Emissionszentrum endet (die Funktion $f(x)$ sei auf 1 normiert). Dann lautet die Abfallfunktion für den Teilchenstrom eines parallelen Strahlenbündels:

$$\varphi(x) = \int_x^\infty f(x)\,dx \qquad \text{mit} \qquad \varphi(0) = 1.$$

Die mittlere Reichweite ist definiert als

$$R = \int_0^\infty x\,f(x)\,dx.$$

I ergibt sich durch elementare Auswertung des Integrals

$$I = \int \dot{N}\,dz \int \varphi\left(\frac{z}{\cos\vartheta}\right)\frac{d\Omega}{4\pi},$$

wobei $d\Omega$ das Raumwinkelelement und z den Abstand des strahlenden Elementes von der Grenzfläche bedeutet, zu

$$I = \tfrac{1}{4}\dot{N}R. \tag{1}$$

Dabei ist nur vorausgesetzt, daß die emittierten Teilchen für große Entfernung von der Quelle stärker als $1/x$ absorbiert werden. Die Beziehung ist vom Absorptionsgesetz unabhängig. Sie besagt: Ein Halbraum strahlt genau so viele Teilchen aus, wie in einer Schicht der Dicke $R/4$ insgesamt emittiert werden.

(b) Anwendung auf α-Teilchen.

Die obige Formel gilt für α-Teilchen sicher, da wegen der endlichen Reichweite die Bedingung $\varphi(x) \to 0$ stärker als $1/x$ bei $x \to \infty$ erfüllt ist. Man kann als Funktion $\varphi(x)$ eine Rechteckfunktion annehmen, d. h. die Reichweitenschwankung (straggling) vernachlässigen; $f(x)$ ist dann die Diracsche δ-Funktion $\delta(x-R)$. Dies ist für den vorliegenden Zweck erlaubt.

Als Halbraum wirkt schon eine Materialschicht, die dicker als die Reichweite ist, da die weiter entfernt ausgesandten Teilchen die Grenzfläche nicht erreichen können. Ebenso braucht die Probe auch in der Grenzflächenebene nicht unendlich ausgedehnt zu sein. Die Funktion I mißt die Zahl der pro Sekunde und Quadratzentimeter das Material verlassenden Teilchen, wenn man nur um die Länge einer Reichweite vom Rande entfernt bleibt. Dies liefert eine Grenze für die Anwendbarkeit der Rechnung auf kleine Strahler, wie sie z. B. radioaktive Einschlüsse in Mineralien darstellen. Die Rechnung ist nur gültig für solche Spuren, die zwischen Emissionszentrum und Photoplatte ein einziges Medium durchdringen. Die verbleibende Fläche muß allerdings genügend viele Spuren aufweisen, um eine Statistik aufstellen zu können.

Bei der Messung mit der photographischen Platte muß zweierlei berücksichtigt werden: 1. tritt das α-Teilchen aus dem strahlenden Halbraum in ein vom emittierenden verschiedenes Medium ein, 2. kann man unter dem Mikroskop nur solche Spuren erkennen, deren Projektion auf die Plattenebene eine Mindestlänge überschreitet.

Für die Messung mit der Ionisationskammer hat EVANS [4] die Grenzflächenaktivität als Funktion der Restreichweite selbst berechnet. I. CURIE und H. YAGODA übertrugen diese Rechnung auf die Messung mit der Photoplatte. Sie ist jedoch nur anwendbar, wenn man die ganze Reichweite mißt, was zur Aufstellung einer Statistik über viele Spuren schwierig ist und Konstanz sowie genaue Kenntnis des Schrumpfungsfaktors der Schicht voraussetzt, dessen Bestimmung ohnehin unsicher ist. Besonders schwierig gestaltet sich eine solche Messung für kurzreichweitige und steile Spuren. Die Rechnung wurde daher für die Restreichweiteprojektionen abgeändert, deren Messung unter dem Mikroskop einfach ist und in deren Bestimmung der Schrumpfungsfaktor nicht eingeht. Das Problem ist also, die Zahl $I(r_0)$ derjenigen in die Platte eintretenden α-Teilchen zu bestimmen, für die die Projektion der Bahnspur auf die Plattenebene $\geq r_0$ ist. Die quantitative Behandlung verläuft folgendermaßen:

Ein α-Teilchen möge an den Rand einer Materialschicht (Reichweite R_1) kommen und in eine andere eindringen, in der es die Reichweite R_2 hat. Dabei sei vorausgesetzt, daß das Bremsvermögen [5] von der Restreichweite nicht abhängt, was in dem hier betrachteten Intervall der α-Reichweiten gerechtfertigt erscheint. Mißt man den zurückgelegten Weg des α-Teilchens in Einheiten der Reichweite, so gilt

$$\frac{a}{R_1} + \frac{b}{R_2} = 1. \tag{2}$$

Für ein in der Tiefe z befindliches Volumelement ist $a = \frac{z}{\cos\vartheta}$, und es sei die Restreichweite-Projektion $b \sin\vartheta = r$, also (vgl. Abb. 1)

$$\frac{z}{R_1 \cos\vartheta} + \frac{r}{R_2 \sin\vartheta} = 1.$$

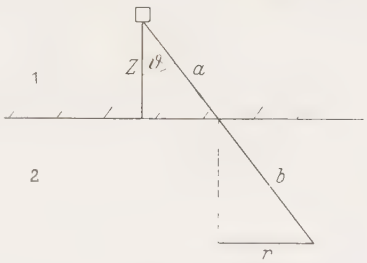

Abb. 1. Schema für den Durchgang eines α-Teilchens durch Material und Photoplatte.

Führt man dimensionslose Größen $\zeta = \frac{z}{R_1}$ und $\chi = \frac{r}{R_2}$ ein, so folgt

$$\zeta + \chi \operatorname{cotg}\vartheta = \cos\vartheta. \tag{3}$$

Gezählt werden Teilchen mit $r \geq r_0$, d. h. $\chi \geq \chi_0$, also nur solche von dV ausgehenden Teilchen, die in ein bestimmtes Winkelintervall $\vartheta_1 < \vartheta < \vartheta_2$ hineingestrahlt werden. Ganz steile Spuren haben eine zu geringe Restreichweite-Projektion, die flachen legen den größten Teil ihres Weges im Material zurück, so daß die Restreichweiten in der Platte kurz werden. Somit muß es also einen oberen und einen unteren Grenzwinkel für die zu zählenden Spuren geben. Diese Grenzwinkel sind die beiden im Intervall 0 bis $\pi/2$ gelegenen Nullstellen der Gleichung

$$\zeta + \chi_0 \operatorname{cotg}\vartheta - \cos\vartheta = 0. \tag{4}$$

Das günstige Winkelintervall ist um so kleiner, je weiter entfernt das Volumelement von der Grenzfläche liegt; es wird zu Null, wenn die beiden Grenzen zusammenfallen. Der zugehörige Wert von ζ ist mit ζ_{Grenz} bezeichnet. Aus der letzten Gleichung erhält man durch Nullsetzen der ersten Ableitung die Beziehung [6].

$$\zeta_{\text{Grenz}} = (1 - \chi_0^{\frac{2}{3}})^{\frac{3}{2}}. \tag{5}$$

Es sind also die in der Berechnung von I auftretenden Integrationsgrenzen über ϑ abhängig von ζ, und das Integral über ζ ist von Null bis ζ_{Grenz} zu erstrecken. Das bedeutet, daß die gezählten Spuren nur aus einer Tiefe $R \cdot \zeta_{\text{Grenz}}$ kommen, was nur im Grenzfall $r \to 0$ in die Reichweite selbst übergeht. Wegen $f(x) = \delta(x - R)$ hat man also

$$I = \dot{N} \iint \frac{dz\, d\Omega}{4\pi} = \frac{1}{2} \dot{N} R_1 \int_0^{\zeta_{\text{Grenz}}} d\zeta \int_{\vartheta_1}^{\vartheta_2} \sin\vartheta \, d\vartheta .$$

Die Funktion I bleibt damit nur noch abhängig von der frei wählbaren Größe χ_0, das ist die Restreichweite-Projektion, unterhalb deren man die Spuren nicht mehr zählen will, ausgedrückt in Einheiten der Plattenreichweite R_2. Also

$$I(\chi_0) = \tfrac{1}{2} \dot{N} R_1 \int_0^{\zeta_{\text{Grenz}}} (\cos\vartheta_1(\zeta) - \cos\vartheta_2(\zeta))\, d\zeta , \tag{6}$$

$$I(\chi_0) = \tfrac{1}{4} \dot{N} R_1 K(\chi_0) . \tag{7}$$

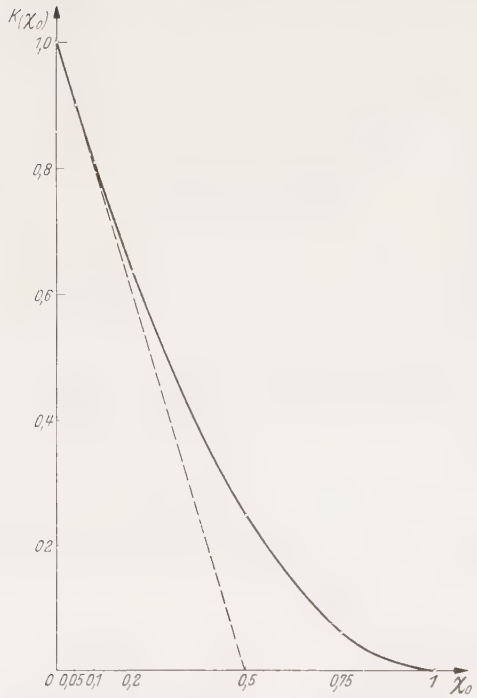

Abb. 2. Die Funktion K in Abhängigkeit von der in Einheiten der Plattenreichweite ausgedrückten Restreichweite-Projektion.

Die Funktion $K(\chi_0)$ muß nach Gleichung (1) für $\chi_0 = 0$ den Wert 1 annehmen und für $\chi_0 \to 1$ gegen Null gehen. Sie wurde numerisch durch Lösung der Gleichung (4) für angenommene Werte von χ_0, Bestimmung von ζ_{Grenz} und graphischer Integration der Gleichung (6) bestimmt und zeigt den in Abb. 2 dargestellten Verlauf. Der anfänglich fast lineare Abfall hat die Steigung -2.

Tabelle 1

χ_0	0	0,05	0,1	0,2	0,5	0,75	1,0
$K(\chi_0)$	1,000	0,900	0,809	0,637	0,249	0,062	0

Funktionswerte der Funktion $K(\chi_0)$, 3. Stelle auf ± 1 genau.

(c) Umrechnung von Materialreichweite auf Luftreichweite

Von den bekannten α-Strahlern sind meist die Luftreichweiten tabelliert (Yagoda S. 74). Zur Umrechnung auf die Reichweiten im Material definiert man das relative atomare Bremsvermögen

$$s = \frac{\varrho_0 \cdot R_0 \cdot W}{\varrho \cdot R \, W_0}$$

(ϱ = Dichte, W = Atomgewicht der durchlaufenen Substanz, Index 0 bedeutet Werte für eine Vergleichssubstanz) und benutzt die empirische Regel von BRAGG und KLEEMAN

$$\frac{s}{\sqrt{W}} = \text{const.}$$

Daraus folgt:

$$\frac{\varrho_1 R_1}{\varrho_2 R_2} = \frac{\sqrt{W_1}}{\sqrt{W_2}}.$$

Für Moluküle und zusammengesetzte Stoffe kann man die Formel durch Einführung der „α-Permeabilität“

$$\psi = \sum_n a_n \sqrt{W_n}$$

(a_n = Anteil des Elementes mit dem Atomgewicht W_n) erweitern:

$$\frac{\varrho_1 R_1}{\varrho_2 R_2} = \frac{\psi_1}{\psi_2}.$$

Für Luft ergibt sich $\psi_{\text{Luft}} = 3{,}839$. Die Dichte der Luft ist bei 15° C und 760 mm Hg $\varrho_{\text{Luft}} = 1{,}226 \cdot 10^{-3}$ g/cm³. Somit hängen Luft- und Materialreichweite durch die Gleichung

$$R_{\text{Mat}} = \frac{R_{\text{Luft}} \varrho_{\text{Luft}} \psi_{\text{Mat}}}{\varrho_{\text{Mat}} \psi_{\text{Luft}}} = 3{,}194 \cdot 10^{-4} \frac{\psi_{\text{Mat}}}{\varrho_{\text{Mat}}} R_{\text{Luft}}$$

zusammen.

Führt man die spezifische α-Emission $\dot{A} = \frac{\dot{N}}{\varrho_{\text{Mat}}}$ ein, d.h. die Anzahl der aus 1 g Material pro Sekunde ausgesandten Teilchen, so lautet Gleichung (7)

$$I(\chi_0) = 7{,}985 \cdot 10^{-5} \psi_{\text{Mat}} \dot{A} \cdot R_{\text{Luft}} K(\chi_0). \tag{8}$$

Das bedeutet, daß die Dichte des strahlenden Materials in die Formel für die Spurenzahl überhaupt nicht eingeht. Die Spurenzahl ist also unabhängig von der Packung des Materials. Man kann sogar prinzipiell einen sehr fein gepulverten Sand mit der Auflagemethode quantitativ untersuchen. Das Bremsvermögen der Photoplatte tritt allein auf in der Größe $\chi_0 = \frac{r_0}{R_{\text{Platte}}}$. Ist $R_{\text{Luft}} = \sigma R_{\text{Platte}}$, so ist $\chi_0 = \frac{r_0 \sigma}{R_{\text{Luft}}}$. r_0 ist das Luftäquivalent der Reichweite-Projektion, von der ab gemessen wird. Die Größe r_0 ist experimentell gegeben.

(d) Grenzflächenaktivität einer Substanz, in der radioaktives Gleichgewicht innerhalb der Zerfallsreihen herrscht.

Besteht in einem Material radioaktives Gleichgewicht innerhalb der Zerfallsreihen, so ist die Zahl der zählbaren Teilchen eine Summe aus Anteilen jedes strahlenden Elementes, und zwar derart, daß aus dem Tochterelement pro Zeiteinheit ebenso viele α-Teilchen emittiert werden wie aus der Muttersubstanz. Bei der Thoriumreihe ist für die C-Produkte das Verzweigungsverhältnis zu berücksichtigen.

Enthält eine Probe als einziges strahlendes Element Th im Gleichgewicht mit seinen Folgeprodukten, und zwar [Th] Gramm Th pro Gramm Material, so zerfallen pro Sekunde $4{,}10 \cdot 10^3 \cdot$ [Th] Atome (Halbwertszeit $1{,}39 \cdot 10^{10}$ a [7]) Thorium und ebenso viele jedes Tochterelementes. Die Gesamtzahl aller pro Quadratzentimeter und Sekunde registrierbaren Teilchen, deren Restreichweite-Projektion größer als

r_0 ist, wird dann gegeben durch

$$\left.\begin{aligned} Z(\sigma r_0) &= [\mathrm{Th}] \cdot 7{,}985 \cdot 10^{-5} \cdot 4{,}10 \cdot 10^3 \, \psi_{\mathrm{Mat}} \sum_i K\left(\frac{\sigma r_0}{R_{i\,\mathrm{Luft}}}\right) R_{i\,\mathrm{Luft}} \\ Z(\sigma r_0) &= [\mathrm{Th}] \cdot \psi_{\mathrm{Mat}} \cdot J_{\mathrm{Th}}(\sigma r_0) \end{aligned}\right\} \qquad (9)$$

(zu summieren über alle α-Strahler der Zerfallsreihe). Das heißt:

$$\frac{\text{Zahl der Spuren} \geq r_0}{\mathrm{cm}^2 \cdot \mathrm{sec}} = \text{Thoriumgehalt} \cdot \psi_{\mathrm{Mat}} \cdot J_{\mathrm{Th}}(\sigma r_0).$$

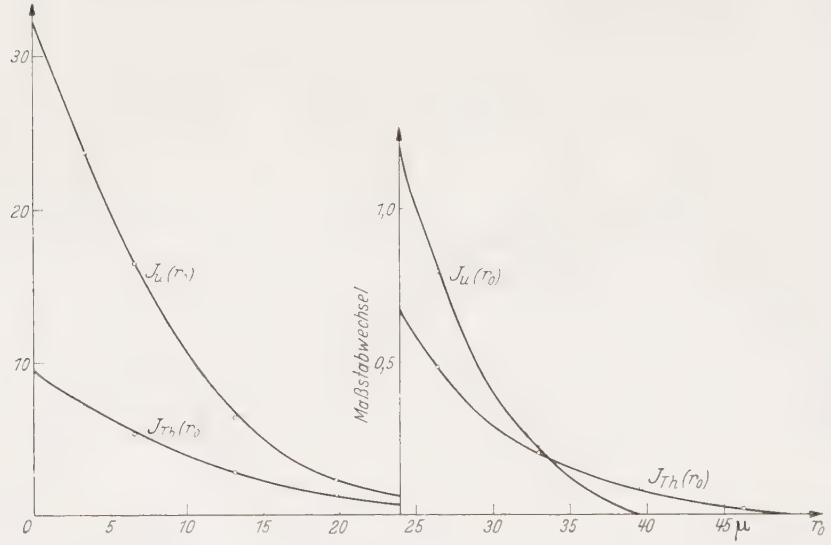

Abb. 3. Graphische Darstellung der Funktionen $J_{\mathrm{U}}(\sigma r_0)$ und $J_{\mathrm{Th}}(\sigma r_0)$ (vgl. Tabelle 2a und 2d).

Da in die Berechnung von ψ_{Mat} der Gehalt [Th] noch einmal eingeht, erhält man im allgemeinen eine in [Th] quadratische Gleichung zur Gehaltsbestimmung. Nur in Fällen ganz geringer Konzentration des strahlenden Elementes spielt der Th-Anteil für ψ keine Rolle.

Ganz entsprechend ergibt sich eine Beziehung für den Fall, daß eine Probe einen Reingehalt von [U] Gramm Uran pro Gramm Material hat, das mit seinen Folgeprodukten im Gleichgewicht steht. Hier muß man bedenken, daß das Uran aus zwei strahlenden Mutterelementen zusammengesetzt ist, nämlich zu 99.28% aus U^{238} und zu 0,72% aus AcU. Man erhält analog wie beim Th, da von 1 g U^{238} pro Sekunde $1{,}23 \cdot 10^4$ (Halbwertszeit $4{,}56 \cdot 10^9$a [8]) und vom AcU pro Sekunde $7{,}86 \cdot 10^4$ (Halbwertszeit $7{,}13 \cdot 10^8$a [8]) Atome zerfallen

$$\left.\begin{aligned} Z(\sigma r_0) &= 0{,}9928\,[\mathrm{U}]\, 7{,}985 \cdot 10^{-5} \cdot 1{,}23 \cdot 10^4 \, \psi_{\mathrm{Mat}} \sum_j K\left(\frac{\sigma r_0}{R_{j\,\mathrm{Luft}}}\right) R_{j\,\mathrm{Luft}} + \\ &\quad + 0{,}0072\,[\mathrm{U}]\, 7{,}985 \cdot 10^{-5} \cdot 7{,}86 \cdot 10^4 \, \psi_{\mathrm{Mat}} \sum_k K\left(\frac{\sigma r_0}{R_{k\,\mathrm{Luft}}}\right) R_{k\,\mathrm{Luft}} \\ Z(\sigma r_0) &= [\mathrm{U}] \cdot \psi_{\mathrm{Mat}} (0{,}9928 \cdot J_{\mathrm{U}^{238}}(\sigma r_0) + 0{,}0072 \cdot J_{\mathrm{AcU}}(\sigma r_0)) \\ Z(\sigma r_0) &= [\mathrm{U}] \cdot \psi_{\mathrm{Mat}} \cdot J_{\mathrm{U}}(\sigma r_0) \end{aligned}\right\} \qquad (10)$$

also

$$\frac{\text{Zahl der Spuren} \geq r_0}{\text{cm}^2 \cdot \text{sec}} = \text{Urangehalt} \cdot \psi_{\text{Mat}} \cdot J_{\text{U}}(\sigma r_0).$$

Für größere Urangehalte tritt auch hier [U] in der Größe ψ auf, so daß zur Gehaltsbestimmung eine quadratische Gleichung zu lösen ist.

Die Tabellen 2a, b, c, d liefern J_{Th}, $J_{\text{U}^{238}}$, J_{AcU} und J_{U} als Funktionen von σr_0. Außerdem sind in Abb. 3 die Funktionen J_{Th} und J_{U} graphisch dargestellt.

Tabelle 2a

Element	Th	RdTh	ThX	Tn	ThA	ThC 35 %	ThC′ 65 %	$\sum_j K_j R_j$	J_{Th}
R_{Luft} *in cm*	2,50	4,00	4,32	5,00	5,64	4,73	8,57		
σr_0 *in cm*	$K(\chi_0) \cdot R_{\text{Luft}}$								
0	2,500	4,000	4,320	5,000	5,640	1,655	5,570	28,685	9,400
0,578	1,464	2,920	3,265	3,900	4,536	1,268	4,836	22,180	7,245
1,155	0,732	1,992	2,324	2,940	3,552	0,940	4,156	16,636	5,440
2,31	0,032	0,712	0,988	1,448	1,976	0,432	2,928	8,516	2,738
3,465		0,096	0,208	0,492	0,856	0,124	1,984	3,760	1,229
4,62				0,060	0,216	0,008	1,172	1,456	0,475
5,775							0,612	0,612	0,2005
6,93							0,2184	0,2184	0,0714
8,085							0,0444	0,0444	0,01457

Die Tabelle gibt Werte der Funktion

$$J_{\text{Th}}(\sigma r_0) = 0{,}328 \left\{ 2{,}5\, K\left(\frac{\sigma r_0}{2{,}5}\right) + 4\, K\left(\frac{\sigma r_0}{4}\right) + 4{,}32\, K\left(\frac{\sigma r_0}{4{,}32}\right) + 5\, K\left(\frac{\sigma r_0}{5}\right) + \right.$$
$$\left. + 5{,}64\, K\left(\frac{\sigma r_0}{5{,}64}\right) + 1{,}655\, K\left(\frac{\sigma r_0}{4{,}73}\right) + 5{,}57\, K\left(\frac{\sigma r_0}{8{,}57}\right) \right\}.$$

Graphische Darstellung s. Abb. 3.

Tabelle 2b

Element	U_I	U_{II}	Io	Ra	Rn	RaA	RaC′	RaF	$\sum_i K_i R_i$	J_{U}
R_{Luft} *in cm*	2,65	3,21	3,11	3,26	4,05	4,66	6,91	3,84		
σr_0 *in cm*	$K(\chi_0) \cdot R_{\text{Luft}}$									
0	2,650	3,210	3,110	3,260	4,050	4,660	6,910	3,840	31,690	31,08
0,578	1,612	2,148	2,052	2,200	2,968	3,548	5,800	2,760	23,088	22,72
1,155	0,858	1,314	1,224	1,344	2,044	2,600	4,772	1,852	16,008	15,705
2,31	0,064	0,256	0,204	0,228	0,744	1,184	3,040	0,616	6,396	6,275
3,465					0,104	0,312	1,712	0,060	2,188	2,155
4,62							0,787		0,787	0,772
5,775							0,221		0,221	0,217
6,93							0		0	0
8,085							0		0	0

Die Tabelle gibt Werte der Funktion

$$J_{\text{U}^{238}}(\sigma r_0) = 0{,}984 \left\{ 2{,}65\, K\left(\frac{\sigma r_0}{2{,}65}\right) + 3{,}21\, K\left(\frac{\sigma r_0}{3{,}21}\right) + 3{,}11\, K\left(\frac{\sigma r_0}{3{,}11}\right) + 3{,}26\, K\left(\frac{\sigma r_0}{3{,}26}\right) + \right.$$
$$\left. + 4{,}05\, K\left(\frac{\sigma r_0}{4{,}05}\right) + 4{,}66\, K\left(\frac{\sigma r_0}{4{,}66}\right) + 6{,}91\, K\left(\frac{\sigma r_0}{6{,}91}\right) + 3{,}84\, K\left(\frac{\sigma r_0}{3{,}84}\right) \right\}.$$

Tabelle 2c

Element	AcU	Pa	RdAc	AcX	An	AcA	AcC	$\sum_k K_k R_k$	J_{AcU}
R_{Luft} *in cm*	3,00	3,57	4,60	4,29	5,67	6,46	5,36		
σr_0 *in cm*	$K(\chi_0) \cdot R_{\text{Luft}}$								
0	3,000	3,570	4,600	4,290	5,670	6,460	5,360	32,950	206,5
0,578	1,964	2,472	3,542	3,244	4,600	5,636	4,268	25,708	161,4
1,155	1,158	1,632	2,584	2,336	3,604	4,368	3,316	18,998	119,0
2,31	0,140	0,492	1,178	0,996	2,052	2,700	1,792	9,35	58,9
3,465		0,028	0,313	0,223	0,908	1,434	0,729	3,635	23,79
4,62			0,018		0,238	0,594	0,150	1,000	6,28
5,775						0,142		0,142	0,891
6,93						0		0	0
8,085						0		0	0

Die Tabelle gibt Werte der Funktion

$$J_{AcU}(\sigma r_0) = 6{,}28 \left\{ 3K\left(\frac{\sigma r_0}{3}\right) + 3{,}57K\left(\frac{\sigma r_0}{3{,}57}\right) + 4{,}6K\left(\frac{\sigma r_0}{4{,}6}\right) + 4{,}29K\left(\frac{\sigma r_0}{4{,}29}\right) + \right.$$
$$\left. + 5{,}67K\left(\frac{\sigma r_0}{5{,}67}\right) + 6{,}46K\left(\frac{\sigma r_0}{6{,}46}\right) + 5{,}36K\left(\frac{\sigma r_0}{5{,}36}\right) \right\}.$$

Als weiteres Mutterelement kommt Io in Frage, da nach Urry [9] in den Tiefseesedimenten Io ohne seine Mutterelemente abgesetzt wird. Die Formel lautet, wenn man über die α-strahlenden Zerfallsprodukte des Io summiert und wenn Io $6{,}965 \cdot 10^8$ Zerfallsakte pro Gramm und Sekunde ausführt.

Tabelle 2d

σr_0 *in cm*	$0{,}0072\, J_{AcU}$	$0{,}9928\, J_{U^{238}}$	J_U
0	1,49	30,85	32,34
0,578	1,16	22,58	23,74
1,155	0,86	15,60	16,46
2,31	0,424	6,23	6,654
3,465	0,171	2,140	2,311
4,62	0,045	0,767	0,812
5,775	0,0064	0,2152	0,2216
6,93	0	0	0
8,085	0	0	0

Die Tabelle gibt Werte der Funktion

$$J_U = 0{,}0072\, J_{AcU} + 0{,}9928\, J_{U^{238}}.$$

$$Z(\sigma r_0) = [\text{Io}]\, \psi_{\text{Mat}}\, 7{,}985 \times$$
$$\times 10^{-5} \cdot 6{,}965 \cdot 10^8 \sum_l K\left(\frac{\sigma r_0}{R_{l\,\text{Luft}}}\right) R_{l\,\text{Luft}}.$$

Ist Radium das Mutterelement der Strahlung und [Ra] der Radiumgehalt, so gilt entsprechend (mit Einschluß des Po!)

$$Z(\sigma r_0) = [\text{Ra}]\, \psi_{\text{Mat}}\, 7{,}985 \times$$
$$\times 10^{-5} \cdot 3{,}7 \cdot 10^{10} \sum_n K\left(\frac{\sigma r_0}{R_{n\,\text{Luft}}}\right) R_{n\,\text{Luft}}.$$

und bei Samarium ([Sm] = Gehalt an Sm. pro Sekunde und Gramm zerfallen 133 Atome [10]):

$$Z(\sigma r_0) = [\text{Sm}]\, \psi_{\text{Mat}}\, 7{,}985 \cdot 10^{-5} \cdot 133 \cdot K\left(\frac{\sigma r_0}{R_{\text{Luft}}}\right) R_{\text{Luft}}.$$

(e) Thorium-Uran-Verhältnis.

Liegt eine Substanz vor, die sowohl Uran als auch Thorium enthält, so gilt

$$Z(\sigma r_0) = \psi_{\text{Mat}}([\text{U}]\, J_U(\sigma r_0) + [\text{Th}]\, J_{\text{Th}}(\sigma r_0)). \tag{11}$$

Will man hier Uran- und Thoriumgehalt getrennt wissen, so muß man zunächst das Th/U-Verhältnis bestimmen. Dazu wurde in Tab. 3a die Funktion $\Phi = \frac{Z(\sigma r_0)}{Z(\sigma b)}$ für $\sigma b = 1{,}155$ cm (d. h. bei Annahme von $\sigma = 1750$ [11] für $r_0 = b = 6{,}6\,\mu$) für verschiedene Werte von Th/U dargestellt. Die Wahl des Normierungswertes b beruht darauf, daß für große σr_0 der Wert von $Z(\sigma r_0)$ so klein ist, daß der statistische Fehler $\sqrt{Z}$ groß wird, während für kurze Spuren der Meßfehler ins Gewicht fällt, der dadurch zustande kommt, daß die steilen Spuren durch den Fixier- und Trockenprozeß, bei dem die Emulsion auf etwa $^1/_3$ ihrer Dicke zusammenschrumpft, ineinandergeschoben werden und dabei die Länge ihrer Projektion auf die Plattenebene ändern können. Empirisch hat sich erwiesen, daß man als Optimum einen Wert in der Umgebung des oben angegebenen $b = 6{,}6\,\mu$ benutzen kann.

Die Schwierigkeit der Bestimmung des Th/U-Verhältnisses liegt darin begründet, daß die Reichweitenverteilung ziemlich unempfindlich gegen die Änderung des Verhältnisses ist. Eine genaue Ermittlung verlangt daher eine große Statistik. Der Vorteil der Methode ist darin begründet, daß die Probe im Verlauf der Messung nicht zerstört zu werden braucht.

Wie man sieht, enthält Gleichung (11) die beiden Unbekannten [U] und [Th], die man aus zwei Messungen bei verschiedenem r_0 bestimmen kann. Wählt man als einen der r_0-Werte den Normierungswert $r_0 = b$ (hier: 6,6 μ), so gibt es für jeden Wert des Th/U-Verhältnisses einen günstigsten zweiten Wert r_{opt}, für den man das Verhältnis mit dem geringsten Fehler angeben kann. Denn zwei Fehlerquellen wirken gegeneinander: Einmal vergrößert sich der statistische Fehler mit wachsendem r_0, da $Z(\sigma r_0)$ abnimmt, andererseits aber ist wegen des Unterschiedes der J-Kurven die Bestimmung des Th/U-Verhältnisses um so genauer, je größer σr_0 wird (vgl. Tabelle 3a).

Tabelle 3a

Th/U	0	0,1	0,2	0,5	1	2	5	10	∞
W	0	0,0909	0,1667	0,3333	0,5000	0,6667	0,8333	0,9090	1,0000
r_0 in μ									
3,3	1,443	1,438	1,431	1,427	1,414	1,398	1,372	1,358	1,331
6,6	1,000	1,000	1,000	1,000	1,000	1,000	1,000	1,000	1,000
13,2	0,404	0,4065	0,4105	0,419	0,4305	0,4470	0,472	0,4865	0,512
19,8	0,1403	0,1428	0,1455	0,1525	0,1616	0,1744	0,1937	0,206	0,226
26,4	0,0493	0,0504	0,0517	0,0547	0,0588	0,0644	0,0730	0,0785	0,0872
33,0	0,01345	0,01418	0,01490	0,01678	0,01935	0,02277	0,02805	0,0314	0,0369
39,6	0	0,000418	0,000814	0,001861	0,00326	0,00522	0,00817	0,0107	0,0132
46,2	0	0,000085	0,000166	0,000380	0,000665	0,001065	0,00167	0,002055	0,00268

Die Tabelle gibt Werte der Funktion $\Phi(b, W) = \frac{Z(\sigma r_0)}{Z(\sigma b)}$ für $\sigma = 1750$, $b = 6{,}6\,\mu$ und verschiedene Werte von W.

Definiert man eine Größe $W \frac{[\mathrm{Th}]}{[\mathrm{U}] + [\mathrm{Th}]}$, die den Anteil von Th an dem Gesamtgehalt strahlender Elemente mißt, so lassen sich die in Tabelle 3a angegebenen Funktionen Φ darstellen durch den Ausdruck [vgl. Gleichung (11)]

$$\Phi(\sigma r_0, W) = \frac{Z(\sigma r_0)}{Z(\sigma b)} = \frac{(1-W)\,J_{\mathrm{U}}(\sigma r_0) + W\,J_{\mathrm{Th}}(\sigma r_0)}{(1-W)\,J_{\mathrm{U}}(\sigma b) + W\,J_{\mathrm{Th}}(\sigma b)}.$$

Ist A die Anzahl der am Normierungspunkt $r_0 = b$ gemessenen Spuren, so ist $\Delta(A\Phi) = \sqrt{A\Phi}$ der statistische Fehler. In erster Näherung ist dann der bei der Angabe von W gemachte Fehler

$$\Delta W(\sigma r_0, W) = \frac{\Delta(A\Phi)}{\frac{\partial}{\partial W}(A\Phi)}.$$

Dieser Ausdruck hat sein Minimum für $r_0 = r_{\mathrm{opt}}$, dort muß gelten

$$\left(\frac{\partial \Delta W}{\partial r_0}\right)_{r_0 = r_{\mathrm{opt}}} = 0.$$

Ausrechnung dieser Gleichung führt auf eine Beziehung $r_{\mathrm{opt}} = r_{\mathrm{opt}}(b, W)$, so daß das günstigste r_{opt} also noch vom Th/U-Verhältnis abhängt. In ganz grober Näherung lassen sich die Funktionen $J_{\mathrm{U}}(\sigma r_0)$ und $J_{\mathrm{Th}}(\sigma r_0)$ durch die Exponentialfunktionen

$$J_{\mathrm{U}}(\sigma r_0) = 48 \cdot e^{-0{,}88\,\sigma r_0}$$
$$J_{\mathrm{Th}}(\sigma r_0) = 12{,}4 \cdot e^{-0{,}67\,\sigma r_0}$$

darstellen, was bis etwa $\sigma r_0 = 4{,}6$ cm, d. h. $r_0 = 26\,\mu$ gestattet ist. Eine analytische Darstellung für $\sigma r_0 > 4{,}6$ cm erübrigt sich, da die günstigsten Werte r_{opt} wegen des Anwachsens des statistischen Fehlers für große r_0 nicht höher liegen.

Tabelle 3b

Th/U	W	r_{opt} in μ	$\sqrt{A} \cdot \Delta W$
0	0	24,5	13,9
0,1	0,0909	24,1	12,3
0,2	0,1667	23,8	11,1
0,5	0,3333	23,1	8,8
1	0,50000	22,5	6,6
2	0,6667	21,7	4,8
5	0,8333	20,9	3,2
10	0,9090	20,5	2,6
∞	1	20,0	2,0

Die Tabelle gibt das günstigste r_0 zur Bestimmung des Th/U-Verhältnisses und den bei der Messung von Z an der Stelle b und r_{opt} in der Angabe der Größe W gemachten Fehler ΔW. A ist die Zahl der Spuren mit $r_0 \geq b$.

Bei $\sigma = 1750$ erhält man die in Tabelle 3b aufgeführten Werte r_{opt} in Abhängigkeit von W. Ebenfalls finden sich dort die Fehlergrenzen ΔW, in denen das gefundene W bei Messungen an den Stellen b und r_{opt} angegeben werden kann.

Praktisch wird man zur Bestimmung des Th/U-Verhältnisses so vorgehen, daß man durch Aufnahme einer geringen Statistik und Vergleich mit Tabelle 3a sich größenordnungsmäßig über den Wert von Th/U und damit von W orientiert und dann eine größere Statistik über alle Spuren $\geq b$ und $\geq r_{\mathrm{opt}}$ aufstellt. Die Bestimmung von Th/U wird um so genauer, je größer die Spurenstatistik ist und kann prinzipiell beliebig gesteigert werden. Zum Beispiel beträgt bei einem Th/U-Verhältnis von 5:1 bzw. 1:2 $r_{\mathrm{opt}} = 20{,}9\,\mu$ bzw. $23{,}1\,\mu$. Der Fehler in W ist also für $A = 3600$ Spuren $W = 0{,}053$ bzw. 0,147, demnach der Fehler in Th/U $(5 \pm 1{,}9)$ bzw. $(0{,}5 \pm 0{,}33)$.

Die von Evans, Goodman und Keevil ausgearbeitete und von Hurley, Larsen u. a. weiterentwickelte α-He-Methode zur Altersbestimmung an schwach aktiven Mineralien und Gesteinen erfordert nur eine verhältnismäßig ungenaue Kenntnis des Th/U-Verhältnisses. Dieses läßt sich, wenn die eingangs erwähnten Voraussetzungen hinsichtlich der Homogenität der untersuchten Materialien erfüllt sind, in der hier beschriebenen Art auf einfache Weise photographisch ermitteln.

3. Experimentelle Nachprüfung der berechneten Funktionen

Die Längenverteilung der Bahnprojektionen wurde für $U_I + U_{II} + AcU$ mittels eines Stückes Uranmetall, für U bzw. Th im Gleichgewicht mit seinen Folgeprodukten mittels einer Pechblende bzw. eines Monazitkristalls geprüft. Um eine möglichst gute Auflage der Materialien auf der Platte zu erreichen, wurden diese einseitig angeschliffen. Die übrige Oberfläche wird zweckmäßig in Paraffin eingegossen, um Störeffekte der von dort ausgehenden Teilchen zu vermeiden.

Die so präparierten Strahler wurden auf je eine Ilford-C_2-Platte (Schichtdicke 50 μ) gepreßt und eine gemessene Zeit exponiert (Uranmetall 10 min, Pechblende 35 min, Monazit 9,5 Std). Die Entwicklung der Platten geschah mit ID 19-Entwickler, Verdünnung 1:2 bei 21° C (Entwicklungsdauer 40 min, dann 20 min in Natriumbisulfit 5% als Stopbad, anschließend 24 Std Fixierbad, schließlich wässern und trocknen). Unter dem Mikroskop sieht man bei geeigneter Vergrößerung die einzelnen α-Spuren als schwarze Striche unterschiedlicher Länge. Das Zählquadrat, das für die meisten der vorliegenden Messungen benutzt wurde, hatte die Größe 132 $\mu \times 132$ μ.

Die Ergebnisse der Auszählung der Uranplatten sind in Tabelle 4 und 5, Spalte 3 zusammengestellt. Zur Umrechnung auf die Zahl der pro Sekunde und Quadratzentimeter entstandenen Spuren müssen diese Zahlen beim Uranmetall mit

$$\frac{1}{10 \cdot 60\,\mathrm{sec}} \; \frac{1}{60 \cdot (132\,\mu)^2} = 1{,}592 \cdot 10^{-1}\,\mathrm{sec}^{-1}\,\mathrm{cm}^{-2}$$

und bei der Pechblende mit

$$\frac{1}{35 \cdot 60\,\mathrm{sec}} \; \frac{1}{60 \cdot (132\,\mu)^2} = 4{,}56 \cdot 10^{-2}\,\mathrm{sec}^{-1}\,\mathrm{cm}^{-2}$$

multipliziert werden.

Für das Uranmetall ist ein Vergleich der Absolutzahlen mit der Theorie möglich, wenn man annimmt, daß das Metall aus 100%igem Uran besteht. Die Erwartungswerte sind in Tabelle 4, Spalte 5 eingetragen. Man erkennt die gute Bestätigung der Theorie.

Die Pechblende wurde dazu benutzt, den Kurvenverlauf $J_U(\sigma r_0)$ zu kontrollieren und gleichzeitig den Urangehalt in unmittelbarer Nähe der Auflagefläche zu bestimmen. Um in Tabelle 5 die experimentelle Längenstatistik (Spalte 4) mit der theoretischen der Spalte 5 vergleichen zu können, wurden in Spalte 6 die Werte der Spalte 4, multipliziert mit einem Normierungsfaktor (hier: 0,178), eingetragen, so daß der Wert bei $r_0 = 6{,}6$ mit dem der Spalte 5 zur Deckung kam. Nach dieser Normierung ist der Vergleich möglich; es zeigt sich eine gute Übereinstimmung zwischen Experiment und Theorie.

Aus dem Wert des Normierungsfaktors läßt sich der Urangehalt der Pechblende bestimmen. Nach Gleichung (10) ist mit den Werten $\sigma = 1750$, $r_0 = 6{,}6$ μ

$$Z(\sigma r_0) = \frac{[U]\,\psi_{Mat}\,J_U(\sigma r_0)}{1 - 0{,}178\,[U]\,\psi_{Mat}}.$$

Der Gehalt [U] geht auch in die α-Permeabilität ein. Nimmt man an, daß pro Gramm Pechblende [U] Gramm U und (1 − [U]) Gramm Beimengungen des durchschnittlichen Atomgewichts 25 enthalten sind, so ist

$$\psi_{Mat} = [U] \cdot 15{,}4 + (1 - [U])\,5 = 10{,}4\,[U] + 5\,.$$

Tabelle 4

Projektion der Restreichweite in Luftäquivalent σr_0 *in cm*	r_0 *in* μ *bei* $\sigma = 1750$	*Zahl der gezählten Spuren*	*Spuren pro cm² und sec*	*Wie Spalte 4, theoretischer Absolutwert für reines Uran**	*Abweichung* %
0,578	3,6	1235	56,3	58,6	3,9
1,155	6,6	709	32,4	33,9	4,6
2,31	13,2	109	4,98	4,89	1,8
3,465	19,8	0	0	0,125	–

* Berechnet nach der Formel $Z = \{0{,}9928\,(J_{U_I} + J_{U_{II}}) + 0{,}0072\,J_{AcU}\} \cdot 15{,}4$.

Vergleich von Experiment und Rechnung an einem Stück Uranmetall. Der Nulleffekt der Platte (Zahl der Spuren außerhalb des Strahlers) ist vernachlässigbar klein. $\psi_{Mat} = \sqrt{238} = 15{,}4 \cdot \sigma = 1750$.

Tabelle 5

Projektion der Restreichweite in Luftäquivalent σr_0 *in cm*	r_0 *in* μ *bei* $\sigma = 1750$	*Zahl der gezählten Spuren*	*Spuren pro cm² und sec*	$J_U\,(\sigma r_0)$	*Werte der Spalte 4, multipliziert mit 0,178*	*Abweichung der Spalte 6 von Spalte 5* %
0,578	3,3	844	134,3	23,74	23,92	0,8
1,155	6,6	580	92,4	16,46	16,46	—
2,31	13,2	229	36,4	6,654	6,48	2,6
3,465	19,8	79	12,58	2,311	2,24	3,1
4,62	26,4	28	4,46	0,812	0,794	2,2
5,775	33,0	8	1,275	0,2216	0,227	2,4
6,93	39,6	0	0	0	0	0

Vergleich zwischen Experiment und Rechnung an einer Pechblende. Aus dem Wert des Faktors 0,178 kann man auf den Urangehalt der Pechblende schließen.

Daraus folgt

$$[U] = 0{,}533 \text{ g U pro g Mat.}$$

Die Pechblende enthält also etwa 53,3% Uran. Unter der Annahme, daß das Uran in der Verbindung U_3O_8 vorliegt, die ihrerseits 84,8% Uran enthält, ist der Gehalt der untersuchten Probe an U_3O_8 etwa 63%. Dieser Wert befindet sich in Einklang mit chemischen Untersuchungen, z. B. liefert Mittelbildung über 20 analysierte Probe der Pechblende Joachimsthal [12], woher auch die vorliegende Probe stammt, einen U_3O_8-Gehalt von $(65{,}705 \pm 16{,}8)\%$. Der Urangehalt variiert in weiten Grenzen, da mit dem Zerfall chemische Wertigkeitsänderungen verknüpft sein können und das ursprüngliche Kristallgitter dadurch zerstört wird.

Bei dem Monazitkristall ist zunächst von Interesse, wie die Aktivität über die Auflagefläche verteilt ist, d. h. ob überhaupt Homogenität des Einbaus des Strahlers in das Gefüge des Mischkristalls aus $CePO_4$ und $ThSiO_4$ besteht. Für einen vollkommenen Mischkristall müßte über Flächen, die groß sind gegen das Quadrat der Reichweite, eine rein statistische Verteilung der Spuren zu erwarten sein, wie man sie etwa bei einem Uranglas erhalten würde. Um dies zu prüfen, muß man die Spurenverteilung über die gesamte Fläche aufnehmen. Dies geschah, indem von jedem $^1/_4$ mm² der Fläche ein Quadrat der Größe $190\,\mu \times 190\,\mu$ herausgegriffen

und darin mit einem Zählnetz die Zahl der Spuren $> 4{,}75\,\mu$ ausgezählt wurde. Dieses Quadrat kann man im statistischen Mittel als Repräsentant des ganzen $^1/_4\,\mathrm{mm}^2$ ansehen. Die so gewonnene Verteilung aller Spuren über 4,75 Längenprojektion ist in Abb. 4 dargestellt. Wie man sieht, ist die Verteilung der Spuren jedenfalls für die natürliche Grenzfläche nicht statistisch, sondern zeigt langsam veränderliche Schwankungen. Abgesehen von einer einzigen Stelle 4mal höherer Aktivität von etwa $200\,\mu$ Durchmesser finden sich „Aktivitätswolken", aus denen sich eventuell Rückschlüsse auf die Bildung des Kristalls, Verarmung der Umgebung an Thorium u. dgl. ziehen lassen.

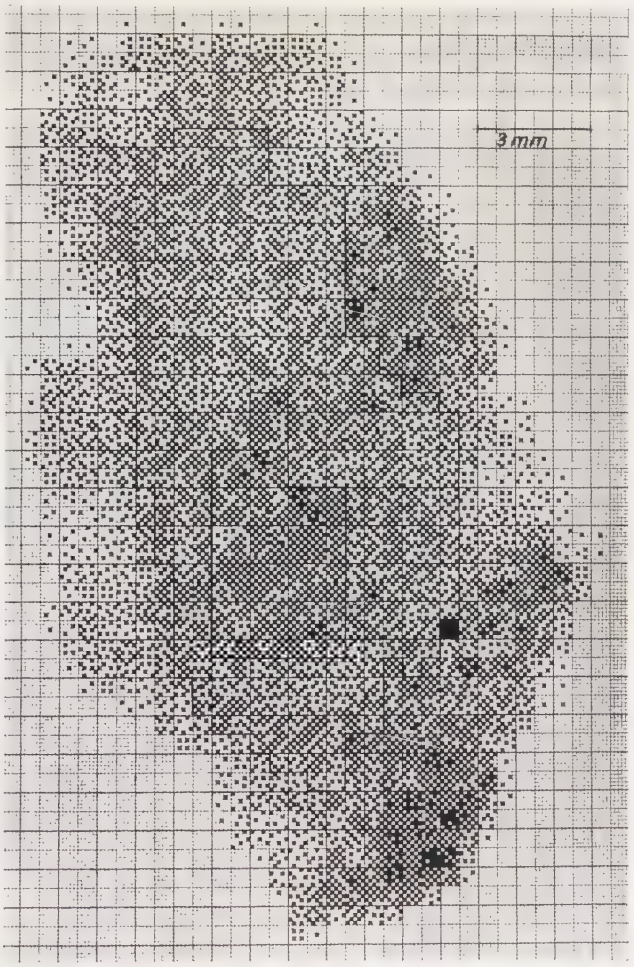

Abb. 4. Aktivitätsverteilung über die Fläche eines Monazitkristalls. Ein Punkt bedeutet 3 Bahneintrittsstellen, d. h. eine Spur im Quadrat = 0 Punkte, 2—4 Spuren = 1 Punkt, 5—7 Spuren = 2 Punkte usw. Der Th-Gehalt wurde in dem Gebiet zwischen den eingezeichneten Grenzlinien bestimmt.

Jedoch gibt es immer noch größere Flächen, auf denen die Aktivität homogen verteilt ist. Zur Feststellung des Gehalts an strahlenden Elementen wurde willkürlich ein größeres, zusammenhängendes Gebiet herausgegriffen und zunächst geprüft, ob die Verteilung der Aktivität dort homogen ist. Als Kriterium dafür wurde die Tatsache benutzt, daß die von einem homogenen Strahler ausgesandten Teilchen in genügend kleinen Flächeneinheiten nach dem Poissongesetz der Wahrscheinlichkeitstheorie verteilt sein müssen. Abb. 5 zeigt die Häufigkeitsverteilung der insgesamt 337 Quadrate über die darin gezählten Teilchenzahlen. Die ausgezogene Kurve ist die für den Mittelwert 27,083 berechnete Poissonverteilung. Wie man aus dem Vergleich sieht, ist die Übereinstimmung gut, nur ist die Verteilung in der Nähe des Maximums etwas steiler; dies erklärt sich ohne weiteres dadurch, daß durch die nach Augenmaß durchgeführte Auswahl einer zusammenhängenden homogenen Fläche eine leicht unternormale Wahrscheinlichkeitsdispersion bewirkt wurde. Diese Unstimmigkeit stört jedoch nicht wesentlich.

Innerhalb dieses Gebietes läßt sich nun die Aktivität bestimmen und die Reichweiteverteilung untersuchen. Dazu wurden in 100 willkürlich herausgegriffenen, aber über das ganze Gebiet verstreuten Quadraten alle enthaltenen Spuren gezählt und eine Reichweitenstatistik aufgenommen. Das Resultat zeigt Tabelle 6, Spalte 3. Die Spalte 4 gibt die mit dem Umrechnungsfaktor

$$\frac{1}{9{,}5 \cdot 60 \cdot 60 \text{ sec}} \cdot \frac{1}{100 \cdot (132\,\mu)^2} = 1{,}68 \cdot 10^{-3}\ \text{sec}^{-1}\ \text{cm}^{-2}$$

auf 1 cm² und 1 sec umgerechneten Meßwerte.

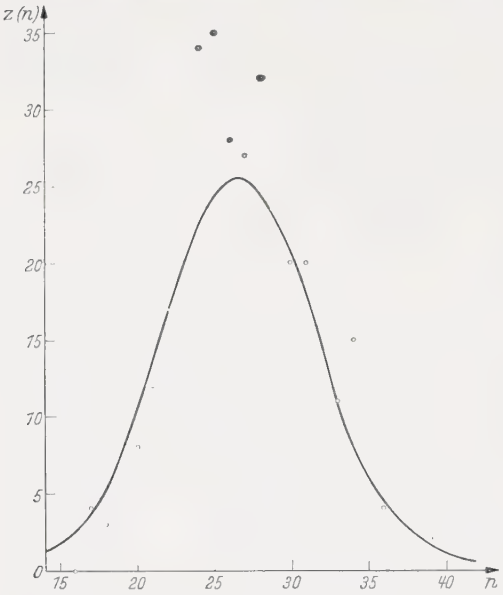

Abb. 5. Zur Homogenität der Aktivitätsverteilung in einem Monazitkristall. n = Zahl der in einem Quadrat gezählten Spuren.

Spalte 5 gibt den theoretischen Wert von J_{Th}, d. h. für einen Thoriumgehalt von 100 % und $\psi_{\mathrm{Mat}} = 1$. Wie im Falle der Pechblende mußten die experimentellen Werte in Spalte 4 mit einem Faktor (hier 2,96) multipliziert werden, um sie mit denen der Spalte 5 vergleichen zu können. Es zeigt sich eine gute Übereinstimmung mit der theoretisch für reines Th gewonnenen Verteilung der Bahnprojektionen. Die α-Aktivität des Monazits läßt sich also in ihrer Längenstatistik durch einen reinen Thoriumgehalt verstehen. Eine Diskussion der Fehlergrenzen auf Grund des hier gezählten Spurenmaterials ergibt nach Tabelle 3b

$$\Delta W = \frac{2{,}0}{\sqrt{1444}} = \frac{1}{19}\,,$$

also

$$W > \frac{18}{19}\,, \qquad \text{d. h.} \qquad \frac{[\mathrm{U}]}{[\mathrm{Th}]} < 0{,}05\,.$$

Tabelle 6

Projektion der Restreichweite in Luftäquivalent σr_0 *in cm*	r_0 *in* μ *bei* $\sigma = 1750$	*Zahl der gezählten Spuren*	*Spuren pro cm² und sec*	$J_{\mathrm{Th}}(\sigma r_0)$	*Werte der Spalte 4, multipliziert mit 2,96*	*Abweichung der Spalte 6 von Spalte 5* %
0,578	3,3	1444	2,42	7,245	7,160	1,2
1,155	6,6	1057	1,775	5,440	5,250	3,5
2,31	13,2	561	0,943	2,783	2,783	—
3,465	19,8	259	0,436	1,229	1,289	4,9
4,62	26,4	97	0,163	0,475	0,482	1,5
5,775	33,0	41	0,0688	0,2005	0,2035	1,5
6,93	39,6	17	0,0286	0,0714	0,0846	(18,5)
8,085	46,2	3	0,00503	0,01457	0,0149	2,3

Vergleich von Experiment und Rechnung an einem Monazitkristall. Aus dem Wert des Faktors 2,96 kann man auf den Thoriumgehalt schließen.

Aus dem Wert des Faktors 2,96 kann man auf den Thoriumgehalt in unmittelbarer Nachbarschaft der gezählten Fläche schließen: Nach Gleichung (9) ist mit den Werten für $r_0 = 13{,}2\ \mu$

$$Z(\sigma r_0) = [\mathrm{Th}]\, \psi_{\mathrm{Mat}}\, J_{\mathrm{Th}}(\sigma r_0)$$

$$1 = [\mathrm{Th}]\, \psi_{\mathrm{Mat}} \cdot 2{,}96\,.$$

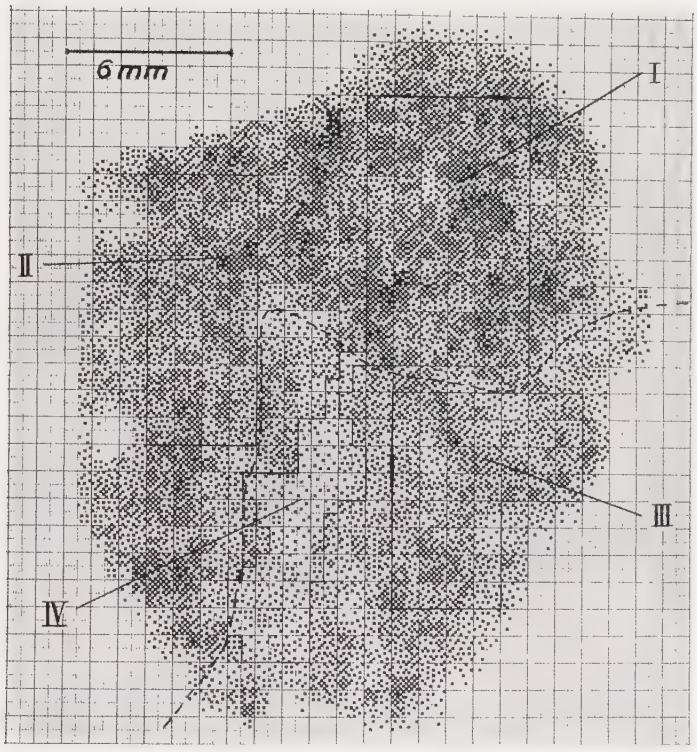

Abb. 6. Aktivitätsverteilung über die Fläche eines Zirkonkristalls. Ein Punkt bedeutet 2 Bahneintrittsstellen im repräsentierenden Quadrat (s. Text). Das Auge erhält durch die Tatsache ein etwas falsches Bild, daß alle ungeraden Zahlen aufgerundet wurden.

Monazit ist chemisch ein Mischkristall aus $CePO_4$ und $ThSiO_4$. Die α-Permeabilität ergibt sich zu

$$\psi_{\mathrm{Mat}} = 8{,}88 + 3{,}4\,[\mathrm{Th}]\,.$$

Damit ergibt sich insgesamt

$$[\mathrm{Th}] = 0{,}038\ \mathrm{g\ Th\ pro\ g\ Mat}.$$

Der Kristall enthält also im untersuchten Gebiet 3,8 % Th. Eine Zählung aller mehr als 1 mm von der Kristallbegrenzung entfernten Spuren ergab für den Thoriumgehalt 3,94 %. Diese Angaben beziehen sich selbstverständlich nur auf eine dünne Schicht über der Auflagefläche.

Chemische Analysen von Monaziten der gleichen Herkunft (Divino de Ubà, Brasilien) ergaben 5,091 % Th [14] und 5,167 % Th [13].

4. Aktivitätsanalyse an einem Zirkon-Einkristall

Als Anwendungsbeispiel wird die Untersuchung eines Zirkonkristalls gezeigt. Die Zirkone verdienen in der Mineralogie besonderes Interesse, da Zirkoneinschlüsse sowohl in Eruptiv- als auch in Sedimentgesteinen die Träger eines großen Prozentsatzes der Gesamtaktivität sind [15]. Diese Zirkone besitzen ihrerseits relativ hohe Gehalte an den radioaktiven Elementen Th und U, die von der Größenordnung einiger Prozente sein können. Es besteht daher die Hoffnung, die Zirkone ebenso wie andere ähnlich hochaktive Schwermineralbestandteile in den Gesteinen als „radioaktive Leitmineralien" bei Gesteinsanalysen zu benutzen, und zwar in zweierlei Hinsicht:

1. zum Zwecke der Altersbestimmung etwa nach der Bleimethode,

2. um aus der spezifischen Aktivität der Zirkoneinschlüsse in Gesteinen etwas über lokale und genetische Zusammenhänge zu erfahren, da der U- und Th-Gehalt bzw. das Th/U-Verhältnis in den Zirkonen ein verhältnismäßig leicht meßbares Charakteristikum derselben darstellt.

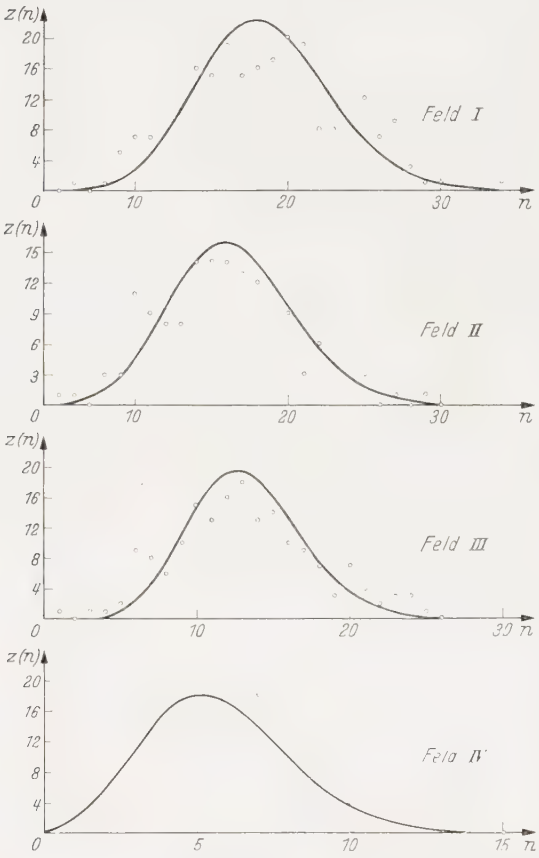

Abb. 7. Zur Homogenität der Aktivitätsverteilung der ausgewählten Felder in einem Zirkonkristall. n = Zahl der in einem Quadrat gezählten Spuren.

Es wurde daher eine Arbeit in Angriff genommen, die zum Ziele hatte, den U- und Th-Gehalt sowie das Th/U-Verhältnis an Zirkoneinschlüssen in verschiedenen Gesteinen zu messen mit dem Ziel, zu prüfen, wieweit diese Größen für Zirkoneinschlüsse im gleichen Gestein variieren [16]. Bei Durchführung dieser Arbeiten erwies es sich als erforderlich, zunächst die Aktivitätsverteilung an gut ausgebildeten, großen Zirkoneinkristallen zu messen, um zu sehen, wieweit diese sich als homogen voraussetzen läßt.

Zur Verfügung stand ein Einkristall von etwa 5 cm Durchmesser (Near Eganville, Renfrew County, Ontario Canada), von dem eine natürliche Kristallfläche (Prismenfläche C-Achse) bei einer Belichtungszeit von 449,5 Std die in Abb. 6 dargestellte Aktivitätsverteilung lieferte. Für die Auszählung der Spuren wurde ein Quadrat der Seitenlänge 135 μ als Repräsentant eines $^1/_4$ mm^2 gewählt, wobei in der Aktivitätskarte je 2 Bahnspuren des repräsentierenden Quadrats durch einen Punkt angedeutet sind. Daher bedeutet jeder Punkt $2 \cdot (\frac{500}{135})^2 = 27{,}4$ Spuren.

Wie beim Monazit zeigen sich auch hier — im Gegensatz zu den radioaktiven Einschlüssen, wie man sie z. B. in Graniten findet [15], [17] — Aktivitätswolken,

Tabelle 7

r_0 in μ	*Feld I*		*Feld II*		*Feld III*		*Feld IV*	
	gemessene Spuren-zahl	*normiert auf* $r_0 = 6{,}6\,\mu$	*gemessene Spuren-zahl*	*normiert auf* $r_0 = 6{,}6\,\mu$	*gemessene Spuren-zahl*	*normiert auf* $r_0 = 6{,}6\,\mu$	*gemessene Spuren-zahl*	*normiert auf* $r_0 = 6{,}6\,\mu$
3,3	1161	1,461	1082	1,578	878	1,559	1232	1,489
6,6	795	1,000	687	1,000	566	1,000	828	1,000
13,2	324	0,407	273	0,398	235	0,415	365	0,441
19,8	111	0,1398	95	0,1382	87	0,1535	149	0,180
26,4	40	0,0503	27	0,0393	35	0,0618	50	0,0604
33,0	7	0,0088	5	0,00727	11	0,01945	14	0,0169
39,6	2	0,00252	1	0,00146	3	0,0053	1	0,00121
46,2	0	0	1	0,00146	0	0	0	0
Daraus Th/U	0		0		$0{\cdot}2 < \mathrm{Th/U} < 1$		$1 < \mathrm{Th/U} < 5$	
Zahl der gezählten Felder	75		75		75		200	

Tabelle zur Bestimmung des Th/U-Verhältnisses eines Zirkonkristalls. Die Werte der vorletzten Zeile entstammen einem Vergleich mit Tabelle 3a.

d. h. langsam veränderliche Verteilungen der Aktivität auf Entfernungen, die groß gegen die Reichweite sind. Man unterscheidet leicht zwei Teile, deren Grenzlinie man auch schon mit dem bloßen Auge an etwas unterschiedlicher Oberflächenbeschaffenheit (Reflexionsvermögen und Farbe) erkennen kann.

Tabelle 8

Feld	*Urangehalt in g U pro g Mat.*	Th/U
I	$3{,}3 \cdot 10^{-4}$	0
II	$2{,}85 \cdot 10^{-4}$	0
III	$2.0 \cdot 10^{-4}$	0.5
IV	$7{,}75 \cdot 10^{-5}$	2

Urangehalt sowie Th/U-Verhältnis auf den Teilgebieten der natürlichen Kristallfläche eines Zirkoneinkristalls.

Zur quantitativen Untersuchung wurden aus der Gesamtfläche vier zusammenhängende Teilgebiete ausgewählt und geprüft, ob sich diese der jeweils gültigen Poissonverteilung anpassen. Wie man aus Abb. 7 sieht, ist dies in allen 4 Fällen mit genügender Genauigkeit der Fall, was bedeutet, daß die Aktivität in jedem Gebiet als homogen angesehen werden kann. In jedem Teilgebiet wurde nun eine Längenstatistik der Bahnspurprojektionen aufgenommen und die Ergebnisse in Tabelle 7 zusammengestellt. Die Meßwerte wurden auf den Wert bei $r_0 = 6{,}6\,\mu$ normiert und erlauben so in Verbindung mit Tabelle 3a eine Abschätzung des Thorium-Uran-Verhältnisses. Hiermit läßt sich dann nach Gleichung (11) auf die spezifische Aktivität eines jeden Feldes schließen. Dazu wird angenommen:

Feld I $[\mathrm{Th}] = 0$ $\quad Z_1(\sigma r_0) = [\mathrm{U}]_1 J_{\mathrm{U}}(\sigma r_0)$

Feld II $[\mathrm{Th}] = 0$ $\quad Z_2(\sigma r_0) = [\mathrm{U}]_2 J_{\mathrm{U}}(\sigma r_0)$

Feld III $[\mathrm{Th}] = 0{,}5\,[\mathrm{U}]$ $\quad Z_3(\sigma r_0) = [\mathrm{U}]_3 \{J_{\mathrm{U}}(\sigma r_0) + 0{,}5\, J_{\mathrm{Th}}(\sigma r_0)\}$

Feld IV $[\mathrm{Th}] = 2\,[\mathrm{U}]$ $\quad Z_4(\sigma r_0) = [\mathrm{U}]_4 \{J_{\mathrm{U}}(\sigma r_0) + 2\, J_{\mathrm{Th}}(\sigma r_0)\}$

Hieraus ergeben sich die $[U]_i$, wenn man

$$\begin{aligned} \psi_{(ZrSiO_4)} &= 6{,}96 \\ \text{Belichtungszeit} &= 449{,}5\ \text{Std} = 1{,}618 \cdot 10^6\ \text{sec} \\ \text{Fläche} &= \text{Feldzahl} \cdot 132 \cdot 132 \cdot 10^{-8}\ \text{cm}^2 \end{aligned}$$

und die Meßwerte für $r_0 = 6{,}6\ \mu$ zugrunde legt (s. Tabelle 8).

Die uneinheitliche Kristallnatur kommt weniger stark in der Spurenverteilung über die Fläche zum Ausdruck, sondern besonders deutlich im Thoriumgehalt der Komponenten. Der Urangehalt nimmt deutlich von der einen Seite des Kristalls her ab, während der Thoriumgehalt gleichzeitig von Null auf einen endlichen Wert anwächst. Es liegt also der Schluß nahe, daß die beiden Teile des Kristalls zu verschiedenen Zeiten gebildet sind.

5. Zusammenfassung

1. Es wurde für ein homogenes Material für die Auflagemethode die Häufigkeit der austretenden Bahnspuren in Abhängigkeit von der Projektion der Restreichweite berechnet.

2. Es werden Formeln angegeben, um aus der Dichte der Spuren auf den Gehalt an strahlenden Elementen zu schließen. Durch Untersuchung von einem Stück Uranmetall, einer Uranpechblende und einem Monazitkristall wurden die gefundenen Formeln für die Längenstatistik der Bahnspurprojektionen bestätigt und dabei der spezifische Gehalt von Uran in der Pechblende und von Thorium im Monazit bestimmt.

3. Es wird eine Methode entwickelt, die erlaubt, wenigstens die Größenordnung des Uran-Thoriumverhältnisses in einem homogenen Material aus der Längenstatistik der Bahnspurprojektionen zu ermitteln.

4. An zwei großen Kristallen (einem Monazit und einem Zirkon) wurde durch Vergleich der Bahnspurdichte mit einer statistischen Poissonverteilung für begrenzte Gebiete der Größenordnung einiger Quadratmillimeter die Homogenität des Einbaues strahlender Elemente festgestellt. Ferner wurden bei beiden Krystallen langsam veränderliche Schwankungen in der Aktivität und beim Zirkon im Th/U-Verhältnis gefunden.

Den Herren Prof. Dr. C. W. Correns, Prof. Dr. H. Schumann und Prof. Dr. H. Winkler vom Mineralogischen Institut der Universität Göttingen sind wir dankbar für die Überlassung der untersuchten Mineralien und ihnen sowie Herrn Dr. E. Picciotto für zahlreiche anregende Diskussionen. Herrn Dr. M. Teucher vom Max-Planck-Institut für Physik, Göttingen, für seine wertvolle Hilfe durch technische Ratschläge und den Optischen Werken Ernst Leitz, Wetzlar, insbesondere den Herren Ludwig Leitz und Dr. H. Claussen, für die großzügige Unterstützung der Arbeit mit optischen Hilfsmitteln.

Literatur

[1] Vgl. Baranov, V. I. u. Kretschmer, S. I.; Compt. rend. acad. sci. URSS. 1935 **1** 543. I. Curie J. Phys. et Ra. VII 11 (1946). Picciotto, E.; s. [3]. Eine vollständige Bibliographie und zahlreiche technische Einzelheiten s. H. Yagoda, Radioactive Measurements with Nuclear Emulsions, New York

1949. [2] Im Rahmen der Arbeit werden nur diese betrachtet. [3] Picciotto, E.; Bull. de la Soc. belge de Géol., de Paléontol. et d'Hydrol. LVIII 1 S. 75. [4] Evans, R. D. u. Goodman, C.; Phys. Rev. 1944 **65** 216. [5] Definition siehe 2c. [6] Diese Formel ist weiterhin von Nutzen, wenn es sich darum handelt, etwa einen Dünnschliff zu untersuchen, dessen Dicke geringer ist als die maximale Reichweite der emittierten Teilchen. Man wird dann nach der Formel ein minimales r_0 finden können, oberhalb dessen sich die Längenstatistik der Bahnspurprojektionen und die Aktivitätsbestimmung durchführen läßt. [7] Kovaric u. Adams; Phys. Rev. 1938 **54** 713. [8] Nier; Phys. Rev. 1939 **55** 153. [9] Urry; Trans. N. Y. Acad. Sci. II, 1948 **10** 63. [10] Picciotto, E.; C. R. [11] Dieser Wert wird übereinstimmend von den Ilford-Werken (Ilford Research Laboratories, June 27th 1947) und von Yagoda S. 132 für C_2-Emulsionen angegeben. [12] Doelter; Handbuch der Mineralogie, IV 2 S. 910ff. [13] Guimaraes, D.; Bull. de la Soc. Géol. de France 1949 **19** 657. [14] Fenner; J. Am. Sci. 1928 **16** 382. [15] Picciotto, E.; Bull. du Centre de Phys. Nucl. de l'Univ. Libre de Bruxelles Note No. 16 (1950); Vgl. a.: Morgan, I. H. u. Auer, M. I.; Am. J. of Sci. 1949 **239** No. 1. Evans, R. D. u. Williams, H.; J. Am. Sci. 1935 **29** 441. Keevil, N. D., Larsen, E. S. u. Wank, F. J.; Am. J. of Sci. 1944 **242** 345. [16] Buttlar, H. v.; Diplomarbeit Göttingen, II. Phys. Inst. d. Universität (1950). [17] Houtermans, F. G.; Naturw. (1951).

Geochimica et Cosmochimica Acta, 1951, Vol. 2, pp. 62 to 75. Pergamon Press Ltd., London

Zur Geochemie des Kohlenstoffs

H. Borchert, Clausthal

(Received 14 May 1951)

ABSTRACT

The "small cycle" of carbon takes place between the atmosphere and the present organic world. For the "big cycle" in the lithosphere the most important processes are being characterized and a quantitative balance established. Some of the earlier data have to be corrected in essential points.

I. Das geochemische Verhalten des Kohlenstoffs in der Lithosphäre

In neuerer Zeit hat K. Kalle [1] eine quantitative Bilanz des Kohlenstoffs entwickelt, die in Abb. 1 wiedergegeben ist. Hierbei steht jedoch der äußere „kleine Kreislauf" stark bevorzugt im Mittelpunkt der Betrachtung, während der „große Kreislauf" des Kohlenstoffs in der Erdkruste nur mit wenigen Zahlen beteiligt ist.

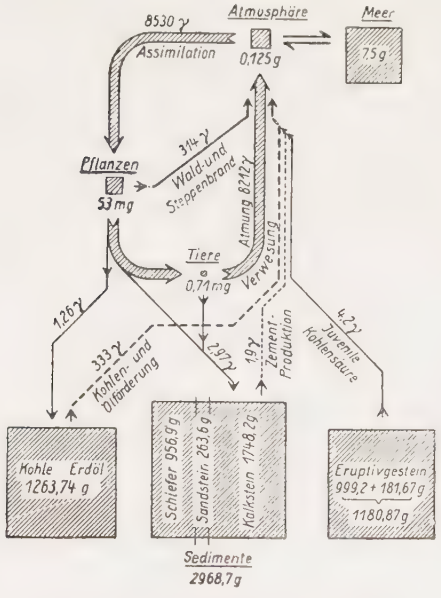

Abb. 1. Der Kreislauf des Kohlenstoffs (nach K. Kalle).

Bevor diese Zahlen im einzelnen näher untersucht werden sollen, mögen zunächst die Vorgänge der Fixierung von Kohlenstoff in der Lithosphäre und das Verhalten bei der Metamorphose an Hand von Abb. 2 gekennzeichnet werden.

Der fein gegliederte und quantitativ belegte „kleine Kreislauf" der Biosphäre mit der Atmosphäre ist hier auf einen kleinen Auszug beschränkt worden. Dagegen ist stärker hervorgehoben, daß sich in den ozeanen Räumen ein gewaltiger Kreislauf des Kalkes — als dem wichtigsten Kohlenstoffträger voll zieht; er ist wesentlich dadurch gekennzeichnet, daß in der kalten Tiefsee kalkuntersättigtes Wasser die Schalen der absinkenden Organismenreste auflöst (wobei die Verwesungskohlensäure beim Auflösen hilft!) und warmes Oberflächenwasser wiederum durch Kalkübersättigung kalkschalenbauende Tiere zu intensiver Lebenstätigkeit anregt. Endgültige Fixierung des Kalkes in Sedimenten aber vollzieht sich überwiegend in flacheren warmen Meeresräumen. Die hier vorliegenden Verhältnisse sind ausgezeichnet von C. W. Correns [2] herausgearbeitet worden. In Festlandnähe wird der kalkreiche „Globigerinenschlamm" durch reichlicher Festlandsdetritus als „Blauschlick" „verdünnt"; roter Ton der tiefsten Meeresräume ist durch starke Herauslösung der Kalkschalen gekennzeichnet. In den mittleren Zwischenregionen ist der Globigerinenschlamm

das typische, äußerst kalkreiche Sediment. Im großen betrachtet, hat für quantitative Bilanzen *diese* Fixierung des Kalkes sicher das Übergewicht; im einzelnen aber wirken die gewaltigen Riffe heißer Flachseeregionen (Großes Barriere-Riff Australiens usw.) imposanter. — Die Aufklärung der äußerst komplizierten physikalisch-chemischen Verhältnisse der Kalksättigung sind durch die bahnbrechenden Untersuchungen von H. WATTENBERG [3] entscheidend gefördert worden.

Der Kohlenstoffanteil, welcher als organische Substanz in Sedimenten fixiert wird, ist wesentlich kleiner gegenüber der C-Bindung als Karbonat. Auf dem Schema

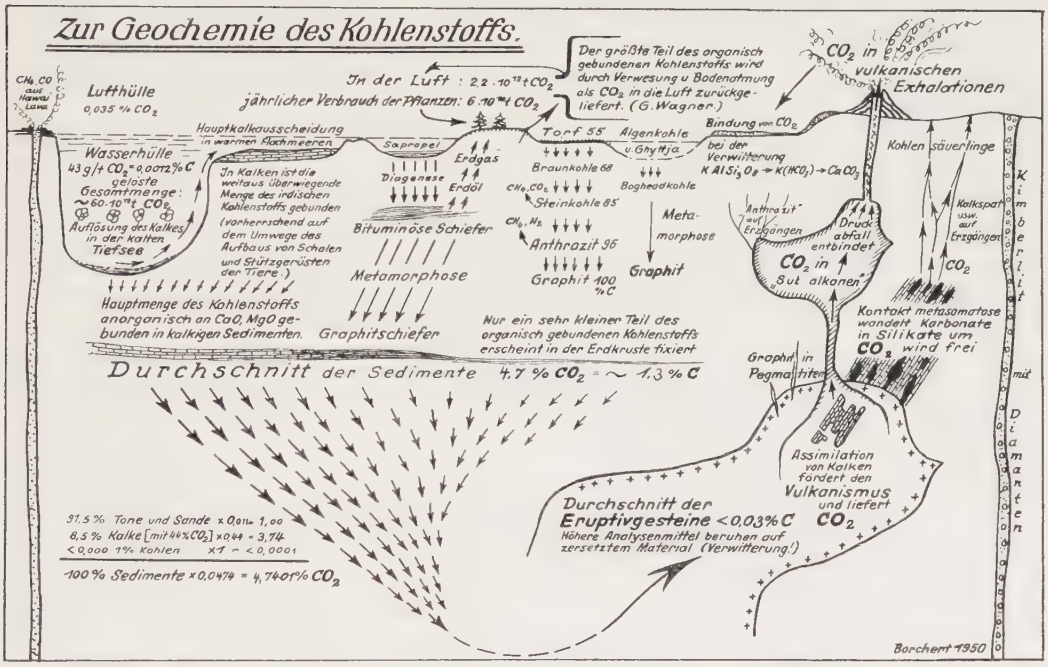
Zur Geochemie des Kohlenstoffs.
Lufthülle
0,035 % CO₂
In der Luft : 2,2 · 10¹² t CO₂
jährlicher Verbrauch der Pflanzen: 6 · 10¹⁰ t CO₂
Der größte Teil des organisch gebundenen Kohlenstoffs wird durch Verwesung u. Bodenatmung als CO₂ in die Luft zurückgeliefert. (G. Wagner.)
CO₂ in vulkanischen Exhalationen
Wasserhülle
43 g/t CO₂ = 0,0012 % C
gelöste Gesamtmenge: ~60 · 10¹⁵ t CO₂
Auflösung des Kalkes in der kalten Tiefsee
Hauptkalkausscheidung in warmen Flachmeeren
In Kalken ist die weitaus überwiegende Menge des irdischen Kohlenstoffs gebunden (vorherrschend auf dem Umwege des Aufbaus von Schalen und Stützgerüsten der Tiere.)
Sapropel
Diagenese
Erdgas
Erdöl
Bituminöse Schiefer
Metamorphose
Graphitschiefer
Torf 55
Algenkohle u. Gyttja
Braunkohle 68
Bogheadkohle
Steinkohle 85
Anthrazit 96
Graphit 100 % C
Meta-morphose
Graphit
Bindung von CO₂ bei der Verwitterung
K Al Si₃ O₈ → K(HCO₃) → Ca CO₃
Kohlensäuerlinge
Anthrazit auf Erzgängen
Druck-abfall entbindet
CO₂ in Sut alkanen
Kalkspat usw. auf Erzgängen
CO₂
Kimberlit
Kontakt metasomatose wandelt Karbonate in Silikate um
CO₂ wird frei
Graphit in Pegmatiten
mit Diamanten
Hauptmenge des Kohlenstoffs anorganisch an CaO, MgO gebunden in kalkigen Sedimenten.
Nur ein sehr kleiner Teil des organisch gebundenen Kohlenstoffs erscheint in der Erdkruste fixiert
Durchschnitt der Sedimente 4,7 % CO₂ = ~ 1,3 % C
Assimilation von Kalken fördert den Vulkanismus und liefert CO₂
Durchschnitt der Eruptivgesteine < 0,03 % C CO₂
Höhere Analysenmittel beruhen auf zersetztem Material (Verwitterung!)
91,5 % Tone und Sande x 0,01 = 1,00
8,5 % Kalke [mit 44 % CO₂] x 0,44 = 3,74
< 0,000 1 % Kohlen x 1 = < 0,0001
100 % Sedimente x 0,0474 = 4,74 % CO₂
Borchert 1950

Abb. 2. Das Verhalten des Kohlenstoffs in der Lithosphäre.

sind die Bildungsbedingungen von Erdölmuttergesteinen (vgl. die Zusammenfassung von K. KREJCI-GRAF [4]) angedeutet, ebenso wie die Bildung von Algenkohlen und Torf in Gebieten, deren säkulare Absenkung bei hohem Grundwasserstand gerade *das* Ausmaß hat, daß das Pflanzenwachstum damit Schritt halten kann. Zu geringe Absenkung führt zu Oxydation und Verwesung des jährlich produzierten „Holzes": zu starke Absenkung bedingt zu starke Verdünnung durch „gewöhnliche Sedimente" (Tone und Sande) in dann wassererfüllten Senken.

Es sei jedoch an dieser Stelle gleich hervorgehoben, daß solche Übergangsbedingungen — wo also nicht ein mächtiges Torflager geschaffen wird, sondern spärlich eingestreute Organismenreste in einer Unmasse von „normalen Sedimenten" in solcher Verdünnung enthalten sind, daß an eine Gewinnung solcher „Kohlenflöze" oder Bitumenreste nie gedacht werden kann, in der Gesamtbilanz eine entscheidende Rolle spielen; gewinnbare Kohlen und Erdöle machen nur einen geringen Bruchteil des in der Erde fixierten Kohlenstoffs aus.

Bei der Metamorphose von Faulschlämmen, Gyttjen und Torfen spielen sich die bekannten Veränderungen ab, die in der Bildung von hexagonalem Graphit ihr Endglied haben. Die geologischen Bedingungen solcher Veränderungen durch Druck- und Temperaturerhöhung — wesentlich ist offenbar mehr die Temperatur als der Druck, wie eine soeben erschienene Arbeit von M. u. R. Teichmüller [5] belegt — können hier nicht genauer gekennzeichnet werden; Versenkung der organogenen Sedimente in tiefere Regionen der Erdkruste in absinkenden Sedimentationströgen bringt das Wesentlichste hervor; Gebirgsfaltung und Heizung durch eindringende Magmen wirken als weitere Faktoren der Metamorphose. Eine starke Abgabe von Wasser, CO_2 und CH_4 aus torfartigen Sedimenten und eine Mobilisation von gasförmigen Kohlenwasserstoffen und flüssigen Erdölen aus Faulschlämmen ist die Folge, die in allen Fällen in den Gesteinen einen immer C-reicheren Rückstand zurückläßt.

Im Endergebnis wandeln sich alle organischen Verbindungen schließlich in Graphit um, wobei wiederum der Anteil, der für die geochemische Bilanz quantitativ ausschlaggebend ist, nicht durch die wenigen „Schungit"-Flöze (aus wesentlich Humuskohle) und die abbaufähigen Graphitlager in kristallinen Schiefern (vielfach aus ehemaligen Faulschlämmen entstanden) gebildet wird. Mengenmäßig hervorragend sind auch hier wieder die mehr oder weniger verdünnt vorliegenden „Graphit-Flitter" in der überwiegenden Masse der „normalen" kristallinen Schiefer.

Festzuhalten ist im großen, daß der Hauptanteil des C-Gehaltes der Erdkruste als Karbonat vorliegt. Dieses Kalkkarbonat bleibt bis zum Metamorphosestadium „epizonaler kristalliner Schiefer" weitgehend erhalten. Dann aber vollzieht sich zunehmend die Umwandlung von Karbonat in Silikat. Hierbei müssen entsprechend große Mengen von Kohlensäure frei werden und aufsteigen, die teilweise als Bikarbonatlösungen bei abnehmenden Temperaturen und Drucken zur Wiederausscheidung von Kalkspat in Mineralgängen führen können, der sicher weitaus größere Teil aber erreicht in Form von Mofetten und Kohlensäuerlingen die Erdoberfläche und wird damit dem Kreislauf der Atmosphäre zurückgegeben. Diese Zusammenhänge werden weiter unten quantitativ verfolgt werden.

Um die Darstellung der Vorgänge aber nicht zu kompliziert werden zu lassen, ist die Metamorphose der Sedimente — ohne die eben angedeuteten Zwischenphasen der Bildung kristalliner Schiefer — gleich bis zum Stadium der Ultrametamorphose, d. h. der Wiederaufschmelzung, durchgeführt worden. Daß solche Bedingungen der Wiederaufschmelzung stets dann gegeben sind, wenn normales Sialkrustenmaterial in Geosynklinalregionen in mehr als rund 20 km Tiefe versenkt wird, ist in einer Arbeit von H. Borchert und E. Tröger [6] näher ausgeführt. Das geochemisch wichtigste Ereignis der gesamten Metamorphosevorgänge für den Kohlenstoff ist jedenfalls, daß — spätestens bei der tatsächlichen Wiederschmelzung — die weitaus überwiegende Menge sowohl des elementaren wie des Karbonatkohlenstoffs in Form von CH_4, CO und insbesondere CO_2 mobilisiert wird.

Über die Gleichgewichte der hierbei ablaufenden C-Reaktionen ist leider sehr wenig bekannt. Die entsprechenden Systeme CO_2 — CO — C — CH_4 — H_2 — H_2O müßten bei Temperaturen von 700—1200° und Drucken von 5—10000 atm und in Gegenwart von SiO_2, FeO, S, H_2S usw. untersucht werden. Wir verdanken T. A. Jaggar [1] der bahnbrechend bei der Probenahme und Untersuchung von Gasproben der Hawaii-Vulkane gewirkt hat, eine gründliche Studie über die Zusammensetzung dieser Gase, wobei auf den Mangel an gründlichen einschlägigen physikalisch-chemischen Untersuchungen dringlich hingewiesen wird. Diese Vorgänge in den

Silikatschmelzen sind auch für die Geochemie des Kohlenstoffs derart bedeutsam, daß ich die Probleme an Hand einer „reinen Papierchemie" herausstellen möchte, um damit gründliche Studien anzuregen.

$$
\begin{aligned}
C &+ H_2O \rightleftharpoons CO + H_2\\
2\,C &+ 2\,H_2O \rightleftharpoons CO + CH_4\\
2\,CH_4 &+ H_2O \rightleftharpoons CO + CH_4 + H_2\\
3\,C &+ 2\,H_2O \rightleftharpoons CO_2 + CO + CH_4\\
CO_2 &+ H_2 \rightleftharpoons CO + H_2O + 10000\ \text{cal}\\
FeO &+ H_2O \rightleftharpoons Fe_3O_4 + H_2 + 15400\ \text{cal}\\
2\,SiO_2 &+ 3\,CH_4 \rightleftharpoons 2\,SiH_4 + 3\,CO + H_2O + H_2
\end{aligned}
$$

Bei zwei der obigen Gleichungen konnte die Wärmetönung aus der Arbeit von T. A. Jagger entnommen werden, der außerdem zu der vorletzten Gleichung bemerkt, daß die Umsetzung von links nach rechts über 570° steigende Bedeutung gewinnt.

T. A. Jagger betont die bedeutsame Beteiligung von Wasserstoff in „vulkanischen Gasen", deren höchst wechselnde Zusammensetzung bisher jeglichen Versuchen einer klaren Unterscheidung zwischen „juvenilen" und „vadosen" Komponenten getrotzt hat. Erwarten sollte man nach allgemeiner heutiger Auffassung, daß die Gase der doch sicher „maximal juvenilen" Basalte Hawaiis am allerbesten die Zusammensetzung wirklich „juveniler Gase" widerspiegeln sollten und gerade bei diesen glaubte E. S. Shepherd [8] resigniert feststellen zu müssen, daß dies völlig unmöglich sei, wegen vielfacher Umsetzungen mit Zwischenkondensationsprodukten und tiefreichenden Oxydationsprozessen durch Beteiligung atmosphärischer Luft.

Tatsache ist, daß in den Hawaii-Gasen CO_2 eine überragende Rolle spielt, während CH_4 und H_2 nur in ganz geringen Mengen beteiligt sind. Gerade von Basalten, die sicher aus tieferen Regionen der Erdkruste stammen als die saueren Andesite oder Granite, aber sollte man erwarten, daß sie das niedrigste Oxydationspotential demonstrieren sollten, daß sie am meisten CH_4 und H_2 aufweisen sollten und nur wenig CO_2, SO_2 oder gar SO_3. Tatsache ist nun aber, daß gerade die sauren Gesteine und Laven vielfach die höchsten Gehalte an H_2 und CH_4 aufweisen (z. B. Gase des Andesit-Domes des Mt. Pelée und der sauren Andesite von Santorin).

Die Erklärung dieser Tatsache dürfte aus der Perspektive der Auffassung, daß Andesite, Rhyolithe und Granite durch fraktionierte Kristallisation rein juveniler subkrustaler Magmen entstanden seien, sehr schwer sein. Aus der Perspektive, daß die sauren Magmen und Gesteine ganz überwiegend aus der Wiederaufschmelzung von Sedimenten hervorgegangen sind, wird der tatsächliche Sachverhalt leichter verständlich: erst im Laufe der Erdgeschichte ist es, *seit es Organismen gibt*, zur Fixierung wesentlicher Mengen von elementarem Kohlenstoff in Sedimenten gekommen (vorher gab es eine wahrscheinlich CO_2-reiche, sauerstoffarme Atmosphäre!). Erst seit solche Sedimente in den tieferen Krustenkreislauf einbezogen wurden, wurde ein stärker reduzierendes Milieu in tiefere Erdkrustenteile getragen. Erst die Wiederaufschmelzung solchen relativ SiO_2-reichen Sial-Materials konnte *und kann heute noch* die CH_4- und H_2-reichsten Gase liefern. So ergibt sich aus der Betrachtung der Geochemie des Kohlenstoffs wiederum ein kleines weiteres Argument für die Grundauffassung, daß die weitaus überwiegende Menge der Granodiorite bis Granite *palingenen* und *nicht juvenilen Ursprungs* ist.

Im großen und ganzen ist unter den Gasen, die in der Tiefe unter hohen Drucken homogen in die Schmelzen aufgenommen werden und die erst beim Aufsteigen dieser Magmen und Durchbrüchen an die Erdoberfläche (Drucknachlaß!) als Gase entbunden werden, CO_2 weitaus häufiger als CO und CH_4. Die Begründung ergibt sich aus der bisher schon behandelten Geochemie des Kohlenstoffs: Karbonatkohlenstoff ist ungleich häufiger als elementarer C, der sich mit H_2O bei hohen Temperaturen *und Drucken* zu CH_4, CO usw. umsetzen könnte. Daß die Zusammensetzung gerade auch der vulkanischen Gase in so außerordentlich weiten Grenzen schwankt, hat seine wesentlichste Begründung in dem örtlich sehr verschiedenen Aufschmelzungsmaterial. Bei aller Anerkennung sekundärer und tertiärer Gasreaktionen beim Aufstieg durch die höhere Erdkruste wäre eine *derart verschiedene* Zusammensetzung der „juvenilen" Gase nicht zu verstehen, wenn *ein* juveniles subkrustales Magma der mengenmäßig ausschlaggebende Bestandteil des Magmatismus wäre.

Kurz hingewiesen sei auf die CO_2-Mobilisation durch Kontaktmetasomatose und auf die Rolle, welche Kalkassimilation vielfach auf den Einzelablauf vulkanischer Erscheinungen ausübt. Das klassische Beispiel hierfür ist durch A. Rittmann [9] der Vesuv geworden.

Für die Grobübersicht der Geochemie des Kohlenstoffs ist mit der Kohlensäure, welche durch Vulkane sowie durch entsprechende postvulkanische Mofetten und Kohlensäuerlinge wieder in die Lithosphäre geliefert wird, der „große Kreislauf" des Kohlenstoffs in der Lithosphäre geschlossen. Quantitativ spielen offenbar die CO_2-, CO- und CH_4-Mengen, die mit den wohl wirklich juvenilen Basalten an die Atmosphäre geliefert werden, sicher eine recht untergeordnete Rolle. Daß aber Kohlenstoff dennoch auch in der Geochemie der tieferen Erdkruste beteiligt ist, wird unmittelbar durch die Tatsache des Auftretens von Diamanten in den Kimberlitschloten belegt und indirekt weist darauf die Tatsache, daß die Steinmeteoriten nach W. Noddack [10] durchschnittlich 0,039 % C aufweisen und daß auch die Eisenmeteoriten einen mittleren Gesamt-C-Gehalt von 0,034 % haben.

Der Anteil von intrakrustalen Ausscheidungen von Kohlenstoff aus magmatischen Restlösungen spielt mengenmäßig keine Rolle, ist aber geochemisch doch recht interessant. Gelegentlich kann es in solchem Zusammenhang ja bekanntlich doch sogar zu bauwürdigen Graphitlagerstätten in Pegmatiten kommen (Ceylon, Madagaskar usw.). Die einfachste Umsetzungsgleichung dafür lautet $CH_4 + CO_2 \rightleftharpoons 2\,C + 2\,H_2O$.

Daß solche C-Verbindungen auch noch im hydrothermalen Bereich vorkommen, zeigt das nicht seltene, wenn auch mengenmäßig völlig belanglose Auftreten von „Anthrazit" auf vielen Erzgängen. Es ist sicher kein Zufall, daß die berüchtigte Co-Ni-Ag-Bi-U-Erzformation besonders durch derartige „mineralogische" Funde ausgezeichnet ist.

Rein anorganisch nach der obigen Gasgleichung entstanden ist sicher auch der „Anthrazit", der sich örtlich reichlicher im Verband der Roteisenerze des Lahn-Dill-Typus findet. Während der Kohlenstoff, welcher in der Torf-Fazies und in der marinen Faulschlammfazies entstanden ist, ein jeweils höchst charakteristisches Spektrum von Spurenelementen aufweist, das vom Verfasser gleichzeitig mit V. M. Goldschmidt, K. Krejci-Graf und H. Witte [11] untersucht worden ist und daher nicht zur Veröffentlichung gekommen ist, sind die „submarin-exhalativen" Anthrazite des Lahn-Dill-Typus ganz ungewöhnlich frei von Verunreinigungen; sie sind auch für die Maßstäbe empfindlicher Quarzspektrographen „rein" wie reinste Spektralkohle.

II. Quantitative Bilanz der Geochemie des Kohlenstoffs

Nach diesem Überblick über das geochemische Verhalten des Kohlenstoffs im Kreislauf der Lithosphäre soll im folgenden nun eine quantitative Bilanz versucht werden.

Nach F. W. Clarke [12] verdanken wir V. M. Goldschmidt [13] die ersten Grundlagen zu quantitativen Bilanzen der äußeren Erdhüllen. Indem V. M. Goldschmidt (*loc.cit.* S. 128—136) für die drei Elemente Na, Ca und Mg die Verteilung in den Eruptivgesteinen, in den Sedimenten und im Meerwasser erfaßte, ermittelte er den Gesamtstoffumsatz im Verlauf der Erdgeschichte. Es ergeben sich handliche Zahlen, wenn man diesen Umsatz stets in Gramm je 1 cm^2 Erdoberfläche (g/cm_e^2) ausdrückt.

Wenn man mit C. W. Correns [14] die Menge der verwitterten Eruptivgesteine mit E, die der daraus entstandenen Sedimente mit S, die des Meeres mit M bezeichnet und wenn man für ein Element X die prozentualen Gehalte in den Eruptivgesteinen mit e_x, in den Sedimentgesteinen mit s_x und im Meerwasser mit m_x kennzeichnet, so ergibt sich die einfache Bilanz der quantitativen Verteilung eines Elementes X als

$$E \cdot e_x = S \cdot s_x + M \cdot m_x .$$

Bei der Durchrechnung ist für die Kohlenstoffbilanz sehr wichtig, daß V. M. Goldschmidt für die Elemente Ca und Mg den karbonatischen und silikatischen Anteil scharf getrennt hat (*loc.cit.* S. 131, 133, 135). Tonschiefer und Sandsteine sind demgemäß Ca-Mg-karbonatfrei angesetzt worden, indem deren tatsächlicher Gehalt an solchen Karbonaten auf reine Kalke und Dolomite umgerechnet worden ist. Durch die Nichtberücksichtigung dieser Tatsache kommt K. Kalle (*loc.cit.* S. 205/206) zu falschen Zahlen für den C-Gehalt der Sedimente; sie liegen zu hoch, weil $CaCO_3$ und $(CaMg)CO_3$ doppelt in Ansatz gebracht worden sind. Die Gesamtbilanz von V. M. Goldschmidt besagt, daß je cm_e^2 160 kg Eruptivgesteine im Laufe der Erdgeschichte zerfallen sind in 155 kg Tonschiefer und Sandstein (karbonatfrei gerechnet!), 10,2 kg Kalkstein und 4,4 kg Dolomit. Ergänzend hat W. v. Engelhardt [15] eine weitere saubere Trennung der Tonkomponente in rein tonige Sedimente und tonfreie Sandsteine durchgeführt, deren Anteil dann 87 bzw. 13 % beträgt.

Tabelle 1. Im Laufe der Erdgeschichte sind aus 190 kg/cm_e^2 Eruptivgesteinen die folgenden Sedimente entstanden

Komponenten	*Menge* *kg/cm_e^2*	*Mächtigkeit* *m*
Tonschiefer	184	700
Sandstein	27	100
Kalk	13,6	50
Dolomit	5,4	20
Gesamtsedimente . .	230	870

In einer umfassenden Betrachtung der geochemischen Bilanz hat C. W. Correns [14] erhärtet, daß die Größenordnung des Stoffumsatzes von V. M. Goldschmidt sicher richtig getroffen ist. C. W. Correns hat für die vier Elemente Na, K, Ca und Mg obere und untere Grenzwerte der Verteilung berechnet. Die mögliche Streuung dieser Werte zeigt nun in der graphischen Darstellung von C. W. Correns (*loc.cit.* S. 8) einen deutlichen Schwerpunkt der wahrscheinlich besten Werte, der besagt, daß im Laufe der Erdgeschichte tatsächlich 190 kg/cm_e^2 Eruptiva in 230 kg Sedimente zerfallen sind. Es scheint mir sinnvoll und notwendig, diesem Sachverhalt Rechnung zu tragen, um damit zu einer immer besseren Gesamtbilanz aller Stoffe und Elemente zu kommen. Die obenstehende Tabelle gibt die derart korrigierten Werte, wobei über die letzte Dezimale stets derart abrundend verfügt wurde, wie es der Genauigkeit der Zahlenwerte (u. a. auch für die Gesteinsdichten) tatsächlich entspricht; man sollte sich in der Geochemie von dem Ballast der 3. und 4. Dezimalen frei machen.

Es braucht hier nicht näher ausgeführt zu werden, daß es sich hierbei in erster Linie um Erfassung des Stoffhaushaltes im Verlauf der Erdgeschichte handelt. Für den tatsächlichen durchschnittlichen Aufbau der Erdkruste ist neben der sehr verschiedenen Zusammensetzung der einzelnen Krustenteile zu berücksichtigen, daß

die Zersetzung von Magmatiten zu Sedimenten und die Umsetzung von Sedimenten in kristalline Schiefer und Eruptivgesteine einzelne Teile mehrfach erfaßt haben kann. Entscheidend ist jedoch, daß aus solchen Bilanzen mit einiger Sicherheit zu entnehmen ist, z. B. wieviel Kohlenstoff insgesamt als Karbonat im Laufe der Erdgeschichte in „jungen" Sedimenten festgelegt worden ist.

70 m Kalke und Dolomite haben mit ihren Anteilen von 13,6 kg Kalk und 5,4 kg Dolomit einen durchschnittlichen C-Gehalt von 12,3 %. So ergibt sich aus 70 m Karbonaten je cm^2 Erdoberfläche ein C-Gehalt der Sedimente von 2340 g. Der Gehalt an elementarem Kohlenstoff von 800 m tonigen und sandigen Gesteinen, der durch die Lebenstätigkeit von Organismen bebildet worden ist, wird vielfach zu hoch angesetzt; 0,9 % C sind zweifellos viel zu viel. V. M. Goldschmidt (*loc.cit.* S. 141) mit seiner umfassenden geochemischen Erfahrung hält 0,2 % C für die richtige Größenordnung; äußerstenfalls könnten es 0,5 % C sein.

Um im Endergebnis eine quantitative Bilanz der gesamten Erdkruste zu bekommen, wird im folgenden stets derart vorgegangen, daß ein wahrscheinlichster Mittelwert kalkuliert worden ist, dem obere und untere Grenzwerte gegenübergestellt werden. Für die tonig-sandigen Sedimente ist dieser Mittelwert mit 0,3 % C angesetzt worden gegenüber oberen und unteren Grenzwerten von 0,9 % und 0,1 % C. Als Mittelwert enthalten demnach 211 kg Tonschiefer und Sandstein 633 g elementaren C je cm^2_e, während die Grenzwerte 1900 und 211 g C/cm^2_e lauten (vgl. Tabelle 2).

Für den äußeren Kreislauf des Kohlenstoffs dürfen die quantitativen Daten von K. Kalle (*loc.cit.* S. 205) als beste Zusammenfassung der bisherigen Ermittlungen betrachtet werden. Wenn wir nunmehr aber die genaueren Gehalte der gesamten Lithosphäre ermitteln wollen, so müssen zunächst die grundlegenden Voraussetzungen erörtert werden. Die geochemischen Erwägungen beziehen sich vorherr-

Tabelle 2

		km	*kg/cm^2_e*	*Maximalwerte* C %	*Maximalwerte* C *g/cm^2_e*	*Mittelwerte* C %	*Mittelwerte* C *g/cm^2_e*	*Minimalwerte* C %	*Minimalwerte* C *g/cm^2_e*
Kalk und Dolomit		**0,07**	**19**	12,3	2340	**12,3**	**2340**	12,3	2340
Tonschiefer und Sandstein . . .		**0,80**	**211**	0,9	1900	**0,3**	**633**	0,1	211
A. Gesamtsedimente		**0,87**	**230**	1,84	4240	**1,3**	**2973**	1,1	2551
B. kristalline Schiefer	I	8	2240	0,2	4480	0,1	2240	0,05	1120
	II	**7**	**1960**	0,2	3920	**0,1**	**1960**	0,05	980
	III	6	1680	0,2	3260	0,1	1680	0,05	840
C. Granodiorite bis Granite (palingene Eruptiva)	I	5	1350	0,09	1215	0,03	405	0,01	135
	II	**7**	**1890**	0,09	1701	**0,03**	**567**	0,01	189
	III	9	2430	0,09	2187	0,03	729	0,01	243
D. Basalte, Quarzgabbros bis Dunite	I	2,13	618	0,03	186	0,01	62	0,003	19
	II	**1,13**	**328**	0,03	99	**0,01**	**33**	0,003	10
	III	0,13	38	0,03	11	0,01	4	0,003	1
16 km = Erdkruste		**16,00**	**4408**	0,23	10121	**0,13**	**5533**	0,08	3635

schend auf eine 16 km dicke Kruste. Diese besteht neben den Sedimenten aus kristallinen Schiefern, sauren Eruptivgesteinen (Granodiorite bis Granite) und basischen Magmatiten (Basalte, Quarzgabbros bis Dunite).

In der Tabelle 2 sind für diese Gruppen der wichtigsten Gesteinstypen die Gehalte an Gesamtkohlenstoff geschätzt worden, also Karbonatkohlenstoff + elementarer Kohlenstoff. Mangels wirklich repräsentativer Durchschnittsanalysen haben alle diese Zahlen einen erheblich größeren Unsicherheitsfaktor. So sind die kristallinen Schiefer mit einem Mittelwert von 0,1 % C veranschlagt, bei einem oberen Grenzwert von 0,2 % und einem unteren von 0,05 % C. Hierbei ist zu berücksichtigen, daß epizonale kristalline Schiefer infolge höherer Karbonatanteile und auch höherer elementarer C-Gehalte sicher höhere Durchschnittswerte aufweisen, während meso- und katazonale kristalline Schiefer ebenso sicher unter den angenommenen Werten liegen werden.

Die Eruptivgesteine erscheinen in ihren Analysen meist mit zu hohen C-Werten infolge eines Karbonatanteils, der wesentlich erst durch Zersetzungs- und Verwitterungsprozesse hineingekommen ist. Für die sauren Eruptivgesteine mit der Hauptmasse der Granodiorite bis Granite scheinen Werte zwischen 0,09 und 0,01 mit einem Mittelwert von 0,03 % C angemessen. Für die basischen Magmatite in Gestalt von Basalten, Quarzgabbros bis Duniten sind Grenzwerte von 0,03 und 0,003 % C mit einem Mittelwert von 0,01 % C angesetzt worden.

Wenn wir nun die C-Gehalte der 16 km dicken Erdkruste quantitativ erfassen wollen, so müssen die Mengenanteile der vier obigen wichtigsten Gesteinsfamilien bekannt sein. Das ist nun ganz und gar nicht zutreffend. Herkömmlich rechnet man bei geochemischen Erwägungen mit 95 % Eruptivgesteinen und 5 % Sedimentgesteinen. Es weiß nun jeder, daß dies falsch ist, indem in die „Eruptivgesteine" normalerweise stets die kristallinen Schiefer einfach eingerechnet werden, obwohl wiederum jeder weiß, daß die Durchschnittszusammensetzung der kristallinen Schiefer mit Sicherheit nicht dem „Durchschnitt der Eruptivgesteine" entspricht. Wie der Durchschnitt der Eruptivgesteine zusammengesetzt ist, weiß man aus dem Durchschnitt nach F. W. Clarke [12] und noch besser aus dem gewogenen Durchschnitt von J. H. L. Vogt [16]. Diese Eruptivgesteine sind aus mancherlei Gründen in Granodiorite bis Granite einerseits und Basalte, Gabbros bis Dunite andererseits aufgeteilt worden, wobei hier nur deren C-Gehalte interessieren.

Es ist hier nun erstmalig versucht worden, die tatsächlichen Anteile der Eruptivgesteine und der kristallinen Schiefermengen mengenmäßig nach ihren Anteilen am Aufbau der 16-km-Kruste abzuschätzen, um damit zu den wahrscheinlichsten C-Werten zu gelangen.

Die Grundlage dieser Abschätzung ist die einigermaßen gesicherte Bilanz einer durchschnittlichen Beteiligung von 870 m Sedimenten. Die Anteile der übrigen Gesteine sind jeweils mit oberen, mittleren und unteren Grenzwerten veranschlagt worden. Abb. 3 gibt eine Übersicht dier Mengenabschätzungen, wobei die im folgenden erläuterten mittleren Gehalte in Gramm je cm^2 Erdoberfläche (g/cm^2) umgerechnet und mit eingetragen sind. Tabelle 2 gibt die entsprechenden Zahlenwerte. *Fett gedruckt sind die Mittelwerte*, die einstweilen als die wahrscheinlichsten angenommen werden dürfen und die als Grundlage für die geochemische Bilanz des Kohlenstoffs benutzt werden sollen.

Eine letzte Voraussetzung zur Aufstellung einer solchen Bilanz des Kohlenstoffs muß noch erörtert werden. Wenn die kristallinen Schiefer im Mittel mit 7 km Mächtigkeit und 0,1 % C-Gehalt und entsprechend mit 1960 g cm^2, Kohlenstoff angesetzt sind, so bedeutet das, daß ihr jetziger Gehalt diesem Wert entspricht. Es ist jedoch klar, daß diese kristallinen Schiefer (ganz überwiegend) aus Sedimenten hervorgegangen sind. Man könnte zunächst rechnen, daß die kristallinen Schiefer ursprünglich den gleichen durchschnittlichen C-Gehalt wie die derzeitigen nichtmetamorphen Sedimente gehabt hätten. Das würde ergeben, daß in 7 km kristallinen Schiefern ursprünglich 23900 g/cm^2_e enthalten gewesen wären, die bei der Metamorphose bis auf den derzeitigen Gehalt von 1960 g/cm^2_e als CO_2 und CH_4 mobilisiert worden wären. Das wäre jedoch sicher ein falscher Ansatz.

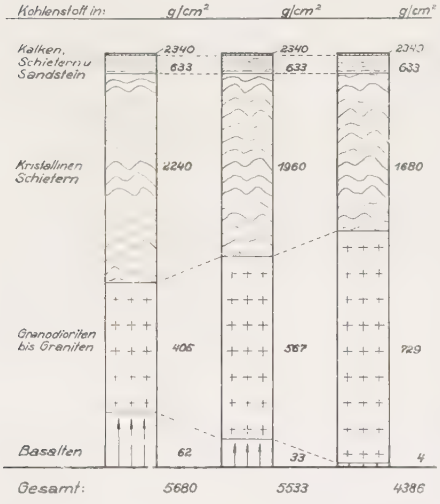

Abb. 3. Die Beteiligung von nichtmetamorphen Sedimenten, kristallinen Schiefern, sauren Eruptivgesteinen und basaltischen Differentiaten am Aufbau der 16-km-Erdkruste. Die beigegebenen Zahlen zeigen die durchschnittlichen Kohlenstoffgehalte.

Zu einer besseren Kalkulation kommt man, wenn man Intensität und Ablauf der geochemischen Prozesse während der ganzen Erdgeschichte berücksichtigt. W. Noddack [10] hat dies für die Erfassung des biochemischen Kohlenstoffkreislaufes getan und die von ihm ermittelten Zahlen haben größtenteils als Grundlage für die von K. Kalle ([1] S. 207) errechneten Werte gedient. W. Noddack betont mit Recht, daß die jetzige Lebensintensität nicht während der ganzen Erdgeschichte geherrscht hat und er berechnet die jährliche Produktion von Kalk (der ja auch größtenteils über den Umweg von Schalen und Stützgerüsten der Tiere zur Sedimentation gelangt ist) und organischem Kohlenstoff auf der Grundlage, daß die jetzige Lebensintensität nur während einem Viertel der Gesamtlebenszeit, d. h. während 250 Millionen Jahren, bestanden hat.

Grundsätzlich diesem Vorgehen folgend, darf man annehmen, daß in 1000 Millionen Jahren der rund 2 Milliarden Jahre währenden Erdgeschichte Verhältnisse geherrscht haben, die immerhin mit den heutigen schon vergleichbar sind. Die vielfach betonte Intensivierung vieler geochemischen Prozesse hat aber erst in der Devonzeit vor rund 400 Millionen Jahren mit der Besiedlung des Festlandes mit Landpflanzen angefangen, wodurch die Verwitterungsprozesse und damit insbesondere auch der Karbonatkreislauf ebenso angestiegen ist wie die Produktion an organischer Substanz. Dieser Prozeß hat ganz offensichtlich eine ständige Steigerung bis zur Gegenwart erfahren, wie neuerdings wieder von C. W. Correns ([14] S. 12) stark hervorgehoben worden ist.

Diese Tatsache aber muß sich auch entscheidend in den Durchschnittsgehalten der kristallinen Schiefer an elementarem und Karbonatkohlenstoff auswirken. Wenn es nun auch bekanntermaßen recht „junge" kristalline Schiefer gibt, die während der Jura-, Kreide- und Tertiärzeit erst sedimentiert worden sind, so wird der Großteil der kristallinen Schiefer doch von paläozoischen und präpaläozoischen Sedimenten

gebildet, für die wesentlich niedrigere Gehalte an Karbonat- und elementarem Kohlenstoff angesetzt werden müssen.

Führt man die Rechnung der Kohlenstoffbilanz für die Gesamtlebenszeit von rund 1 Milliarde Jahren durch, so wird für die kristallinen Schiefer für diese ganze Zeitspanne, die mit heutigen geochemischen Prozeßabläufen immerhin vergleichbar ist, mit ursprünglich nur $^1/_3$ des Durchschnittsgehaltes der jüngeren Sedimente gerechnet. Das ergibt als ursprünglichen Gehalt 8000 g/cm^2_r Gesamtkohlenstoff und würde bedeuten, daß in 10^9 Jahren 8000 — 1960 = 6040 g Kohlenstoff als CO_2 und CH_4 mobilisiert worden sind und in den Kreislauf der Atmosphere zurückgekehrt sind. Daraus errechnet sich ein Jahresdurchschnitt von 6,2 γ cm^2_e, der aus der Lithosphäre in den atmosphärischen Kreislauf zurückgekehrt ist, wenn man durch Kontaktmetasomatose noch 0,16 γ mobilisiert sein läßt.

Entsprechende Zahlen lassen sich für die Ultrametamorphose der kristallinen Schiefer zu palingenen sauren Eruptivgesteinen überschlagen. Beträgt der Anteil palingener Granodiorite bis Granite 7 km von der 16-km-Kruste und setzt man den ursprünglichen Gehalt dieses Materials in der gleichen Größenordnung an wie den der kristallinen Schiefer, so würden in 7 km ursprünglich 1960 g/cm^2_r Gesamtkohlenstoff enthalten gewesen sein. Vielleicht erscheint bei diesem Ansatz der ursprüngliche Gehalt reichlich hoch, da bekanntermaßen nur die epizonalen kristallinen Schiefer wesentliche Anteile von fein verteiltem Karbonatkohlenstoff aufweisen (Kalkphyllite usw.), während in der Mesozone schon stark der Umbau von Ca-Mg-Karbonaten in Ca-Mg-Silikate vor sich geht. An der Granitisation sind aber wesentlich katazonale kristalline Schiefer beteiligt, die ihren Karbonatkohlenstoff schon vorher weitgehend verloren haben. Wenn dennoch der obige Ansatz mit ursrpünglich gleichen Durchschnittsgehalten beibehalten worden ist, so war dafür der Gesichtspunkt leitend, daß kompakte Kalke und Dolomite (im Gegensatz zu Mergeln) sich äußerst resistent verhalten und daher erst bei wirklichen Wiederaufschmelzungsprozessen erfaßt werden. Die Ultrametamorphose setzt demnach 1960 — 567 = 1393 g/cm^2_e Kohlenstoff wieder in Freiheit, die in Form von wesentlich CO_2 aus Vulkanen in die Atmosphäre zurückgeliefert werden. Daraus resultiert ein Jahresdurchschnitt von $1{,}39 \cdot 10^9\,\gamma : 1 \cdot 10^9$ Jahre = 1,4 γ/cm^2_e.

Am unsichersten sind die Zahlenschätzungen, daß 1,13 km Basalt und Gabbro-Dunit 33 g/cm^2_e Gesamtkohlenstoff enthalten und daß ein Jahresdurchschnitt von 0,1 γ/cm^2_e aus solchen juvenilen Magmen als CO_2, CH_4 und CO in die Atmosphäre befördert worden ist.

Die soeben abgeleiteten Zahlen sind zusammenfassend auf Abb. 4 übersichtlich dargestellt. In dem Diagramm verarbeitet sind ferner die Daten über den biochemischen Kreislauf entsprechend dem Kohlenstoffkreislauf von K. Kalle ([1] S. 205). Neben einer Dezimalenabrundung, wie sie für geochemische Bilanzen sinnvoll ist, sind jedoch einige wichtige Daten über den Verwitterungskreislauf einbezogen worden. In der Abb. 4 sind alle jeweils auf kürzere Zeit (Pflanzen und Tiere) oder für längere Zeiträume fixierten oder konstanten C-Mengen in g oder mg je cm^2_r und gewöhnlich durch die Eintragung in festen Umrissen gekennzeichnet. Die γ-Werte entsprechen dem Jahresumsatz in millionstel Gramm je cm^2_e.

Es ist zunächst klar, daß bei der Verwitterung gewaltige CO_2-Mengen gebunden werden. G. Wagner [17] (S. 696) hat berechnet, daß die gesamte Luftkohlensäure

in Menge von 0,125 g/cm^2_e durch die Verwitterung einer knapp 2 cm dicken Feldspatschicht gebunden werden würde. Dabei werden zunächst wesentlich Alkalikarbonate gebildet, während die endgültige Fixierung des so gebundenen CO_2 vorherrschend in Form von Ca-Mg-Karbonaten und vorherrschend im Meer erfolgt. Wenn man berücksichtigt, daß die Erdkruste vorherrschend aus Feldspäten besteht und daß die sonst stark vertretenen Silikate in gleicher Weise bei der Verwitterung CO_2 binden, so besagt das, daß die Luftkohlensäure binnen sehr kurzer Zeit erschöpft sein würde, wenn nicht — abgesehen vom „kleinen Kreislauf" der Organismen — dauernd für Nachschub gesorgt würde.

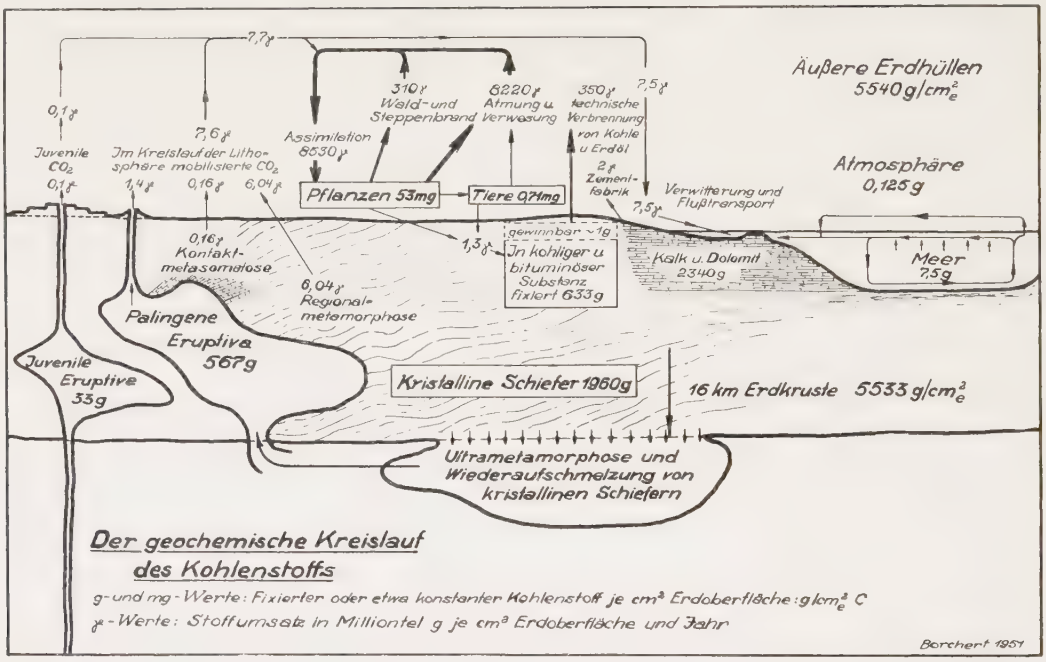

Abb. 4. Quantitative Bilanz des irdischen Kohlenstoffs.

Um welche Mengen es sich bei diesen Verwitterungsprozessen handelt, hat V. M. Goldschmidt ([13], S. 144) an Hand der Zusammensetzung der Flußwässer, welche ja die Verwitterungskarbonate in den Ozean tragen, berechnet. Er kommt zu einem jährlichen Umsatz von 30 γ/cm^2_e, ein Wert, der mindestens geviertelt werden muß, wenn man den Gesamtdurchschnitt über 10^9 Jahre kennzeichnen will.

Zu dem Pfeilring im Meer sei nur erinnert, daß der durchschnittliche Gesamtgehalt an CO_2, bezogen auf C-Gehalt je cm^2_e 7,5 g beträgt und daß daraus laufend nach K. Kalle (*loc.cit.* S. 205) 3 γ/cm^2_e als Karbonat in kalkigen Sedimenten fixiert werden. Hierauf wird unten noch zurückzukommen sein. Wichtig ist, daß die Kohlensäure der Atmosphäre im Gleichgewicht und Austausch mit dem CO_2-Gehalt der Ozeane steht.

Die Gesamtbilanz besagt, daß das Lebensgleichgewicht zwischen Pflanzen und Tieren mit rund 8530 γ/cm^2_e einigermaßen ausgewogen sein dürfte, wobei der Anteil von 1,3 γ/cm^2_e (von K. Kalle übernommen), welcher dem oberflächlichen Kreislauf

durch kohlige und bituminöse Sedimente entzogen wird, mengenmäßig nicht wesentlich ins Gewicht fällt.

Ohne die menschliche Technik würden durchschnittlich 6,2 γ durch Metamorphose, 1,4 γ durch palingenen Magmatismus und 0,1 γ durch juvenilen Vulkanismus der Atmosphäre jährlich zugeführt werden. Da der jährliche Entzug durch die Verwitterung und dessen Fixierung in Kalksedimenten im Gesamtdurchschnitt von 10^9 Jahren 7,7 γ betragen dürfte und die Bindung in Form von organischem Kohlenstoff nur 1,3 γ ausmacht, so erscheint der „natürliche" geochemische Kreislauf bemerkenswert ausgewogen. Es bleibt ein Fehlbetrag von nur 0,6 γ C/cm$_e^2$ an „juveniler" Kohlensäure. Ich möchte ausdrücklich betonen, daß dies Ergebnis bei vollkommen unbefangener Durchrechnung aller Daten zustande gekommen ist. Jeder Geochemiker weiß, daß man rückwärts rechnend auch 10fache Werte leicht auf 0 bringen könnte. Der Spielraum des Anteils der einzelnen Gesteine an der 16-km-Kruste ebenso wie die Prozentgehalte dieser Gesteine sind ja meist in der vorletzten Stelle noch keineswegs gesichert.

Die Bilanz verschiebt sich allerdings um Größenordnungen, wenn die Eingriffe des Menschen in den geochemischen Haushalt berücksichtigt werden. Durch die Energie- und Kraftwirtschaft werden jährlich rund 350 γ (entsprechend rund 2 Milliarden t Kohlenstoff in Form von Kohle und Erdöl!) in die Atmosphäre zurückgeliefert. Für den Kreislauf der Organismen bedeutet dies einen Anteil von nur etwa 0,4 %, weshalb dieser Kreislauf auch nicht grob ersichtlich auf die „Industrialisierung" reagiert.

Für den übrigen geochemischen Kreislauf bedeuten 350 γ aus technischen Verbrennungsprozessen und 2 γ aus der Zementfabrikation einen ganz beachtlichen Überschuß über den durchschnittlichen Verbrauch während geologischer Epochen. Kohlenstoff, der in Jahrmillionen reduziert und in der Erdkruste als Kohle und Erdöl fixiert wurde, wird durch den Menschen sehr kurzfristig der Atmosphäre zurückgegeben. „Sehr kurzfristig" bedeutet, daß die Vorräte an gewinnbarem Kohlenstoff in etwa 3000 Jahren bei derzeitiger Förderhöhe wieder in die Luft gejagt sein würden. Eine Übersicht der wichtigsten Zahlen gibt die Tabelle 3.

Gewisse Diskrepanzen in der Darstellung von Abb. 4 sind nicht zu vermeiden. Das Hauptbemühen ging dahin, für die gesamte Lebenszeit von 1 Milliarde Jahren

Tabelle 3

Gramm je cm² Erdoberfläche g/cm²$_e$	*Erdoberfläche 5,1 · 10^{18} cm²*	*Gewichtsmengen*
1	C in den gewinnbaren Kohlen und Erdölen . . .	5,1 · 10^{12} t
4408000	Gewicht einer 16 km dicken Erdkruste	2,25 · 10^{19} t
5533	C-Gehalt der 16 km dicken Erdkruste.	2,82 · 10^{16} t
2340	C-Gehalt der Karbonate der Sedimente	1,2 · 10^{16} t
633	Elementarer C-Gehalt der Sedimente	3,2 · 10^{15} t
1960	Gesamt-C-Gehalt der kristallinen Schiefer	1,0 · 10^{16} t
567	Gesamt-C-Gehalt der palingenen Eruptiva	2,9 · 10^{15} t
33	Gesamt-C-Gehalt der juvenilen Eruptiva	1,7 · 10^{14} t
7,5	C im CO_2 der Ozeane	3,8 · 10^{13} t
0,125	C im CO_2 der Atmosphäre	6,4 · 10^{11} t
0,054	C in den Organismen	2,8 · 10^{11} t

eine Bilanz aufzustellen, wobei das Schwergewicht im Kreislauf der Lithosphäre liegt und liegen muß, wenn man wirklich über Zeiträume von 10^9 Jahren zu mitteln versucht. Demgegenüber bezieht sich der „kleine Kreislauf" der Organismen naturgemäß auf die derzeitigen biologischen Verhältnisse. Eine rohe Berücksichtigung der um Größenordnungen geringeren Lebensintensität im Präkambrium könnte auch diese „Gegenwarts"-Zahlen über 10^9 Jahre auszugleichen versuchen. Das Verfahren würde entsprechend den oben mehrfach berührten Gesichtspunkten einfach darin bestehen, daß die Zahlen gevierteilt würden, um den Durchschnitt über 10^9 Jahre zu repräsentieren. Auf diese Reduktion ist verzichtet worden, auch weil es völlig sinnlos werden würde, wenn man die rund 350 γ, die durch die moderne Industrialisierung erst seit wenigen Jahrzehnten oder Jahrhunderten anfallen, auch auf 10^9 Jahre auszugleichen versuchte.

Die aus diesen Gründen unvermeidlicher Diskrepanz der Zahlen zwischen dem „großen lithosphärischen" und dem „kleinen biologischen" Kreislauf darf aber insofern wohl in Kauf genommen werden, als beide sauber getrennt zur Darstellung gebracht sind und wiederum gesondert die „kurzfristige Sonderproduktion" durch die moderne Industrie mit zwei offenen Sonderpfeilen gekennzeichnet ist. Das Großbild, das sich uns bietet, kann auf die einfache Formel gebracht werden, daß sowohl der „kleine Kreislauf" wie auch der „große Kreislauf" bemerkenswert ausgewogen erscheint und nur „momentan" ein beachtlicher Überschuß von C in Form von CO_2 durch die moderne Technik in die Atmosphäre zurückgepumpt wird.

Einige Dinge werden durch die vorliegende geochemische Bilanz noch schärfer beleuchtet:

Es ist keinesfalls zu erwarten, daß die letzte bedeutsame Steigerung des Kohlenstoffkreislaufes durch die menschliche Industrie sich schon geochemisch in den Sedimenten bemerkbar machen kann. Der gewaltige Puffer der Organismenwelt wird diesen Überschuß leicht verarbeiten. Mit Sicherheit aber wird hierdurch auch der CO_2-Gehalt der Flußwässer gesteigert und den Ozeanen werden mehr als 30 γ/cm^2_e zugeführt. Letztlich muß verstärkte Kalksedimentation die Hauptfolge sein. Für die Gesamtmengen spielt im übrigen das eine g/cm^2_e gewinnbaren Kohlenstoff wiederum gar keine Rolle.

Aber auch ohne diese menschlich bedingte kurzfristige Rückgabe von fixiertem Kohlenstoff in den Kreislauf ist eine bedeutsame Steigerung der Kalksedimentation während der jüngeren Erdgeschichte unverkennbar. Der jetzige Wert von 30 γ/cm^2_e Verwitterungskohlensäure würde in 10^9 Jahren 30 kg cm^2_e C in Form von Karbonatsedimentation ausmachen können (also mehr als das doppelte des *maximal* und fast das fünffache des *wahrscheinlich* in der ganzen 16-km-Kruste überhaupt vorhandenen Kohlenstoffs), während in Wirklichkeit nur 2,34 kg Karbonatkohlenstoff im Laufe der Erdgeschichte fixiert worden sind. Auch wenn man nur $^1/_4$ des derzeitigen Wertes für die erdgeschichtliche Vergangenheit ansetzt, ergibt das immer noch mehr als die dreifache Menge gegenüber dem tatsächlichen gebundenen Karbonatkohlenstoff. Da aber über geologische Zeiträume sicher keine wesentlichen Überschüsse in der Bilanz bestehen können, bleibt nur die Schlußfolgerung (und für den Mineralogen die Bestätigung), daß die Kalksedimentation in der jüngeren geologischen Vergangenheit um eine Größenordnung gegenüber dem Paläozoikum und noch mehr gegenüber dem Präkambrium gewachsen ist.

III. Schlussbemerkung

W. Noddack ([10], S. 510) hat aus seiner Bilanz des Kohlenstoffhaushalts die Folgerung gezogen, daß bereits $^3/_4$ des in der Erdrinde vorhandenen Kohlenstoffs in Sedimenten festgelegt worden sind und daß bei gleicher Kreislaufgeschwindigkeit wie bisher die Organismen nur noch $^1/_4$ ihrer Gesamtlebensperiode von 10^9 Jahren zur Verfügung haben würden. W. Noddack sieht hierbei nur den Ausweg, daß die lebendige Substanz das Meisterstück schafft, mit dem Rückgriff auf Kalk und Kohle ihr Leben über 250 Millionen Jahre zu verlängern. In dieser Form aber droht der organischen Welt sicher keine Gefahr, solange die Erdkruste „atmet"; daß sie das tut, wird uns durch Vulkan- und Erdbebentätigkeit ebenso bewiesen wie durch das offenbar ganz ungewöhnlich starke Relief, welches die Erdoberfläche einschließlich der Tiefseegräben zeigt. Zwar wird durch den Menschen selbst der Kalkkreislauf „momentan" — auf längere Sicht spielt das eine g/cm_c^2 gewinnbaren Kohlenstoffs entsprechend rund 5 Billionen Tonnen kaum eine Rolle — stark forciert und damit die ohnehin im Gang befindliche Steigerung der Kalksedimentation „augenblicklich" weiter verstärkt. Das bedeutet aber wiederum, daß in erdgeschichtlichen Zeiträumen von 250 Millionen Jahren auch kalkreichere Sedimente metamorphosiert und wieder aufgeschmolzen werden als in der geologischen Vergangenheit, so daß die Zufuhr von CO_2 aus der Metamorphose auf mehr als 7,7 γ/cm_c^2 steigen wird. So lange also die Erdkruste „lebendig" bleiben wird — und aus der geologischen Vergangenheit darf man durchaus auf zukünftige Zeiträume gleicher Größenordnung schließen — ist die Welt der Organismen durch CO_2-Mangel keinesfalls bedroht, selbst wenn der Mensch es aufgeben sollte, aus C-Verbindungen Kraft und Energie zu erzeugen.

Literatur

[1] Kalle, K.; Der Stoffhaushalt des Meeres. 2. Aufl., Leipzig 1945. [2] Correns, C. W.; Globigerinenschlamm, Roter Ton und Blauschlick. Naturwiss. 1937 **25** 196–200. [3] Wattenberg, H.; Kohlensäure und Kaliziumkarbonat im Meere. Fortschr. Mineral. usw. 1936 **20** 168–195. [4] Krejci-Graf, K.; Die Entstehung des Erdöls. Naturwiss. 1935 **23** 599. [5] Teichmüller, M. u. R.; Das Inkohlungsbild des niedersächsischen Wealdon-Beckens. Z. d. D. Geol. Ges. 1948 **100** 498–517. [6] Borchert, H. u. Tröger, E.; Zur Gliederung der Erdkruste nach geophysikalischen und petrologischen Gesichtspunkten. Gerlands Beitr. z. Geophys. 1951 **62** H. 2. [7] Jaggar, T.A.; Magmatic Gases. Amer. J. Sc. 1940 **238** 313–353. [8] Shepherd, E. S.; The Gases in Rocks and some related Problems. Amer. J. Sci. 1938 **35**A 311–355. [9] Rittmann, A.; Das Magma in den Vulkanherden. Geol. Rdsch. 1936 **27** 31–43. [10] Noddack, W.; Der Kohlenstoff im Haushalt der Natur. Angew. Chemie 1937 **50** 505–510. [11] Goldschmidt, V. M. †, Krejci-Graf, K. u. Witte, H.; Spuren-Metalle in Sedimenten. Nachr. Ges. d. Wiss. Göttingen, Math.-phys. Kl. 1948 35–52. [12] Clarke, F. W.; The Data of Geochemistry. U.S. Geol. Surv. Bull. 770, Washington 1924. [13] Goldschmidt, V. M.; Grundlagen der quantitativen Geochemie. Fortschr. Mineral. usw. 1933 **17** 112–156. [14] Correns, C. W.; Die geochemische Bilanz. Naturwiss. 1948 **35** 7–12. [15] Engelhardt, W. v.; Die Geochemie des Barium. Chemie der Erde 1936 **10** 187–246. [16] Vogt, J. H. L.; On the average composition of the earth's crust, with particular reference to the contents of phosphoric and titanic acid. Videnskapsselsk. Skr. Oslo, 1931, Nr. 7. [17] Wagner, G.; Leben und Erdgeschehen im chemischen Wechselspiel. Universitas 1949 **4** 691–700, 937–943.

Siehe auch: Rothe, W.; Kohlensäureassimilation und Photosynthese. Forsch. u. Fortschr. 1950 **26** 253–257. Vernadsky, W. J.; Geochemie in ausgewählten Kapiteln. Leipzig 1930. Vernadsky, W. J.; Ozeanographie und Geochemie. Z. Krist. Abt. B, Mineral. Petrogr. Mitt. N. F. 1933 **44** 168–192.

Geochimica et Cosmochimica Acta, 1951, Vol. 2. pp. 76 to 79. Pergamon Press Ltd. London

Gas content and age of tektites

Hans E. Suess*

Institute for Nuclear Studies, University of Chicago, Chicago, Illinois

(Received 13 August 1951)

ABSTRACT

The following experimental findings are discussed: (a) The gas content of bubbles present in tektites is extremely low; (b) tektites give off small amounts of CO_2, CO, H_2, and H_2O when heated to approximately 1200° C; (c) the low content of radiogenic argon permits an upper limit of the order of 10^7 years to be set for the age of the tektites.

The problem of the origin of the tektites is discussed in view of this new experimental evidence.

It may be recalled that certain glassy bodies which are found in several distinct areas, such as certain regions of Czechoslovakia, Australia, the Philippines, and Indo-China are called tektites [1]. These glasses, of greenish, brown or almost black appearance, range from a fraction of a centimeter to several centimeters in diameter. The lack of any satisfactory explanation for the geological development or origin of these bodies has led to the daring assumption that these objects must have fallen from the sky. Besides this conclusion from negative evidence, there seem to be indications which make it appear more plausible to assume that the tektites have formed in free space rather than on the Earth's surface; for example, their peculiar features, which in a large number of cases resemble perfectly the shapes of Laplace rotational figures [2].

On the other hand, the chemical composition of the tektites is entirely different from that of ordinary meteoritic matter, *viz.*, nickel-iron and silicate phases with a continuous series of intermediate mixtures. There are no indications of any intermediate products between tektites and the common meteorites. No tektite fall has ever been observed. The question of the origin of the tektites is still the object of speculative theories, and there is no evidence available which could be interpreted in a conclusive way.

During recent years our knowledge of the composition of cosmic matter and of the possible astrochemical processes which one may expect to occur in space has substantially increased [3]. These advances seem to justify a renewed discussion of the problem of the origin of the tektites and an attempt to obtain some new experimental evidence which might contribute to a solution of this question.

The new experimental evidence which is discussed below has failed to reveal any clue to the conclusive solution of the question of the origin of the tektites but makes it possible to rule out various theories which hitherto suggested a plausible explanation.

First, an attempt was made to measure the pressure and composition of the gases included in the bubbles which are occasionally present in tektites [4].

Dr. Ortley Bayer of Manila has kindly furnished a number of socalled "gas-rich" philippinites, tektites from the Philippines, which are exceptionally rich in bubbles of various sizes.

* Present address: U.S. Geological Survey, Washington 25, D.C.

The contents of the bubbles were released by mechanically crushing a tektite inside an evacuated tube, and the amount of the released gases was measured by means of a McLeod gauge, which also acted as a Toepler pump. The volume of the opened bubbles was calculated from the density of the material before and after crushing. The surprising result of this experiment was that no measurable amount of gas could be detected, and that the content of the bubbles must represent a fairly good vacuum.

Table 1 shows the results of two typical runs.

Table 1. Gas content of the bubbles of "gas-rich" philippinites

	a	*b*
Weight of tektite	5·585 g	5·154 g
Density before crushing	2·385	2·401
Density after crushing	2·420	2·441
Volume of bubbles	0·10 cc	0·085 cc
Amount of gas found	$<10^{-4}$ cc SPT	
Pressure in the bubbles	$<10^{-3}$ atm	

Obviously some gas must have been present to form the bubbles. But an estimate of the pressure necessary to balance the surface tension of the molten tektite glass shows that a pressure of about 1 mm would be sufficient to form the bubbles at zero external pressure. This evidence undoubtedly speaks for an extra-terrestrial origin of the tektites, but unfortunately does not prove it conclusively. It seems possible that the bubbles might have been caused by water vapor which might have subsequently dissolved in the glass at low temperatures and is for this reason no longer detectable. This alternative, however, seems improbable in view of the results of some experiments in which the gases which tektites give off when melted at high temperatures were collected and analyzed.

In agreement with previous investigations of such gases by A. Brun in 1909 [5] it was found that they consist of CO_2, CO, H_2 and water vapor, necessarily in equilibrium at a temperature somewhat below the temperature to which the samples were heated, *i.e.* a temperature at which the equilibrium is readily established.

Table 2 shows the results of the analyses. They indicate the tektites contain traces of oxides of carbon and hydrogen. At high temperatures an equilibrium is established according to the equation;

$$CO_2 + H_2 = CO + H_2O;$$

$$[CO]\,[H_2O]\,[CO_2]\,[H_2] = 0.7 \quad (t = 700\ \text{C}).$$

The two runs in which the amount of water was measured indicate agreement with the known equilibrium constant. The amount of water relative to that of the oxides of carbon present varies widely for the different samples, and seems to depend on the way in which the surface of the samples was purified. In the cases in which sandblasting was applied, which served to remove the uppermost layer by abrasion, the amount of water was much lower than in one sample which was merely chemically purified. This seems to indicate that most of the water was picked up by the tektite at the Earth's surface, and makes it seem unlikely that the bubbles inside the specimens were created by water vapor.

Table 2. Gases released by heating to 1200° C

	Total	Analysis, %				
	cc/g	CO_2	CO	H_2	H_2O	N_2
Brun 1909:						
Billitonite	0·23	43	44	12·8	—	Tr
Moldavite	0·17	17	63	20	—	—
This work:						
Philippinite	0·11	21	56	6	15	—
Australite	0·14	6	92	1·5	Tr	—
Australite†	0·33	6	7	0·5	86	—

† Surface not mechanically purified

The second kind of new experimental evidence is that obtained by Hayden, Inghram, and Suess [6] from a study of the argon content of three tektite samples. The argon was determined by mass spectrometric analysis after a known amount of A^{38} had been added to the gases released from the sample. The A^{38} samples containing 97·5% A^{38} were prepared by neutron radiation of NaCl. From the amount of radiogenic A^{40} present and the potassium content of the samples the age of the tektites can be calculated, since the decay scheme of K^{40} is now known with sufficient accuracy [7]. However, the A^{40} content of the samples was found to be so low that only an upper limit for the age of the investigated tektites could be determined, and this was of the order of 10^7 years.

The experiments have proved conclusively that the age of the tektites studied is less than 1/100 of that of the solar system. It seems probable to the writer that this age may well be practically equal to the age of the including strata at the Earth's surface *.

In the following discussion, the possibility of any terrestrial origin is omitted, although the final justification of such a step should be left entirely in the hands of the geologists. We then have to consider the question of the cosmochemical process which has led to a chemical separation of tektitic matter from the original solar or meteoritic material. The possibility has been suggested and frequently discussed that the tektites may have formed during the process of the burning of a meteorite containing elementary aluminium and silicon while passing through the Earth's atmosphere. It is, however, difficult to see how such a meteorite can have formed from any kind of cosmic matter, because it can be shown from the thermodynamic properties of Si and Al and their relevant compounds, that these elements will not condense in the elementary state from solar matter under any thermodynamic conditions [8].

One other aspect, however, is furnished by the following fact: As has been pointed out previously [9], silicon and aluminium oxides, the main constituents of tektitic matter, are the most volatile compounds present in the ordinary meteoritic silicate phase. Moreover, of the minor constituents, those with higher vapor pressures seem to be enriched in tektites relative to cosmic matter. We may therefore assume that,

* The age of the strata is described in the literature as "practically Recent" for the australites, "mid-Pleistocene" for the philippinites and "Helvetian" for the moldavites.

as a result of some sort of distillation process during the formation of the meteorites or the terrestrial planets, the tektitic matter may have been separated from the bulk of the condensing material. Dr. HAROLD UREY has directed my attention to the fact that this comparatively volatile matter may be expected to have accumulated in the comets, whose main constituents are ice and frozen ammonia [10]. At distances close to the sun the ice and ammonia may completely evaporate, and if the distance is small enough the remaining silicates may be melted to form a cloud of small objects which occasionally may reach the earth's surface. Thanks are also due to Dr. GERARD KUIPER of Yerkes Observatory for discussing the astronomical side of the problem and particularly the question of the probability of such an event, which can be calculated from the average number of comets passing the sun. This probability seems to be in reasonable agreement with the assumption that molten fragments of a comet, forming a swarm of tektites, could reach the earth once in a few million years.

Such an assumption would not necessarily be contradicted by the isotopic composition of the oxygen in tektites, as determined by SOL R. SILVERMAN [11]. According to Dr. SILVERMANs work, the O^{18} content of tektitic oxygen is noticeably higher than that of stony meteorites or igneous rocks and within the range of that of sedimentary rocks. This may be explained by assuming that O^{18} was exchanged in the direction of equilibrium between the water and the oxides during the process of heating and evaporation of the comet.

The idea of a genetic relation between tektite and comets is certainly not a new one, and no claims are made here for presenting the final solution of the problem. In view of the evidence presented, the writer believes that the probability for its being the correct answer seems at the moment somewhat greater than that of the numerous other theories on tektite formation. A comparison with these other possibilities would require an extensive discussion of astronomical and geological questions which would exceed the limits of this paper.

Acknowledgments—The author wishes to express his appreciation to the University of Chicago for a fellowship granted to him during the time when this work was accomplished. Thanks are also due to Dr. H. C. UREY, not only for many stimulating discussions and may valuable suggestions, but also for making the laboratory space available for carrying out the experimental part of this investigation.

REFERENCES

[1] SUESS, F. E.; Jb. d. Geol. Reichsanstalt Wien 1900 **50** 193. Mittlg. Geolog. Ges. Wien 1914 **7** 51; 1932 **25** 115. [2] FENNER, C.; Trans. Roy. Soc. S. Australia 1934 **50** 62; 1935 **59** 125; 1938 **62** 192. [3] GOLDSCHMIDT, V. M.; Geochem. Verteilungsgesetze IX Videnskapsakademien, Oslo 1938. SUESS, H. E.; Z. Naturforschung 1947 **2**a 311, 604. BROWN, HARRISON; Rev. Mod. Physiks, 1949 **21** 625. [4] SUESS, H. E.; Paper given at the Washington Meeting, Geol. Soc. Amer., Nov. 1950. [5] See BECK, R.; Monatsber. d. Deutsch. Geol. Ges. 1910 **62** 240. [6] SUESS, H. E., HAYDEN, R. J. and INGHRAM, M. G.; Nature, Lond. (in press). [7] INGHRAM, M. G., BROWN, HARRISON, PATTERSON, C., and HESS, D. C.; Phys. Rev. 1950 **80** 916. SAWYER, G. A. and WIEDENBECK, M. L.; Phys. Rev. 1950 **79** 690. HOUTERMANS, F. G., HAXEL, O., and HEINTZE, J.; Z. Physik 1950 **128** 657. [8] EUCKEN, A.; Nachr. Gött. Akad. Wiss., Math.-Phys. Kl. 1944 Heft 1; Naturwiss. 1944 **32** 112. UREY, H. C.; Geochem. et Cosmochem. Acta 1951 **1** 281. [9] SUESS, H. E.; Z. Elektrochem. 1949 **53** 237. [10] WHIPPEL, F. L.; Astrophys. J. 1950 **111** 375. [11] SILVERMAN, SOL R.; Geochim. et Cosmochim. 1951 **2** 26.

Book review

AHRENS, L. H.; **Spectrochemical Analysis,** Pp. 269 + 70, Cambridge, Mass., Addison-Wesley Press, 1950. $ 10.—

This book is of particular interest to workers engaged in the analysis of rocks and minerals, as it deals solely with spectrochemical methods using D. C. arc excitation, a source well suited to such materials and in fact often the only method applicable to them. It indicates the possibilities and limitations of spectrochemical analysis for such work, particularly as far as trace elements are concerned. The determination of major constituents is however not ignored. Dr. AHRENS, who is in charge of the Cabot Spectrographic Laboratory in the Department of Geology of the Massachusetts Institute of Technology, has dealt with technique rather than equipment, and has thus concentrated much valuable information into quite small bulk.

But it is not only to the practising analyst that this book will be of value. Every geochemist should read the second part, dealing with the determination of individual elements. Limits of detection, accuracy and ease of determination are treated fully, and an appreciation of the factors involved will enable the geochemist to interpret much more satisfactorily the data which the analyst puts before him.

R. L. MITCHELL

I. General

1. Papers on Geochemistry should be submitted to the editors for the appropriate country or language (*Papers an Cosmochemistry should be sent Prof. F. A. Paneth, F.R.S.*). Papers submitted for publication will naturally be judged from the standpoint of scientific originality and novelty. Technical details of apparatus used in scientific investigation can, however, be presented in brief notes. The preparation of progress reports and review articles will be invited by the Editors from time to time and it is therefore requested that no uninvited contributions of this nature be submitted. The Journal will appear as independent and complete numbers, which will be sold separately and combined into volumes of about 300 pages.

2. Only papers which have not been previously published will be accepted. The publishers retain exclusive publication rights for all papers in all languages and countries, on acceptance an until the 31st December of the year following the year when the printed paper appears. Authors must agree not to publish elsewhere a paper submitted to and accepted by *Geochimica et Cosmochimica Acta*.

3. Authors will receive 75 free reprints of their papers. Additional copies can be purchased if ordered at the time the first proofs are returned.

II. Manuscript Requirements

1. The manuscript must be written in one of the three official languages, English, French, or German.

2. The manuscript should be an original typewritten copy (not a carbon). The text must be ready for printing and should be carefully checked for errors. Authors will receive proofs for correction.

3. Half-tone illustrations are to be restricted to the minimum necessary. They must accompany the manuscript mounted on separate sheets. Line drawings will be redrawn for the sake of uniformity and should therefore include all relevant details. Photographs should be enlarged sufficiently to permit their clear reproduction in half-tone. If words or numbers appear in photographs, two copies are requested, one clearly printed and the other without inscription. All illustrations and tables should be provided with descriptive legends.

4. Only such references to literature should be given as are referred to in the text. Literature references are to be numbered and listed together at the end of the manuscript and not as footnotes. All references should include the standard (according to the *World List of Scientific Periodicals*) abbreviated title of the journal, year, volume number, and first and last page numbers.

5. The text of articles submitted should be concise and in a readily understandable style. The technical description of the methods used should only be given in detail when such methods are new. The essential contents of each paper should be briefly recapitulated in an abstract in English. Such an abstract may, however, be submitted by the author in the language of the original typescript for translation into English by the editorial staff.

6. To conserve space authors are requested to mark less important portions of the paper (such as description of methods, record of experimental results, *etc.*) for printing in smaller size type.

The Unesco Book Coupon Scheme

Under a scheme initiated by the United Nations Educational, Scientific and Cultural Organization, Book Coupons can now be purchased in national currency for the purpose of obtaining publications of a scientific, educational and cultural nature from other parts of the world.

Coupons are available in various denominations at distributing agencies in the following countries:— Burma; Czechoslovakia; Egypt; France; Hungary; India; Indonesia; Israel; Italy; Pakistan; Persia; Thailand; Union of South Africa; at UNESCO Science Co-operation Offices in East Asia, the Middle East and South Asia; and for British, Colonial and Trust Territories from Book Tokens Ltd., 28 Little Russell Street, London, W.C.1.

Since the amount of coupons available is sometimes limited, special priority is given to the needs of educational, scientific and cultural institutions, although the scheme as a whole is operated for the benefit of both individuals and institutions. Purchasers of Book Coupons need not apply personally to the distributing body but can, if they prefer, place their orders with local booksellers, who will themselves undertake all the necessary formalities.

Full details of the scheme and addresses of distributing agencies can be obtained from Lange, Maxwell & Springer Ltd., 41—45 Neal Street, London, W.C.2., or direct from UNESCO's Clearing House for Publications, 19 Avenue Kleber, Paris 16e, France.

FILED IN STACKS

Lange, Maxwell & Springer Ltd.

SCIENTIFIC, MEDICAL AND TECHNICAL BOOKSELLERS

take this opportunity to announce that they have established a special division within their organisation to handle exclusively the supply of Scientific, Technical and Medical literature to Industrial and Educational Research Organisations and Libraries

1 May 65

This division offers the following services:

- **Regular News Service** regarding newly published books and journals in all languages on Scientific, Technical and Medical subjects, contained in the LANGE, MAXWELL & SPRINGER BOOK NEWS sent free of charge on request
- **Supply of books and periodicals** on Subscription, published anywhere and in any language. Prices charged are at the official rate of exchange
- **Supply of Rare and Out-of-Print Books, Sets and Runs of Periodicals**
- **Translations of Foreign language Articles** undertaken
- **Hand-binding in our own bindery:** Speedy service at competitive prices
- **Books sent on approval if required**
- **Purchase or exchange** of surplus books and journals

We invite your inquiries, and particularly we invite you to visit our

SHOWROOMS at 138 SHAFTESBURY AVENUE, LONDON, W.C.2,

which are open from 9 30 a.m. to 6 p.m. on Mondays to Fridays, and from 9 a.m. to 12.30 p.m. on Saturdays

We shall be pleased to arrange for our Representative to call in order to discuss with you any problems you may have with regard to the supply of Scientific, Technical and Medical literature

LANGE, MAXWELL & SPRINGER LTD.

41–45 NEAL STREET, LONDON, W.C.2

Telephone: Temple Bar 1124

Printed by Universitätsdruckerei H. Stürtz AG., Würzburg